Full title (250 characters): **Transmission of West Nile virus and other temperate mosquito-borne viruses occurs at lower environmental temperatures than tropical mosquito-borne diseases**

Short title (70 characters): **Temperature-dependent transmission of temperate mosquito-borne viruses**

Marta S. Shocket[1*] (mshocket@stanford.edu), Anna B. Verwillow[1] (anna19@stanford.edu), Mailo G. Numazu[1] (mnumazu@stanford.edu), Hani Slamani[2] (hanis1@vt.edu), Jeremy M. Cohen[3,4] (jcohen39@wisc.edu), Fadoua El Moustaid[5] (fadoua@vt.edu), Jason Rohr[3,6] (jasonrohr@gmail.com), Leah R. Johnson[2,5] (lrjohn@vt.edu), and Erin A. Mordecai[1] (emordeca@stanford.edu)

[1]Department of Biology, Stanford University, Stanford, CA, USA

[2]Department of Statistics, Virginia Polytechnic Institute and State University (Virginia Tech), Blacksburg, Virginia, United States

[3]Department of Integrative Biology, University of South Florida, Tampa, FL, USA

[4]Department of Forest and Wildlife Ecology, University of Wisconsin, Madison, WI, USA

[5]Department of Biological Sciences, Virginia Polytechnic Institute and State University (Virginia Tech), Blacksburg, Virginia, United States

[6]Department of Biological Sciences, Eck Institute of Global Health, Environmental Change Initiative, University of Notre Dame, South Bend, IN, USA

Keywords: *Culex pipiens*, West Nile virus, Western Equine Encephalitis virus, Eastern Equine encephalitis virus, St. Louis Encephalitis virus, Rift Valley Fever virus, Sindbis virus, Ockelbo disease, mosquito-borne disease, infectious disease, temperature

* Corresponding Author: Marta S. Shocket, mshocket@stanford.edu, phone: 650-723-5923

Availability of data and material: Upon acceptance, all data and code will be submitted to Dryad repository and the appropriate web link will be listed here for publication.

Competing interests: The authors declare that they have no competing interests.

Authors' contributions: EAM, LRJ, and MSS conceived of and designed the study. MN, AV, HS, FEM, and MSS collected trait data. MN and MSS fit models. JC collected West Nile virus case data and climate data. JC and MSS analyzed West Nile virus case data. MSS wrote the first draft of the manuscript. All authors revised and approved the manuscript.

ABSTRACT (427 WORDS)

Temperature is a key driver of mosquito-borne disease because it affects the physiology and life history traits of mosquitoes and the pathogens they transmit. These trait thermal responses are typically nonlinear and vary by species. However, the impact of temperature on many important temperate mosquito-borne diseases has never been quantified, and it is unclear if thermal responses of temperate mosquito-borne diseases differ systematically from the patterns found in better-studied tropical systems. These environment–transmission relationships are critical for understanding current seasonal and geographic distributions of disease and future shifts due to climate change. We used a mechanistic, trait-based approach to characterize temperature-dependent transmission of 10 vector–pathogen pairs in an overlapping network of mosquitoes (*Culex pipiens*, *Cx. quinquefascsiatus*, *Cx. tarsalis*, *Aedes triseriatus*, and others) and viruses (West Nile virus [WNV], Eastern and Western Equine Encephalitis viruses [EEEV and WEEV], St. Louis Encephalitis virus [SLEV], Sindbis virus [SINV], and Rift Valley Fever virus [RVFV]), most of which have predominantly temperate geographic distributions worldwide. We found that several of these temperate pathogens have lower thermal limits (8.6–19.0ºC) and optima (22.7–26.0ºC) that are cooler than those of tropical pathogens (lower thermal limits: 16.2–22.8ºC; optima: 25.4–29.1ºC), as expected based on geography. However, their upper thermal limits (31.9–37.8ºC) were very similar to those of tropical pathogens (31.4–34.5ºC). Together, these patterns led to wider thermal breadths (18.2–27.7ºC) for all but one of the temperate viruses (12.7ºC) compared to the tropical pathogens (11.7–16.7ºC). Among temperate viruses, thermal limits for transmission varied more and were more uncertain than the optima. While the qualitative shapes of trait thermal responses generally matched prior studies, lifespan declined monotonically at temperatures above 14ºC for the temperate *Culex* vectors, in contrast

to unimodal responses observed within this temperature range for tropical species. We validated the mechanistic models with independent data on human disease cases. The incidence of WNV across US counties responded unimodally to temperature and peaked at 23.9ºC, closely matching model predictions (optima for WNV in North American vectors ranged from 23.9–25.2ºC). Additionally, data on the month of onset of cases of WNV, SLEV, and EEEV suggested that temperature is important for determining the seasonality of transmission. The thermal responses for parasite development rate, vector competence, biting rate, and lifespan, all of which varied among species and determined thermal limits in models, are a critical need for future empirical work. Because temperature effects on vector-borne disease transmission are pervasive and nonlinear, and climate regimes are changing rapidly, trait-based models are a key tool for predicting how temperature will affect mosquito-borne disease dynamics.

INTRODUCTION

Temperature is a key driver of transmission of mosquito-borne diseases—including globally important pathogens like malaria and dengue—because the mosquitoes and pathogens are ectotherms whose physiology and life history depend strongly on environmental temperature [1–7]. These temperature-dependent traits drive the biological processes required for transmission. For example, temperature-dependent fecundity, development, and mortality of mosquitoes determine whether vectors are present in sufficient numbers. Temperature also impacts the mosquito biting rate on hosts and probability of becoming infectious.

Mechanistic models based on these traits and guided by principles of thermal biology predict that the thermal response of transmission is unimodal: transmission peaks at intermediate temperatures and is inhibited at extreme cold and hot temperatures [2–11]. This unimodal pattern is predicted consistently across mosquito-borne diseases [2–7] and supported by independent empirical evidence for positive relationships between temperature and human cases in many settings [5,12–15], but negative relationships at extremely high temperatures in other studies [2,15–17]. Accordingly, increasing temperatures due to climate change are expected to shift disease distributions geographically and seasonally, as warming should increase transmission in cooler settings but decrease it in settings near or above the optimum for transmission [18–21]. Thus, mechanistic models have provided a powerful and general rule describing how temperature affects the transmission of mosquito-borne disease. However, thermal responses vary among mosquito and pathogen species and drive important differences in how transmission responds to temperature, including the specific temperatures of the optimum and thermal limits for each vector–pathogen pair [2–7]. We currently lack a framework to describe or predict this variation, even at the broadest scales. For instance, mosquitoes and mosquito-borne diseases

span the tropical–temperate climate gradient, yet it is unclear if there are systematic differences in the way temperature affects transmission of different species across this gradient.

Filling this gap requires comparing mechanistic, temperature-dependent transmission models for many vector–pathogen pairs, which are currently lacking for several reasons. First, the number of relevant vector–pathogen pairs is large because many mosquitoes transmit multiple pathogens and many pathogens are transmitted by multiple vectors. Second, empirical data are costly to produce and existing data are often insufficient because experiments or data reporting were not designed for this purpose. Third, compiling these data is labor-intensive and fitting thermal responses is technically challenging. Accordingly, many vector–pathogen pairs lack temperature-dependent transmission models altogether or have models that only include a subset of the relevant traits. Here, we address these challenges by systematically compiling data and building models for understudied mosquito-borne disease systems. Accurately characterizing the thermal limits and optima for these systems is critical for understanding where temperature currently promotes or suppresses transmission and where climate change will increase, decrease, or have minimal effects on transmission.

In this study, we model the effects of temperature on a suite of widespread, important, and largely temperate mosquito vectors and viruses that currently lack complete temperature-dependent models. We selected this group of mosquito-borne diseases because many of the viruses share common vector species and several vector species transmit multiple viruses (Fig 1). These temperate viruses include: West Nile virus (WNV), St. Louis Encephalitis virus (SLEV), Eastern and Western Equine Encephalitis viruses (EEEV and WEEV), and Sindbis virus (SINV) [22–24] (summarized in Table 1). We also included the primarily tropical Rift Valley fever virus (RVFV) because it shares two key vector species, *Culex pipiens* and *Cx. quinquefasciatus* [25]

(summarized in Table 1). All the viruses cause febrile illness and a variety of severe disease symptoms, including long-term arthralgia and neuroinvasive syndromes with a substantial risk of mortality in severe cases [22–25]. WNV is found across Africa, Europe, Asia, Oceania, and North America. It first invaded North America in 1999 [22] and is now the most common mosquito-borne disease in the US and Canada. SLEV, EEV, and WEEV occur primarily in the US (Table 1), with occasional cases in Canada and Central and South America [26,27]. SINV occurs in northern Europe and southern Africa [24]. RVFV originated in eastern Africa and now also occurs across Africa and the Middle East [25]. These pathogens primarily circulate and amplify in wild bird reservoir hosts (except RVFV, which primarily circulates in livestock). For all six viruses, humans are dead-end or unimportant reservoir hosts [28,29], in contrast to pathogens like malaria, dengue virus, yellow fever virus, and Ross River virus, which can sustain infection cycles between humans and mosquitoes [28,30,31]. Most transmission of RVFV to humans occurs through direct contact with infected livestock, although it also occurs to a lesser extent via the typical mosquito-borne transmission route, i.e., bites from infected vectors [29].

We primarily focus on *Culex pipiens*, *Cx. quinquefasciatus*, and *Cx. tarsalis*, well-studied species that are important vectors for many of the viruses and for which appropriate temperature-dependent data exist for nearly all traits. Although the closely-related *Cx. pipiens* and *Cx. quinquefasciatus* overlap in their home ranges in Africa, they have expanded into distinct regions globally (Fig 2) [32]. *Cx. pipiens* occurs in higher-latitude temperate areas in the Northern and Southern hemisphere, while *Cx. quinquefasciatus* occurs in lower-latitude temperate and tropical areas (Fig 2A). In contrast, *Cx. tarsalis* is limited to North America but spans the tropical-temperate gradient (Fig 2B). In this system of shared pathogens and vectors with distinct geographical distributions, we also test the hypothesis that differences in thermal performance

underlie variation in vector and pathogen geographic distributions, since temperate environments provide cooler temperatures and a broader range of temperatures than tropical environments. Thermal responses from other vector species were also included in some models: *Ae. taeniorhynchus* (SINV and RVFV), *Ae. triseriatus* (EEEV), *Ae. vexans* (RVFV), *Cx. theileri* (RVFV), and *Cs. melanura* (EEEV). Additionally, we compare our results to previously published models [2–4,6,7] for transmission of more tropical diseases by the following vectors: *Ae. aegypti*, *Ae. albopictus*, *Anopheles spp.*, and *Cx. annulirostris*.

We use a mechanistic approach to characterize the effects of temperature on vector–virus pairs in this network using the thermal responses of traits that drive transmission. Specifically, we use experimental data to measure the thermal responses of the following traits: vector survival, biting rate, fecundity, development rate, competence for acquiring and transmitting each virus, and the extrinsic incubation (development) rate of the virus within the vector. We ask: (1) Do these temperate vectors have qualitatively similar trait thermal responses to more tropical vectors? (2) Do temperate vectors transmit disease at lower temperatures, and across a broader temperature range, than tropical vectors? (3) How do the thermal responses of transmission vary across vectors that transmit the same virus and across viruses that share a vector? (4) Which traits limit transmission at low, intermediate, and high temperatures? Broadly, we hypothesize that variation in thermal responses is predictable based on vectors' and viruses' geographic ranges.

Mechanistic models allow us to incorporate nonlinear effects of temperature on multiple traits, measured in controlled laboratory experiments across a wide thermal gradient, to understand their combined effect on disease transmission. This approach is critical when making predictions for future climate regimes because thermal responses are almost always nonlinear,

and therefore current temperature–transmission relationships may not extend into temperatures beyond those currently observed in the field. We use Bayesian inference to quantify uncertainty and to rigorously incorporate prior knowledge of mosquito thermal physiology to constrain uncertainty when data are sparse [3]. The mechanistic modeling approach also provides an independently-generated, *a priori* prediction for the relationship between temperature and transmission to test with observational field data on human cases, allowing us to connect data across scales, from individual-level laboratory experiments, to population-level patterns of disease transmission, to climate-driven geographic variation across populations. Using this approach, we built mechanistic models for 10 vector–virus pairs by estimating thermal responses of the traits that drive transmission. We validated the models using observations of human cases in the US over space (county-level) and time (month-of-onset). The validation focuses on WNV because it is the most common of the diseases we investigated and has the most complete temperature-dependent trait data.

MODEL OVERVIEW

To understand the effect of temperature on transmission and compare the responses across vector and virus species, we used R_0—the basic reproduction number [33]. We use R_0 as a static, relative metric of temperature suitability for transmission that incorporates the nonlinear effects of temperature on multiple traits [1,34] and is comparable across systems, rather than focusing on its more traditional interpretation as a threshold for disease invasion into a susceptible population. Temperature variation creates additional nonlinear effects on transmission [35–38] that are not well-captured by R_0, [9,33,39–41] but could be incorporated in

future work by integrating the thermal performance curves fit here over the observed temperature regime.

The basic R_0 model (eq. 1) [34] includes the following traits that depend on temperature (T): adult mosquito mortality (μ, the inverse of lifespan [*lf*]), biting rate (a, proportional to the inverse of the gonotrophic [oviposition] cycle duration), pathogen development rate (*PDR*, the inverse of the extrinsic incubation period: the time required for exposed mosquitoes to become infectious), and vector competence (*bc*, the proportion of exposed mosquitoes that become infectious). Vector competence is the product of infection efficiency (c, the proportion of exposed mosquitoes that develop a disseminated infection) and transmission efficiency (*b,* the proportion of infected mosquitoes that become infectious, with virus present in saliva). Three parameters do not depend on temperature: mosquito density (M), human density (N), the rate at which infected hosts recover and become immune (r).

$$\text{Basic } R_0\text{: } R_0(T) = \left(\frac{a(T)^2 bc(T) e^{-\frac{\mu(T)}{PDR(T)}} M}{N\, r\, \mu(T)}\right)^{1/2} \qquad \text{eq. 1}$$

As in previous work [2–4,6,7,9], we extend the basic R_0 model to account for the effects of temperature on mosquito density (M) via additional temperature-sensitive life history traits (eq. 2): fecundity (as eggs per female per day, *EFD*), egg viability (proportion of eggs hatching into larvae, *EV*), proportion of larvae surviving to adulthood (*pLA*), and mosquito development rate (*MDR*, the inverse of the development period).

$$\text{Full } R_0\text{: } R_0(T) = \left(\frac{a(T)^2 bc(T) e^{-\frac{\mu(T)}{PDR(T)}} EFD(T) EV(T) pLA(T) MDR(T)}{N\, r\, \mu(T)^3}\right)^{1/2} \qquad \text{eq. 2}$$

Fecundity data were only available as eggs per female per gonotrophic cycle (*EFGC*; for Cx. *pipiens*) or eggs per raft (*ER*; for Cx. *quinquefasciatus*). Thus, we further modified the model to

obtain the appropriate units for fecundity: we added an additional biting rate term to the model (to divide by the length of the gonotrophic cycle, eqs. S1 and S2) and for *Cx. quinquefasciatus* we also added a term for the proportion of females ovipositing (*pO*; eq. S2).

To fit a temperature-dependent R_0 model for each relevant vector–virus pair, we conducted a literature survey to identify studies that measured the focal traits at three or more constant temperatures in a controlled laboratory environment. From these data, we fit thermal responses for each trait using Bayesian inference, which allowed us to quantify uncertainty and formally incorporate prior data [3] to constrain fits when data for the focal species were sparse or only measured on a limited portion of the temperature range (see *Material and Methods*). As in previous work [2–4,6,7], we fit traits with a symmetrical unimodal thermal response with a quadratic function (eq. 3) and traits with an asymmetrical unimodal thermal response with a Briére function [42] (eq. 4). For some asymmetrical responses (e.g., *PDR* for most vector–virus pairs), we did not directly observe a decrease in trait values at high temperatures due to a limited temperature range. In these cases, we chose to fit a Briére function based on previous studies with wider temperature ranges [2,4–6] and thermal biology theory [43]; the upper thermal limit for these fits did not limit transmission in the R_0 models. Lifespan data exhibited a monotonically decreasing thermal response over the range of experimental temperatures available. Based on vector life history, we fit these data using a linear function (eq. 5) that plateaued at coldest observed data point to be conservative. To overwinter, *Cx. pipiens* and *Cx. tarsalis* enter reproductive diapause and hibernate [44,45], and *Cx. pipiens* can survive temperatures at or near freezing (0ºC) for several months [44]. *Cx. quinquefasciatus* enters a non-diapause quiescent state [45,46] and is likely less tolerant of cold stress, but we wanted a consistent approach across models and other traits constrained the lower thermal limit of the *Cx. quinquefasciatus* R_0 model

to realistic temperatures.

Quadratic function: $f(T) = -q(T - T_{min})(T - T_{max})$ eq. 3

Briére function: $f(T) = q \cdot T(T - T_{min})\sqrt{(T_{max} - T)}$ eq. 4

Linear function: $f(T) = -mT + z$ eq. 5

In the quadratic and Briére functions of temperature (T), the trait values depend on a lower thermal limit (T_{min}), an upper thermal limit (T_{max}), and a scaling coefficient (q). In the linear function, the trait values depend on a slope (m) and intercept (z).

Because the magnitude of realized R_0 depends on system-specific factors like breeding habitat availability, reservoir and human host availability, vector control, species interactions, and additional climate factors, we focused on the relative relationship between R_0 and temperature. We rescaled the R_0 model to range from 0 to 1 (i.e., 'relative R_0'), preserving the temperature-dependence (including the absolute thermal limits and thermal optima) while making each model span the same scale. To compare trait responses and R_0 models, we quantify three key temperature values: the optimal temperature for transmission (T_{opt}) and the lower and upper thermal limits (T_{min} and T_{max}, respectively) where temperature is predicted to prohibit transmission ($R_0 = 0$).

RESULTS

Trait thermal responses

We fit thermal response functions from empirical data for most of the vector and virus traits that affect transmission (Table S1 and Fig 1). All mosquito traits were temperature-sensitive (3 main *Cx.* species: Fig 3, Fig 4; *Ae. taeniorhynchus*, *Ae. triseriatus*, *Ae. vexans*, *Cx. theileri*, and *Culiseta melanura*: Fig S1). For most species, the extensive data for larval traits

(mosquito development rate [MDR] and survival [*pLA*]) produced clear unimodal thermal responses with relatively low uncertainty (Fig 3A,B, Fig S1A,B). For biting rate (*a*) and fecundity traits (*pO*, *EFGC, ER*, *EV*), trait data were often more limited and fits were more uncertain, but still consistent with the expected unimodal thermal responses based on previous studies [2,4–6] and theory [43] (Fig 3C, Fig 4, Fig S1C-F). However, adult lifespan (*lf*) data clearly contrasted with expectations from previous studies of tropical mosquitoes. Lifespan decreased linearly over the entire temperature range of available data (coldest treatments: 14–16ºC, Fig 3D; 22ºC, Fig S1D) instead of peaking at intermediate temperatures (optima for tropical species: 22.2–23.4ºC) [2–4,6,7].

In general, the adult mosquito traits (biting rate, lifespan, and fecundity [*a*, *lf*, *pO*, *EFGC, ER*, *EV*]) varied more among species than the larval traits (development rate and survival [*MDR* and *pLA*]), although the high degree of uncertainty resulted in overlapping 95% credible intervals between species for most traits (Fig 3, Fig 4, Fig S1), with two exceptions. First, the thermal response for lifespan (*lf*) for *Cx. tarsalis* was significantly less steep than the response for *Cx. pipiens* (Fig 3D; 95% CIs for slope coefficients: *Cx. tarsalis* = 1.12–2.24, *Cx. pipiens* = 3.83–5.84). Second, although the symmetry of the unimodal functional form was generally consistent for each trait across species, the thermal responses for the proportion ovipositing (*pO*) and egg viability (*EV*) were symmetrical for *Cx. pipiens* and asymmetrical for *Cx. quinquefasciatus* (Fig 4 A,C). The lifespan pattern (thermal response of *Cx. tarsalis* less steep than *Cx. pipiens*) did not match any *a priori* prediction, but the differences for *pO* and EV matched predictions based on the geographic ranges of the vectors: lower-latitude *Cx. quinquefasciatus* performed better at warmer temperatures for *pO* (Fig 3A), and higher-latitude *Cx. pipiens* performed better at cooler temperatures for *EV* (Fig 3C).

The thermal responses for pathogen development rate were similar among most vector–virus pairs (Fig 5), with a few notable exceptions for the median responses: WNV in *Cx. quinquefasciatus* had a warmer lower thermal limit (Fig 5A); WNV in *Cx. univittatus* had a cooler optimum and upper thermal limit (Fig 5A); and SINV in *Ae. taeniorhynchus* had limited data that indicated a very flat thermal response (Fig 5C). By contrast, the thermal response of vector competence varied substantially across vectors and viruses (Fig 6). For example, infection efficiency (*c*) of *Cx. pipiens* peaked at warmer temperatures for WNV than for SINV (Fig 6A,G; 95% CIs: SINV = 14.1–30.5ºC, WNV = 31.9–36.1ºC), transmission efficiency (*b*) of *Cx. tarsalis* peaked at warmer temperatures for WNV and SLEV than for WEEV (Fig 6B,E,H; CIs: WEEV = 19.2–23.2ºC, SLEV = 23.5–29.7ºC, WNV = 23.9–29.3ºC), and the lower thermal limit for vector competence (*bc*) for WNV was much warmer in *Cx. pipiens* than in *Cx. univittatus* (Fig 6C; CIs: *Cx. univittatus* = 1.5–7.1ºC, *Cx. pipiens* = 15.0–17.9ºC). Infection traits for RVFV were only available in *Aedes taeniorhynchus*, a New World species that is not a natural vector for the virus.

Temperature-dependent R_0 models

Relative R_0 responded unimodally to temperature for all the vector–virus pairs, peaking at temperatures (medians: 22.7–26.0ºC, see Table 2 for CIs; Fig 7) that were cooler than or similar to previous results for tropical diseases (medians: 25.4–29.1ºC) [2–4,6,7]. Many models also had lower thermal limits (medians: 8.7–19.0ºC, see Table 2 for CIs; Fig 7) that were cooler than those for the tropical diseases (medians: 16.0–17.8ºC). By contrast, the upper thermal limits were very similar (medians: 31.9–37.8ºC, see Table 2 for CIs; Fig 7) to past models of tropical diseases (medians: 31.4–34.5ºC). Together, these patterns led to wider thermal breadths (18.2–27.7ºC, see Table 2 for CIs; Fig 7) for most of the temperate viruses (all except WNV in *Cx.*

quinquefasciatus: 12.7ºC) compared to the tropical pathogens (11.7– 16.7ºC). Among the temperate vector–virus pairs, the lower thermal limits were more variable than the optima, although confidence intervals overlapped in most cases because thermal limits also had higher uncertainty (Fig 7), as in previous studies [3,4,6,7]. Regardless, the *Ae. taeniorhynchus* models were clear outliers, with much warmer distributions for their upper thermal limits, and optima that trended warmer as well.

Differences in relative R_0 stemmed from variation both in vector traits (e.g., in Fig 7A, with WNV in different vector species) and in virus infection traits (e.g., in Fig 7B, with different viruses in *Cx. tarsalis*). The upper thermal limit was warmer for WNV transmitted by *Cx. pipiens* (34.9ºC [CI: 32.9–37.5ºC] than by *Cx. quinquefasciatus* (31.8ºC [CI: 31.1–32.2ºC]), counter to the prediction based on vector geographic ranges. This result implies that warming from climate change may differentially impact transmission by these two vectors. Additionally, the lower thermal limit for WNV varied widely (but with slightly overlapping 95% CIs) across different vector species (Fig 7D), from 19.0ºC (14.2–21.0ºC) in *Cx. quinquefasciatus* to 16.8ºC (14.9–17.8ºC) in *Cx. pipiens* to 12.2ºC (9.7–15.3ºC) in *Cx. tarsalis* to 11.1ºC (8.1–15.4ºC) in *Cx. univittatus* (an African and Eurasian vector; Table 2). Based on these trends in the thermal limits of R_0, the seasonality of transmission and the upper latitudinal and elevational limits could vary for WNV transmitted by these different species.

Different traits determined the lower and upper thermal limits and optimum for transmission across vector–virus pairs. The lower thermal limit for transmission was most often determined by parasite development rate (*PDR*; WNV and SLEV in *Cx. tarsalis*, WNV in *Cx. quinquefasciatus*) or biting rate (*a*; WNV in *Cx. univitattus*, WEEV in *Cx. tarsalis*, EEEV in *Ae. triseriatus,* RVFV and SINV in *Ae. taeniorhynchus*, SINV in *Cx. pipiens*; Figs S11–19), which

tend to have asymmetric thermal responses with high optima. However, vector competence (*bc*) determined the lower limit for WNV in *Cx. pipiens* (Fig S10). The upper thermal limit was determined by biting rate (*a*) for the three *Cx. tarsalis* models and by adult lifespan (*lf*) for all others, although proportion ovipositing (*pO*) was also important for WNV in *Cx. quinquefasciatus* (Figs S10-S19). In all models, lifespan (*lf*) and biting rate (*a*) had the strongest impact on the optimal temperature for transmission, with biting rate increasing transmission at low temperatures and lifespan decreasing transmission at high temperatures (Figs S10-S19). This result is consistent with previous mechanistic models of tropical mosquito-borne diseases, despite the qualitative difference in the shape of the lifespan thermal response between those tropical mosquitoes and the more temperate mosquitoes investigated here [2–4,6,7].

Model validation with human case data

Incidence of human neuro-invasive West Nile disease in US counties (averaged from 2001-2016) responded unimodally to average summer temperature and peaked at 23.9ºC (Fig 8), closely matching the optima from the mechanistic models for the three North American *Culex* species (23.9–25. 2ºC; Table 2). The data provided little evidence for lower or upper thermal limits at this scale; instead, mean incidence remained flat but positive below ~20ºC and above ~28ºC, although sample size was very low above 28ºC. The month-of-onset for cases of WNV was consistent with predicted transmission, $R_0(T)$ (Fig 9). As expected *a priori* (based on the time required for mosquito populations to increase, become infectious, and bite humans, and for humans to present symptoms and seek medical care [4,6]), there was a two-month lag between initial increases in $R_0(T)$ and incidence: cases began rising in June to the peak in August. The dramatic decline in transmission between September and October corresponds also closely to the

predicted decline in relative R_0. In general, the seasonal patterns of SLEV and EEEV incidence were similar to WNV, but differed by three orders of magnitude from ~20,000 cases of WNV to ~40-50 cases of EEEV and SLEV during the peak month (Fig. 9). However, transmission of SLEV and EEEV are predicted to begin increasing one month earlier than WNV (March versus April, Fig 9), because the mechanistic models predict that the lower thermal limits for SLEV and EEEV are cooler than those for WNV in two of the three North American vectors (*Cx. pipiens* and *Cx. quinquefasciatus*, Fig 7). The month-of-onset data partially support this prediction, as cases of SLEV (but not EEEV) disease begin to increase earlier in the year than WNV, relative to the summer peak.

DISCUSSION

As climate changes, it is critical to understand how changes in temperature will affect the spread of mosquito-borne diseases. Toward this goal, we developed temperature-dependent, mechanistic transmission models for 10 vector–virus pairs. The viruses—West Nile virus (WNV), St. Louis Encephalitis virus (SLEV), Eastern and Western Equine Encephalitis viruses (EEEV and WEEV), Sindbis virus (SINV), and Rift Valley fever virus (RVFV)—occur primarily in temperate areas (except RVFV), and are transmitted by shared vector species, including *Cx. pipiens*, *Cx. quinquefasciatus*, and *Cx. tarsalis* (Fig 1). Transmission of these temperate diseases differed from that of primarily tropical diseases [2–4,6,7]: several had significantly cooler thermal optima or lower thermal limits (Fig 7, Table 2). These results were partially due to the thermal responses of lifespan, which decreased linearly with temperature over the entire temperature range (of available data, > 14ºC) for these temperate *Culex* vectors (Fig 3), whereas lifespan for more tropical *Anopheles*, *Aedes*, and *Culex* spp. responded unimodally with

intermediate optimal temperatures [2–4,6,7]. The thermal limits and optima for transmission also varied among some of the temperate mosquito and virus species (Fig 7, Table 2), largely due to differences in the thermal responses of mosquito biting rate, lifespan, vector competence, and parasite development rate. Human case data for WNV disease across the US exhibited a strong unimodal thermal response (Fig 8), and month-of-onset data for three viruses was consistent with the predicted seasonality of transmission (Fig 9). Thus, the mechanistic models captured geographical and seasonal patterns of human incidence, despite the complexity of the enzootic cycles and spillover into humans. Our key results—maximal transmission at intermediate temperatures—underscore the importance of considering unimodal thermal responses when predicting how climate change will impact mosquito-borne disease transmission.

The monotonically decreasing thermal responses for lifespan in these temperate mosquitoes (Fig 3D) contrast with unimodal responses of tropical species [2,4,6], and may reflect differing thermal physiology between species that use diapause or quiescence, two forms of dormancy, to persist over winter and those that do not (see *Model Overview*) [44–46]. *Ae. albopictus*, a species that occurs in both tropical and temperate zones, exhibits a latitudinal gradient in the United States in which more temperate populations diapause while sub-tropical populations do not [47]. Experiments could test whether the functional form of the thermal response for lifespan differs between the two groups of populations, to test this hypothesis. Despite the fundamental difference in the shape of the thermal response, lifespan plays a similarly important role in temperate and tropical systems, strongly limiting transmission at high temperatures (Figs S10–19). Nonetheless, the linear thermal responses for lifespan ultimately promoted higher transmission at relatively cool temperatures because unlike in primarily tropical species, lifespan did not decline at cool temperatures within the range measured (> 14ºC). At

more extreme temperatures expected to be fatal even for diapausing mosquitoes (i.e., well below 0ºC), we expect lifespan to decline even for these temperate mosquitoes, so that the response over broader temperature ranges is unimodal.

Accordingly, predicted transmission for several of the temperate diseases peaked and extended to cooler temperatures than for the primarily tropical diseases (Fig 7, Table 2). Here, the optimal temperatures for transmission varied from 22.7–25.2ºC (excluding *Ae. taeniorhynchus* models, Fig 7). By contrast, models predict that transmission peaks at 25.4ºC for malaria [2,3], 26.4ºC for Ross River virus [6] and dengue in *Ae. albopictus* [4], 28.9ºC for Zika in *Ae. aegypti* [4], and 29.1ºC for dengue in *Ae. aegypti* [4,7] (Table 2). Additionally, SINV—the virus most geographically restricted to high latitudes (northern Europe and southern Africa) [24]—had the second coolest lower thermal limits (Fig 7, Table 2). Further, lower-latitude *Cx. quinquefasciatus* outperformed higher-latitude *Cx. pipiens* at warmer temperatures for proportion ovipositing (*pO*; Fig 3A), while the reverse happened at cooler temperatures for egg viability (*EV*; Fig 3C). The temperate vector–virus pairs also had substantially wider thermal breadths (18.2–27.7ºC) than the tropical mosquito-borne diseases (11.7–16.7ºC), except for WNV in *Cx. quinquefasciatus* (12.7ºC), which is the vector most restricted to lower latitude, sub-tropical geographic areas (Fig 2). These results match a previous finding that temperate insects had wider thermal breadths than tropical insects [48], and likely reflect thermal adaptation to greater variation in temperature in temperate areas compared to tropical areas [49]. Collectively, these results imply that, to some extent, measurements of physiological traits can predict geographic patterns of transmission at broad scales. However, geographic range differences (Fig 2) did not consistently predict variation in thermal responses among the *Culex* species in this study (e.g., biting rate [*a*, Fig 3C] and adult lifespan [*lf*, Fig 3D]), indicating limits to the extent to which life

history and transmission trait responses at constant temperatures predict the geographic distributions of species. For example, the ability to tolerate temperature extremes may limit species distributions more than their performance at average or constant temperatures [50].

In contrast to the optima, lower thermal limits, and thermal breadths, the upper thermal limits for the temperate vector–virus pairs in this study (31.9–34.9ºC, excluding *Ae. taeniorhynchus* models; Fig 7D, Table 2) closely matched those of tropical diseases (31.5–34.7ºC) [2–4,6,7]. This similarity likely arises because maximum summer temperatures in temperate areas can match or even exceed maximum temperatures in tropical areas [49]. Accordingly, there may be a fundamental upper thermal constraint on transmission (in the absence of thermal adaptation) that applies similarly to all mosquitoes-borne diseases, driven by short mosquito lifespans at high temperatures. (The relatively high upper thermal limits in both *Ae. taeniorynchus* transmission models were driven by the thermal response of lifespan, which was fit to few data points; more data are needed to determine if it reflects the true thermal response in that species [Fig S1]).

Independent human case data support unimodal thermal responses for transmission and the importance of temperature in shaping seasonal and geographic patterns of these mosquito-borne diseases. Human cases of WNV [51–57] and SINV [58,59] are often positively associated with temperature. Here, we found incidence of neuro-invasive WNV disease responded unimodally to temperature across counties in the US (Fig 8), adding to prior evidence for reduced transmission of WNV [60] and other mosquito-borne diseases [2,15–17] at high temperatures. However, we could not detect lower or upper thermal limits at this scale (Fig 8). We hypothesize that temperature variation over time and across microclimates may sustain transmission in regions with low or high mean summer temperatures by providing time windows

suitable for transmission [35,36,38]. The temperature-dependent models also predict the seasonality of human cases of WNV, EEEV, and SLEV (Fig 9). The 2-month lag between climate suitability and the onset of human cases, which matches previous results from other mosquito-borne diseases [4,6], arises from the time following the onset of suitable conditions required for mosquito populations to increase [61], become infectious, and bite humans, and for humans to present symptoms and seek medical care [62,63]. Transmission of the temperate viruses here may incur additional lags because human cases only result from enzootic transmission and multiple rounds of amplification within reservoir hosts may be required before prevalence is sufficiently high to spill over into humans. Additionally, as wild birds disperse in late summer, both *Cx. pipiens* and *Cx. tarsalis* shift their feeding preferences from birds to humans, increasing transmission to people and influencing the seasonal dynamics of WNV [64]. Drought, precipitation, and reservoir immunity also strongly drive transmission of WNV [5,54,55,57] and may interact with temperature. SLEV, EEEV, and WEEV are less common in nature, and thus less well-studied, but the lower thermal limits in our study support previous findings that transmission WEEV is favored over SLEV in cooler conditions [65]. Additionally, the seasonal patterns of incidence data (Fig 9) provide some support for the model prediction that SLEV transmission is possible at cooler temperatures than WNV by North American vectors (Table 2). By contrast, mean temperature is not associated with outbreaks of RVFV, although they are highly predictable based on precipitation driven by El Niño–Southern Oscillation cycles [66,67]. Thus, disease dynamics depend on the interaction between temperature and other environmental factors, and the relative importance of temperature versus other drivers varies across systems.

Most prior studies with mechanistic models for temperature-dependent transmission of WNV do not capture the unimodal thermal response that our mechanistic models predict and that we observe in the human case data (Table 3). Two previous models predicted that transmission of WNV would increase up to the warmest temperatures they considered, 28ºC [68] and 35ºC [69]. In both cases, the daily survival rates estimated from lab experiments were far less sensitive to temperature than our measure of adult lifespan, and neither model was validated with field data. A third study with models for *Cx. pipiens*, *Cx. quiquefasciatus*, and *Cx. tarsalis*, like our study, predicted unimodal thermal responses for transmission, with very similar optima but with lower thermal limits that were ~5ºC warmer, resulting in much narrower thermal breadths (Fig S22) [5]. This model [5] was validated with annual, state-level WNV human case data (in contrast to our county-level data averaged over time), and detected a positive effect of temperature, with no decline at high temperatures [5]. These differences in modeling and validation approaches can lead to strongly divergent predictions for the impact of climate change.

Given the unimodal relationship between temperature and transmission of these temperate mosquito-borne pathogens, we expect climate warming to lead to predictable shifts in disease transmission [18,20,21]. Warming should extend the transmission season earlier into the spring and later into the fall and increase transmission potential in higher latitudes and altitudes, although this prediction may be impacted by changes in bird migrations. However, the thermal optima for these temperate vector–virus pairs are relatively cool, so in many locations, warming could result in summer temperatures that exceed the thermal optima for transmission more frequently, reducing overall transmission or creating a bimodal transmission season [70]. Still, warming is unlikely to eliminate any of these temperate pathogens since the upper thermal limits

for transmission are well above temperatures pathogens regularly experience in their current geographic ranges. More generally, our results raise concerns about the common practice of extrapolating monotonic relationships between temperature and disease incidence fit from observational data into warmer climate regimes to predict future cases [54,56].

While the data-driven models presented here represent the most comprehensive synthesis to date of trait thermal response data and their impact on transmission for these temperate mosquitoes and pathogens, additional temperature-dependent trait data would increase the accuracy and decrease the uncertainty in these models where data were sparse or missing. We recommend prioritizing parasite development rate (*PDR*) and vector competence (*bc*) data (both estimated from the same experiments) and biting rate (*a*) data, because those thermal responses varied widely among vector–virus pairs and determined the lower thermal limits and optima for transmission in many models. Additionally, vector competence and/or parasite development rate data were missing (WNV in *Cx. quinquefasciatus*, EEEV in *Cs. melanura*, RVFV in vectors from endemic areas, transmission efficiency [*b*] for SINV) or sparse (EEEV and WNV in *Cx. univittatus*) in many cases, as were biting rate data (*Cx. univittatus*, RVFV vectors). Lifespan data—key for determining transmission optima and upper thermal limits—were the missing for *Ae. triseriatus*, *Cs. melanura*, *Cx. univittatus*, and RVFV vectors, and at temperatures below 14 ºC for all vector species, so it was unclear which functional form these thermal responses should take (linear or quadratic). While the other mosquito demographic traits did not determine thermal limits for transmission in models here, fecundity (typically as *EFD*), larval-to-adult survival (*pLA*), and egg viability (*EV*) determined thermal limits for malaria [2] and Ross River virus [6]. Thus, we recommend collecting more fecundity data (missing for *Cx. tarsalis*, *Cx. univittatus*, and *Ae. triseriatus*; sparse for *Cx. pipiens* and *Cx. quinquefasciatus*) as well. New data are

particularly important for RVFV, which has a tropical distribution but for which the model depends on traits measured in *Cx. pipiens* collected from temperate regions and infection traits measured in *Ae. taeniorhynchus*, a North American species. RVFV is spread by a diverse community of vectors across the African continent, but we suggest prioritizing hypothesized primary vectors (e.g., *Ae. circumluteolus* or *Ae. mcintoshi*) or secondary vectors that already have partial trait data (e.g., *Ae. vexans* or *Cx. theileri*) [25,71]. Although temperature itself does not predict the occurrence of RVFV outbreaks, it may affect the size of epidemics once they are triggered by precipitation. Additionally, the thermal response of vector competence may vary across vector populations and/or virus isolates even within the same species, so more data may also improve the accuracy of models without missing data.

As carbon emissions continue to increase and severe climate change becomes increasingly inevitable [72], it is critical that we understand how temperature will shape transmission of mosquito-borne diseases in a warmer future world. While data gaps are still limiting, the comparative approach is powerful for predicting similarities and differences across vectors and viruses, including systematic differences between primarily tropical and temperate diseases. Future trajectories of these diseases will depend not just on climate suitability but on land use, which governs mosquito–wildlife–human interactions, vector control activities, human and wildlife immune dynamics, thermal adaptation of vectors and viruses, and potential future emergence and spread of new vectors and viruses.

MATERIALS AND METHODS

All analyses were conducted using R 3.1.3 [73].

Vector species range maps

The distributions of *Cx. pipiens* and *Cx. quinquefasciatus* are georectified maps adapted from [32,74]. The northern boundary of *Cx. tarsalis* was taken from [75]. For the southern boundary, we drew a convex polygon using five datasets [76–80] in the Global Biodiversity Information Facility (https://www.gbif.org/).

Temperature-dependent R_0 models

We found 39 studies with appropriate temperature-dependent trait data [5,51,81–117]. When necessary, we digitized the data using Web Plot Digitizer [118], a free online tool. When lifespan data were reported by sex, only female data were used. Vector competence trait data (*b*, *c*, or *bc*) were only included if time at sampling surpassed the estimated extrinsic incubation period (*EIP*, the inverse of *PDR*) at that temperature, which resulted in the exclusion of some studies [119,120].

We fit trait thermal responses using Bayesian inference with the 'r2jags' package [121,122]. In the likelihood functions, we truncated all thermal response functions at zero when $T < T_{min}$ and $T > T_{max}$ (for eq. 3 and 4) or when $T > -z/m$ (eq. 5) to prevent trait values from becoming negative (i.e., set trait value to 0). For traits with ambiguous functional responses, we fit the quadratic and Briere and used the deviance information criterion (DIC) [123] to pick the best fit. For traits that were proportions or probabilities, we truncated the predicated values at 1. For the linear thermal responses, we also calculated the predicted trait values in a piecewise manner in order to be conservative: for temperatures at or above the coldest observed data point, we used the trait values predicted by the fitted thermal response (i.e., the typical method); for temperatures below the coldest observed data point, we substituted the trait estimate at the

coldest observed data point (i.e., forcing the thermal response to plateau, rather than continue increasing beyond the range of observed data). For data-informed priors, we used gamma distributions with parameters estimated from thermal responses fit using a 'leave-one-out' approach. In other words, we fit a thermal response using all the data for a given trait except for the focal vector or vector–virus pair (e.g., for the prior for biting rate for *Cx. pipiens*, we used the biting rate data for all species except *Cx. pipiens*). The pool of data used to fit priors also included data from other temperate *Ae.* and *Cx.* species [83,85,94,98,103,104,124–129].

When data were missing for a vector–virus pair, we substituted the most conservative (i.e., least restrictive of transmission) trait thermal response from a vector species that occurs within the geographic range of disease transmission (Table 2). When there were was more than one option for how to parameterize a model (e.g., vector competence data for WEEV in *Cx. tarsalis* were available in two forms: separately as *b* and *c,* and combined as *bc*), we calculated R_0 both ways. The results were very similar, except for the model for RVFV with lifespan data from *Cx. pipiens* lifespan in place of *Ae. taeniorhynchus* (Fig S21). See Supplement for sensitivity and uncertainty methods and results (Fig S10-19).

Model validation: spatial analysis

We obtained county-level (n = 3,109) neuro-invasive WNV disease data from 2001-2016 for the contiguous US through the CDC's county-level disease monitoring program [130]. Data were available as total human cases per year, which we adjusted to average cases per 1,000 people (using 2010 US county-level census data) to account for population differences. We averaged cases across years beginning with the first year that had reported cases in a given county to account for the initial spread of WNV and the strong impact of immunity on

interannual variation [5]. Ninety-eight percent of human cases of WNV in the US occur between June and October (data described below), and cases of mosquito-borne disease often lag behind temperature by 1–2 months [6,61]. Thus, we extracted monthly mean temperature data between the months of May–September for all years between 2001-2016 and averaged the data to estimate typical summer conditions for each county. Specifically, we took the centroid geographic coordinate for every county in the contiguous US with the 'rgeos' package [131] and extracted corresponding historic climate data (Climate Research Unit 3.1 rasters) [132] from $0.5°^2$ cells (approx. 2,500-3,000 km^2) using the 'raster' package [133]. We used the 'loess' function in base R 'stats' package [73] to fit a locally estimated scatterplot smoothing (LOESS) regression for average incidence as a function of average summer temperature to county-level data with span (smoothing parameter) = 0.6. See Fig S23 for the model fit across varying span values.

Model validation: seasonality analysis

We calculated monthly temperature-dependent relative R_0 to compare with month-of-onset data for neuro-invasive WNV, EEEV, and SLEV disease aggregated nationwide from 2001-2016 [130,134,135], using the same monthly, county-level temperature data as above. For WNV, we used the subset of counties with reported cases (68% of counties). For SLEV and EEEV we used all counties from states with reported cases (16 and 20 states, respectively). We weighted each county $R_0(T)$ by its population size to calculate a national estimate of $R_0(T)$. For WNV, the county-level estimates of $R_0(T)$ used models for three *Culex* species (*Cx. pipiens*, *Cx. quinquefasciatus*, and *Cx. tarsalis*) weighted according to the proportion of WNV+ mosquitoes reported at the state level, reported in [5]. SLEV and EEEV both only had one R_0 model. The

estimated monthly temperature-dependent relative R_0 values and month-of-onset data were compared visually.

Funding

EAM, MSS, JC, LRJ, and MN were supported by the National Science Foundation (NSF, DEB-1518681; https://nsf.gov/). LRJ was supported by the NSF (DMS- 1750113). AV and MN were supported by the Stanford Vice Provost for Undergraduate Education Summer Research Program in the Biology Department; MN was supported by the Introductory Seminars Program at Stanford University. HS was supported by a Luther and Alice Hamlett Undergraduate Research Scholarship at Virginia Tech. EAM was also supported by the Stanford Woods Institute for the Environment (https://woods.stanford.edu/research/environmental-venture-projects), the Hellman Fellowship (http://www.hellmanfellows.org/), and the Terman Fellowship.

Acknowledgements

We gratefully acknowledge the students of the Spring 2017 Stanford University Introductory Seminar course BIO 2N: Global Change and the Ecology and Evolution of Infectious Diseases, who helped with preliminary literature searches, data collection, and model fitting: Uche Amakiri, Michelle Bach, Isabelle Carpenter, Phillip Cathers, Audriana Fitzmorris, Alex Fuentes, Margaux Giles, Gillian Gittler, Emma Leads Armstrong, Erika Malaspina, Elise Most, Stephen Moye, Jackson Rudolph, Simone Speizer, William Wang, and Ethan Wentworth. We thank the Stanford University Introductory Seminars program for support. We thank Michelle Evans for creating Figure 2. We thank Lyle Peterson, Marc Fischer, and Nicole

Lindsey at the CDC for providing the month-of-onset case data, and Sara Paull for providing state-level data for proportion of WNV vectors. We thank Nicholas Skaff for guidance with EEEV vector ecology.

REFERENCES

1. Rogers DJ, Randolph SE. Climate Change and Vector-Borne Diseases. Advances in Parasitology. 2006;62: 345–381. doi:10.1016/S0065-308X(05)62010-6

2. Mordecai EA, Paaijmans KP, Johnson LR, Balzer C, Ben-Horin T, de Moor E, et al. Optimal temperature for malaria transmission is dramatically lower than previously predicted. Ecology letters. 2013;16: 22–30. doi:10.1111/ele.12015

3. Johnson LR, Ben-Horin T, Lafferty KD, McNally A, Mordecai E, Paaijmans KP, et al. Understanding uncertainty in temperature effects on vector-borne disease: A Bayesian approach. Ecology. 2015;96: 203–213. doi:10.1890/13-1964.1

4. Mordecai EA, Cohen JM, Evans MV, Gudapati P, Johnson LR, Lippi CA, et al. Detecting the impact of temperature on transmission of Zika, dengue, and chikungunya using mechanistic models. PLOS Neglected Tropical Diseases. 2017;11: e0005568. doi:10.1371/journal.pntd.0005568

5. Paull SH, Horton DE, Ashfaq M, Rastogi D, Kramer LD, Diffenbaugh NS, et al. Drought and immunity determine the intensity of West Nile virus epidemics and climate change impacts. Proceedings of the Royal Society B: Biological Sciences. 2017;284: 20162078. doi:10.1098/rspb.2016.2078

6. Shocket MS, Ryan SJ, Mordecai EA. Temperature explains broad patterns of Ross River virus transmission. eLife. 2018;7. doi:10.7554/eLife.37762

7. Tesla B, Demakovsky LR, Mordecai EA, Ryan SJ, Bonds MH, Ngonghala CN, et al. Temperature drives Zika virus transmission: evidence from empirical and mathematical models. Proceedings of the Royal Society B: Biological Sciences. 2018;285: 20180795. doi:10.1098/rspb.2018.0795

8. Martens WJM, Jetten TH, Focks DA. Sensitivity of malaria, schistosomiasis and dengue to global warming. Climatic Change. 1997;35: 145–156. doi:10.1023/A:1005365413932

9. Parham PE, Michael E. Modeling the effects of weather and climate change on malaria transmission. Environmental Health Perspectives. 2010;118: 620–626. doi:10.1289/ehp.0901256

10. Liu-Helmersson J, Stenlund H, Wilder-Smith A, Rocklöv J. Vectorial capacity of *Aedes aegypti*: Effects of temperature and implications for global dengue epidemic potential. PLoS ONE. 2014;9. doi:10.1371/journal.pone.0089783

11. Wesolowski A, Qureshi T, Boni MF, Sundsøy PR, Johansson MA, Rasheed SB, et al. Impact of human mobility on the emergence of dengue epidemics in Pakistan. Proceedings of the National Academy of Sciences. 2015;112: 11887–11892. doi:10.1073/pnas.1504964112

12. Siraj AS, Bouma MJ, Santos-Vega M, Yeshiwondim AK, Rothman DS, Yadeta D, et al. Temperature and population density determine reservoir regions of seasonal persistence in highland malaria. Proceedings of the Royal Society B: Biological Sciences. 2015;282: 20151383. doi:10.1098/rspb.2015.1383

13. Werner AK, Goater S, Carver S, Robertson G, Allen GR, Weinstein P. Environmental drivers of Ross River virus in southeastern Tasmania, Australia: towards strengthening public health interventions. Epidemiology and Infection. 2012;140: 359–371. doi:10.1017/S0950268811000446

14. Lowe R, Stewart-Ibarra AM. Climate and Non-Climate Drivers of Dengue Epidemics in Southern Coastal Ecuador. The American Journal of Tropical Medicine and Hygiene. 2013;88: 971–981. doi:10.4269/ajtmh.12-0478

15. Peña-García VH, Triana-Chávez O, Arboleda-Sánchez S. Estimating Effects of Temperature on Dengue Transmission in Colombian Cities. Annals of Global Health. 2017;83: 509. doi:10.1016/j.aogh.2017.10.011

16. Perkins TA, Metcalf CJE, Grenfell BT, Tatem AJ. Estimating Drivers of Autochthonous Transmission of Chikungunya Virus in its Invasion of the Americas. PLoS Currents. 2015; doi:10.1371/currents.outbreaks.a4c7b6ac10e0420b1788c9767946d1fc

17. Gatton ML, Kay BH, Ryan PA. Environmental predictors of Ross River virus disease outbreaks in Queensland, Australia. Am J Trop Med Hyg. 2005;72: 792–799. doi:72/6/792 [pii]

18. Lafferty KD. The ecology of climate change and infectious diseases. Ecology. 2009;90: 888–900. doi:10.1890/09-1656.1

19. Rohr JR, Dobson AP, Johnson PTJ, Kilpatrick AM, Paull SH, Raffel TR, et al. Frontiers in climate change-disease research. Trends in Ecology & Evolution. 2011;26: 270–277. doi:10.1016/j.tree.2011.03.002

20. Lafferty KD, Mordecai EA. The rise and fall of infectious disease in a warmer world. F1000Research. 2016;5: 2040. doi:10.12688/f1000research.8766.1

21. Ryan SJ, McNally A, Johnson LR, Mordecai EA, Ben-Horin T, Paaijmans KP, et al. Mapping physiological suitability limits for malaria in Africa under climate change. Vector borne and zoonotic diseases. 2015;15: 718–25. doi:10.1089/vbz.2015.1822

22. Kilpatrick AM. Globalization, Land Use, and the Invasion of West Nile Virus. Science. 2011;334: 323–327. doi:10.1126/science.1201010

23. Weaver SC, Barrett ADT. Transmission cycles, host range, evolution and emergence of arboviral disease. Nature Reviews Microbiology. 2004;2: 789–801. doi:10.1038/nrmicro1006

24. Adouchief S, Smura T, Sane J, Vapalahti O, Kurkela S. Sindbis virus as a human pathogen-epidemiology, clinical picture and pathogenesis: Sindbis virus as a human pathogen. Reviews in Medical Virology. 2016;26: 221–241. doi:10.1002/rmv.1876

25. Linthicum KJ, Britch SC, Anyamba A. Rift Valley Fever: An Emerging Mosquito-Borne Disease. Annual Review of Entomology. 2016;61: 395–415. doi:10.1146/annurev-ento-010715-023819

26. Centers for Disease Control and Prevention. St. Louis Encephalitis: Statistics and Maps. [Internet]. 2018 Dec. Available: https://www.cdc.gov/sle/technical/epi.html

27. Centers for Disease Control and Prevention. Eastern Equine Encephalitis: Epidemiology & Geographic Distribution [Internet]. 2018 Sep. Available: https://www.cdc.gov/easternequineencephalitis/tech/epi.html

28. Go YY, Balasuriya UBR, Lee C. Zoonotic encephalitides caused by arboviruses: transmission and epidemiology of alphaviruses and flaviviruses. Clinical and Experimental Vaccine Research. 2014;3: 58. doi:10.7774/cevr.2014.3.1.58

29. Sang R, Arum S, Chepkorir E, Mosomtai G, Tigoi C, Sigei F, et al. Distribution and abundance of key vectors of Rift Valley fever and other arboviruses in two ecologically distinct counties in Kenya. Bird B, editor. PLOS Neglected Tropical Diseases. 2017;11: e0005341. doi:10.1371/journal.pntd.0005341

30. Harley D, Sleigh A, Ritchie S. Ross River Virus Transmission, Infection, and Disease: a Cross-Disciplinary Review. Clinical Microbiology Reviews. 2001;14: 909–932. doi:10.1128/CMR.14.4.909

31. Gonçalves BP, Kapulu MC, Sawa P, Guelbéogo WM, Tiono AB, Grignard L, et al. Examining the human infectious reservoir for Plasmodium falciparum malaria in areas of differing transmission intensity. Nature Communications. 2017;8. doi:10.1038/s41467-017-01270-4

32. Farajollahi A, Fonseca DM, Kramer LD, Marm Kilpatrick A. “Bird biting” mosquitoes and human disease: A review of the role of Culex pipiens complex mosquitoes in epidemiology. Infection, Genetics and Evolution. 2011;11: 1577–1585. doi:10.1016/j.meegid.2011.08.013

33. Diekmann O, Heesterbeek JAP, Roberts MG. The construction of next-generation matrices for compartmental epidemic models. Journal of the Royal Society Interface. 2010;7: 873–885. doi:10.1098/rsif.2009.0386

34. Dietz K. The estimation of the basic reproduction number for infectious diseases. Statistical Methods in Medical Research. 1993;2: 23–41. doi:10.1177/096228029300200103

35. Paaijmans KP, Blanford S, Bell AS, Blanford JI, Read AF, Thomas MB. Influence of climate on malaria transmission depends on daily temperature variation. Proceedings of the National Academy of Sciences of the United States of America. 2010;107: 15135–9. doi:10.1073/pnas.1006422107

36. Murdock C, Evans M, McClanahan T, Miazgowicz K, Tesla B. Fine-scale variation in microclimate across and urban landscape changes the capacity of Aedes albopictus to vector arboviruses. PLoS Neglected Tropical Diseases. 2017;11: e0005640. doi:10.5061/dryad.s3953

37. Huber JH, Childs ML, Caldwell JM, Mordecai EA. Seasonal temperature variation influences climate suitability for dengue, chikungunya, and Zika transmission. Althouse B, editor. PLOS Neglected Tropical Diseases. 2018;12: e0006451. doi:10.1371/journal.pntd.0006451

38. Lambrechts L, Paaijmans KP, Fansiri T, Carrington LB, Kramer LD, Thomas MB, et al. Impact of daily temperature fluctuations on dengue virus transmission by Aedes aegypti. Proceedings of the National Academy of Sciences. 2011;108: 7460–7465. doi:10.1073/pnas.1101377108

39. Bacaër N. Approximation of the Basic Reproduction Number R 0 for Vector-Borne Diseases with a Periodic Vector Population. Bulletin of Mathematical Biology. 2007;69: 1067–1091. doi:10.1007/s11538-006-9166-9

40. Bacaër N, Ait Dads EH. On the biological interpretation of a definition for the parameter R 0 in periodic population models. Journal of Mathematical Biology. 2012;65: 601–621. doi:10.1007/s00285-011-0479-4

41. Bacaër N, Guernaoui S. The epidemic threshold of vector-borne diseases with seasonality: The case of cutaneous leishmaniasis in Chichaoua, Morocco. Journal of Mathematical Biology. 2006;53: 421–436. doi:10.1007/s00285-006-0015-0

42. Briere J-F, Pracros P, Le Roux A-Y, Pierre J-S. A Novel Rate Model of Temperature-Dependent Development for Arthropods. Environmental Entomology. 1999;28: 22–29. doi:10.1093/ee/28.1.22

43. Amarasekare P, Savage V. A Framework for Elucidating the Temperature Dependence of Fitness. The American Naturalist. 2012;179: 178–191. doi:10.1086/663677

44. Vinogradova EB. Culex pipiens pipiens mosquitoes taxonomy, distribution, ecology, physiology, genetics, applied importance and control. Sofia: Pensoft; 2000.

45. Nelms BM, Macedo PA, Kothera L, Savage HM, Reisen WK. Overwintering biology of Culex (Diptera: Culicidae) mosquitoes in the Sacramento Valley of California. J Med Entomol. 2013;50: 773–790.

46. Diniz DFA, de Albuquerque CMR, Oliva LO, de Melo-Santos MAV, Ayres CFJ. Diapause and quiescence: dormancy mechanisms that contribute to the geographical expansion of mosquitoes and their evolutionary success. Parasites & Vectors. 2017;10. doi:10.1186/s13071-017-2235-0

47. Urbanski JM, Benoit JB, Michaud MR, Denlinger DL, Armbruster P. The molecular physiology of increased egg desiccation resistance during diapause in the invasive mosquito,

Aedes albopictus. Proceedings of the Royal Society B: Biological Sciences. 2010;277: 2683–2692. doi:10.1098/rspb.2010.0362

48. Deutsch CA, Tewksbury JJ, Huey RB, Sheldon KS, Ghalambor CK, Haak DC, et al. Impacts of climate warming on terrestrial ectotherms across latitude. Proceedings of the National Academy of Sciences. 2008;105: 6668–6672. doi:10.1073/pnas.0709472105

49. Sunday JM, Bates AE, Dulvy NK. Global analysis of thermal tolerance and latitude in ectotherms. Proceedings of the Royal Society B: Biological Sciences. 2011;278: 1823–1830. doi:10.1098/rspb.2010.1295

50. Overgaard J, Kearney MR, Hoffmann AA. Sensitivity to thermal extremes in Australian *Drosophila* implies similar impacts of climate change on the distribution of widespread and tropical species. Global Change Biology. 2014;20: 1738–1750. doi:10.1111/gcb.12521

51. Reisen WK, Fang Y, Martinez VM. Effects of Temperature on the Transmission of West Nile Virus by *Culex tarsalis* (Diptera: Culicidae). Journal of Medical Entomology. 2006;43: 309–317. doi:10.1603/0022-2585(2006)043[0309:EOTOTT]2.0.CO;2

52. Platonov AE, Fedorova MV, Karan LS, Shopenskaya TA, Platonova OV, Zhuravlev VI. Epidemiology of West Nile infection in Volgograd, Russia, in relation to climate change and mosquito (Diptera: Culicidae) bionomics. Parasitology Research. 2008;103: 45–53. doi:10.1007/s00436-008-1050-0

53. Hahn MB, Monaghan AJ, Hayden MH, Eisen RJ, Delorey MJ, Lindsey NP, et al. Meteorological Conditions Associated with Increased Incidence of West Nile Virus Disease in the United States, 2004–2012. The American Journal of Tropical Medicine and Hygiene. 2015;92: 1013–1022. doi:10.4269/ajtmh.14-0737

54. Marcantonio M, Rizzoli A, Metz M, Rosà R, Marini G, Chadwick E, et al. Identifying the Environmental Conditions Favouring West Nile Virus Outbreaks in Europe. Gourbiere S, editor. PLOS ONE. 2015;10: e0121158. doi:10.1371/journal.pone.0121158

55. Ahmadnejad F, Otarod V, Fathnia A, Ahmadabadi A, Fallah MH, Zavareh A, et al. Impact of Climate and Environmental Factors on West Nile Virus Circulation in Iran. J Arthropod Borne Dis. 2016;10: 315–327.

56. Semenza JC, Tran A, Espinosa L, Sudre B, Domanovic D, Paz S. Climate change projections of West Nile virus infections in Europe: implications for blood safety practices. Environmental Health. 2016;15. doi:10.1186/s12940-016-0105-4

57. Shand L, Brown WM, Chaves LF, Goldberg TL, Hamer GL, Haramis L, et al. Predicting West Nile Virus Infection Risk From the Synergistic Effects of Rainfall and Temperature. Journal of Medical Entomology. 2016;53: 935–944. doi:10.1093/jme/tjw042

58. Brummer-Korvenkontio M, Vapalahti O, Kuusisto P, Saikku P, Manni T, Koskela P, et al. Epidemiology of Sindbis virus infections in Finland 1981–96: possible factors explaining a

peculiar disease pattern. Epidemiology and Infection. 2002;129. doi:10.1017/S0950268802007409

59. Jalava K, Sane J, Ollgren J, Ruuhela R, Rätti O, Kurkela S, et al. Climatic, ecological and socioeconomic factors as predictors of Sindbis virus infections in Finland. Epidemiology and Infection. 2013;141: 1857–1866. doi:10.1017/S095026881200249X

60. Mallya S, Sander B, Roy-Gagnon M-H, Taljaard M, Jolly A, Kulkarni MA. Factors associated with human West Nile virus infection in Ontario: a generalized linear mixed modelling approach. BMC Infectious Diseases. 2018;18. doi:10.1186/s12879-018-3052-6

61. Stewart Ibarra AM, Ryan SJ, Beltrán E, Mejía R, Silva M, Muñoz Á. Dengue Vector Dynamics (Aedes aegypti) Influenced by Climate and Social Factors in Ecuador: Implications for Targeted Control. Mores CN, editor. PLoS ONE. 2013;8: e78263. doi:10.1371/journal.pone.0078263

62. Jacups SP, Whelan PI, Markey PG, Cleland SJ, Williamson GJ, Currie BJ. Predictive indicators for Ross River virus infection in the Darwin area of tropical northern Australia, using long-term mosquito trapping data. Tropical Medicine and International Health. 2008;13: 943–952. doi:10.1111/j.1365-3156.2008.02095.x

63. Hu W, Tong S, Mengersen K, Oldenburg B. Rainfall, mosquito density and the transmission of Ross River virus: A time-series forecasting model. Ecological Modelling. Elsevier; 2006;196: 505–514. doi:10.1016/j.ecolmodel.2006.02.028

64. Kilpatrick AM, Kramer LD, Jones MJ, Marra PP, Daszak P. West Nile Virus Epidemics in North America Are Driven by Shifts in Mosquito Feeding Behavior. Ostfeld R, editor. PLoS Biology. 2006;4: e82. doi:10.1371/journal.pbio.0040082

65. Hess AD, Cherubin CE, Lamotte LC. Relation of Temperature to Activity of Western and St. Louis Encephalitis Viruses *. The American Journal of Tropical Medicine and Hygiene. 1963;12: 657–667. doi:10.4269/ajtmh.1963.12.657

66. Anyamba A, Chretien J-P, Small J, Tucker CJ, Formenty PB, Richardson JH, et al. Prediction of a Rift Valley fever outbreak. Proceedings of the National Academy of Sciences. 2009;106: 955–959. doi:10.1073/pnas.0806490106

67. Linthicum KJ, Anyamba A, Tucker CJ, Kelley PW, Myers MF, Peters CJ. Climate and satellite indicators to forecast Rift Valley fever epidemics in Kenya. Science. 1999;285: 397–400.

68. Vogels CBF, Hartemink N, Koenraadt CJM. Modelling West Nile virus transmission risk in Europe: effect of temperature and mosquito biotypes on the basic reproduction number. Scientific Reports. 2017;7. doi:10.1038/s41598-017-05185-4

69. Kushmaro A, Friedlander TA, Levins R. Temperature Effects on the Basic Reproductive Number (R0) Of West Nile Virus, Based On Ecological Parameters: Endemic Vs. New

Emergence Regions. Journal of Tropical Diseases. 2015;s1. doi:10.4172/2329-891X.1000S1-001

70. Molnár PK, Kutz SJ, Hoar BM, Dobson AP. Metabolic approaches to understanding climate change impacts on seasonal host-macroparasite dynamics. Ecology letters. 2013;16: 9–21. doi:10.1111/ele.12022

71. Braack L, Gouveia de Almeida AP, Cornel AJ, Swanepoel R, de Jager C. Mosquito-borne arboviruses of African origin: review of key viruses and vectors. Parasites & Vectors. 2018;11. doi:10.1186/s13071-017-2559-9

72. Climate Change 2014: Synthesis Report. Contribution of Working Groups I, II and III to the Fifth Assessment Report of the Intergovernmental Panel on Climate Change. Geneva, Switzerland: IPCC; 2014 pp. 1–151.

73. R Core Team. R: A language and for statistical computing. Vienna, Austria: R Foundation for Statistical Computing; 2016.

74. Smith JL, Fonseca DM. Rapid assays for identification of members of the Culex (Culex) pipiens complex, their hybrids, and other sibling species (Diptera: culicidae). Am J Trop Med Hyg. 2004;70: 339–345.

75. Darsie Jr, Richard F, Ward, Ronald A. Identification and Geographical Distribution of the Mosquitoes of North America, North of Mexico. University Press of Florida; 2016.

76. Huerta Jiménez H. Actualización de la Colección de Artrópodos con importancia médica (CAIM), Laboratorio de Entomología, InDRE [Internet]. Comisión nacional para el conocimiento y uso de la biodiversidad; 2018. doi:10.15468/y2rff2

77. López Cárdenas J. Apoyo para la infraestructura de la colección de artrópodos con y sin importancia médica del Laboratorio estatal de Salud Pública del estado de Guanajuato [Internet]. Comisión nacional para el conocimiento y uso de la biodiversidad; 2018. doi:10.15468/5mjcse

78. Ortega Morales AI. Catálogo digital y clave ilustrada de los mosquitos (Diptera: Culicidae) de las zonas áridas de los estados de Nuevo León y Tamaulipas, México [Internet]. Comisión nacional para el conocimiento y uso de la biodiversidad; 2018. doi:10.15468/otexwf

79. Ponce García G. Computarización de la Colección de insectos y ácaros de importancia médica de la Facultad de Ciencias Biológicas, Universidad Autónoma de Nuevo León [Internet]. Comisión nacional para el conocimiento y uso de la biodiversidad; 2018. doi:10.15468/sma9a5

80. Walter Reed Biosystematics Unit. Mosquito Occurrence Dataset [Internet]. Smithsonian Institution; 2018. doi:10.15468/tw2y9b

81. Andreadis SS, Dimotsiou OC, Savopoulou-Soultani M. Variation in adult longevity of *Culex pipiens f. pipiens*, vector of the West Nile Virus. Parasitology Research. 2014;113: 4315–4319. doi:10.1007/s00436-014-4152-x

82. Brust RA. WEIGHT AND DEVELOPMENT TIME OF DIFFERENT STADIA OF MOSQUITOES REARED AT VARIOUS CONSTANT TEMPERATURES. The Canadian Entomologist. 1967;99: 986–993. doi:10.4039/Ent99986-9

83. Buth JL, Brust RA, Ellis RA. Development time, oviposition activity and onset of diapause in *Culex tarsalis*, *Culex restuans* and *Culiseta inornata* in southern Manitoba. J Am Mosq Control Assoc. 1990;6: 55–63.

84. Chamberlain RW, Sudia WD. The effects of temperature upon the extrinsic incubation of eastern equine encephalitis in mosquitoes. Am J Hyg. 1955;62: 295–305.

85. Ciota AT, Matacchiero AC, Kilpatrick AM, Kramer LD. The Effect of Temperature on Life History Traits of *Culex* Mosquitoes. Journal of Medical Entomology. 2014;51: 55–62. doi:10.1603/ME13003

86. Cornel AJ, Jupp PG, Blackburn NK. Environmental Temperature on the Vector Competence of *Culex univittatus* (Diptera: Culicidae) for West Nile Virus. Journal of Medical Entomology. 1993;30: 449–456. doi:10.1093/jmedent/30.2.449

87. Dodson BL, Kramer LD, Rasgon JL. Effects of larval rearing temperature on immature development and West Nile virus vector competence of *Culex tarsalis*. Parasites & Vectors. 2012;5: 199. doi:10.1186/1756-3305-5-199

88. Dohm DJ, O'Guinn ML, Turell MJ. Effect of environmental temperature on the ability of *Culex pipiens* (Diptera: Culicidae) to transmit West Nile virus. Journal of Medical Entomology. 2002;39: 221–225. doi:10.1603/0022-2585-39.1.221

89. Kilpatrick AM, Meola MA, Moudy RM, Kramer LD. Temperature, viral genetics, and the transmission of West Nile virus by *Culex pipiens* mosquitoes. PLoS Pathogens. 2008;4. doi:10.1371/journal.ppat.1000092

90. Kramer LD, Hardy JL, Presser SB. Effect of temperature of extrinsic incubation on the vector competence of *Culex tarsalis* for western equine encephalomyelitis virus. Am J Trop Med Hyg. 1983;32: 1130–1139.

91. Li J, Zhu G, Zhou H, Tang J, Cao J. Effect of temperature on the development of *Culex pipiens pallens*. Chin J Vector Biol & Control. 2017;28: 35–37.

92. Loetti V, Schweigmann N, Burroni N. Development rates, larval survivorship and wing length of *Culex pipiens* (Diptera: Culicidae) at constant temperatures. Journal of Natural History. 2011;45: 2203–2213. doi:10.1080/00222933.2011.590946

93. Lundström JO, Turell MJ, Niklasson B. Effect of environmental temperature on the vector competence of *Culex pipiens and Cx. torrentium* for Ockelbo virus. Am J Trop Med Hyg. 1990;43: 534–542.

94. Madder DJ, Surgeoner GA, Helson BV. Number of generations, egg production, and developmental time of Culex pipiens and Culex restauns (Diptera: Culicidae) in southern Ontario. J Med Entomol. 1983;20: 275–287.

95. Mahmood F, Crans WJ. A thermal heat summation model to predict the duration of the gonotrophic cycle of Culiseta melanura in nature. J Am Mosq Control Assoc. 1997;13: 92–94.

96. Mahmood F, Crans WJ. Effect of temperature on the development of Culiseta melanura (Diptera: Culicidae) and its impact on the amplification of eastern equine encephalomyelitis virus in birds. J Med Entomol. 1998;35: 1007–1012.

97. McHaffey DG. Photoperiod and temperature influences on diapause in eggs of the floodwater mosquito *Aedes vexans* (Meigen) (Diptera: Culicidae). J Med Entomol. 1972;9: 564–571.

98. Mogi M. Temperature and Photoperiod Effects on Larval and Ovarian Development of New Zealand Strains of *Culex quinquefasciatus* (Diptera: Culicidae). Annals of the Entomological Society of America. 1992;85: 58–66. doi:10.1093/aesa/85.1.58

99. Mpho M, Holloway GJ, Callaghan A. A comparison of the effects of organophosphate insecticide exposure and temperature stress on fluctuating asymmetry and life history traits in *Culex quinquefasciatus*. Chemosphere. 2001;45: 713–720.

100. Mpho M, Callaghan A, Holloway GJ. Temperature and genotypic effects on life history and fluctuating asymmetry in a field strain of *Culex pipiens*. Heredity. 2002;88: 307–312. doi:10.1038/sj.hdy.6800045

101. Mpho M, Callaghan A, Holloway GJ. Effects of temperature and genetic stress on life history and fluctuating wing asymmetry in *Culex pipiens* mosquitoes. European Journal of Entomology. 2002;99: 405–412. doi:10.14411/eje.2002.050

102. Nayar JK. Effects of constant and fluctuating temperatures on life span of *Aedes taeniorhynchus* adults. Journal of Insect Physiology. 1972;18: 1303–1313. doi:10.1016/0022-1910(72)90259-4

103. Oda T, Mori A, Ueda M, Kurokawa K, others. Effects of temperatures on the oviposition and hatching of eggs in *Culex pipiens molestus* and *Culex pipiens quinquefasciatus*. Tropical Medicine. 1980;22: 167–180.

104. Oda T, Uchida K, Mori A, Mine M, Eshita Y, Kurokawa K, et al. Effects of high temperature on the emergence and survival of adult *Culex pipiens molestus* and *Culex quinquefasciatus* in Japan. J Am Mosq Control Assoc. 1999;15: 153–156.

105. Rayah EAE, Groun NAA. Effect of temperature on hatching eggs and embryonic survival in the mosquito Culex quinquefasciatus. Entomologia Experimentalis et Applicata. 1983;33: 349–351. doi:10.1111/j.1570-7458.1983.tb03281.x

106. Reisen WK, Milby MM, Presser SB, Hardy JL. Ecology of Mosquitoes and St. Louis Encephalitis Virus in the Los Angeles Basin of California, 1987–1990. Journal of Medical Entomology. 1992;29: 582–598. doi:10.1093/jmedent/29.4.582

107. Reisen WK, Meyer RP, Presser SB, Hardy JL. Effect of temperature on the transmission of western equine encephalomyelitis and St. Louis encephalitis viruses by *Culex tarsalis* (Diptera: Culicidae). J Med Entomol. 1993;30: 151–160.

108. Reisen WK. Effect of temperature on *Culex tarsalis* (Diptera: Culicidae) from the Coachella and San Joaquin Valleys of California. J Med Entomol. 1995;32: 636–645.

109. Rueda LM, Patel KJ, Axtell RC, Stinner RE. Temperature-dependent development and survival rates of *Culex quinquefasciatus* and *Aedes aegypti* (Diptera: Culicidae). J Med Entomol. 1990;27: 892–898.

110. Ruybal JE, Kramer LD, Kilpatrick AM. Geographic variation in the response of *Culex pipiens* life history traits to temperature. Parasites & Vectors. Parasites & Vectors; 2016;9. doi:10.1186/s13071-016-1402-z

111. Shelton RM. The effect of temperatures on development of eight mosquito species. Mosquito News. 1973;33: 1–12.

112. Tekle A. The Physiology of Hibernation and Its Role in the Geographical Distribution of Populations of the *Culex Pipiens* Complex. The American Journal of Tropical Medicine and Hygiene. 1960;9: 321–330. doi:10.4269/ajtmh.1960.9.321

113. Teng H-J, Apperson CS. Development and Survival of Immature *Aedes albopictus* and *Aedes triseriatus* (Diptera: Culicidae) in the Laboratory: Effects of Density, Food, and Competition on Response to Temperature. Journal of Medical Entomology. 2000;37: 40–52. doi:10.1603/0022-2585-37.1.40

114. Trpiš M, Shemanchuk JA. EFFECT OF CONSTANT TEMPERATURE ON THE LARVAL DEVELOPMENT OF *AEDES VEXANS* (DIPTERA: CULICIDAE). The Canadian Entomologist. 1970;102: 1048–1051. doi:10.4039/Ent1021048-8

115. Turell MJ, Rossi CA, Bailey CL. Effect of Extrinsic Incubation Temperature on the Ability of *Aedes Taeniorhynchus* and *Culex Pipiens* to Transmit Rift Valley Fever Virus. The American Journal of Tropical Medicine and Hygiene. 1985;34: 1211–1218. doi:10.4269/ajtmh.1985.34.1211

116. Turell MJ, Lundström JO. Effect of environmental temperature on the vector competence of *Aedes aegypti* and *Ae. taeniorhynchus* for Ockelbo virus. Am J Trop Med Hyg. 1990;43: 543–550.

117. Van der Linde TCD. Development rates and percentage hatching of Culex (Culex) theileri; Theobald (Diptera: Culicidae) eggs at various constant temperatures. Journal of the Entomological Society of Southern Africa,. 1990;53: 17–26.

118. Rohatgi A. WebPlotDigitizer [Internet]. 2018. Available: https://automeris.io/WebPlotDigitizer

119. Vogels CBF, Fros JJ, Göertz GP, Pijlman GP, Koenraadt CJM. Vector competence of northern European Culex pipiens biotypes and hybrids for West Nile virus is differentially affected by temperature. Parasites & Vectors. 2016;9. doi:10.1186/s13071-016-1677-0

120. Fros JJ, Geertsema C, Vogels CB, Roosjen PP, Failloux A-B, Vlak JM, et al. West Nile Virus: High Transmission Rate in North-Western European Mosquitoes Indicates Its Epidemic Potential and Warrants Increased Surveillance. Liang S, editor. PLOS Neglected Tropical Diseases. 2015;9: e0003956. doi:10.1371/journal.pntd.0003956

121. Su Y-S, Yajima M. R2jags: A Package for Running jags from R. 2009.

122. Plummer M. JAGS: A program for analysis of Bayesian graphical models using Gibbs sampling. Proceedings of the 3rd International Workshop on Distributed Statistical Computing. 2003; 1–10. doi:ISSN 1609-395X

123. Spiegelhalter DJ, Best NG, Carlin BP, van der Linde A. Bayesian measures of model complexity and fit. Journal of the Royal Statistical Society: Series B (Statistical Methodology). 2002;64: 583–639. doi:10.1111/1467-9868.00353

124. Kiarie-Makara MW, Ngumbi PM, Lee D-K. Effects of Temperature on the Growth and Development of *Culex pipiens* Complex Mosquitoes (Diptera: Culicidae). Journal of Pharmacy and Biological Sciences. 2015;10: 1–10.

125. McHaffey DG, Harwood RF. Photoperiod and Temperature Influences on Diapause in Eggs of the Floodwater Mosquito, *Aedes Dorsalis* (Meigen) (Diptera: Culicidae)1. Journal of Medical Entomology. 1970;7: 631–644. doi:10.1093/jmedent/7.6.631

126. McHaffey DG. Photoperiod and temperature influences on diapause in eggs of the floodwater mosquito *Aedes nigromaculis* (Ludlow) (Diptera : Culicidae). Mosquito News. 1972;32: 51–61.

127. Muturi EJ, Lampman R, Costanzo K, Alto BW. Effect of Temperature and Insecticide Stress on Life-History Traits of Culex restuans and Aedes albopictus (Diptera: Culicidae). Journal of Medical Entomology. 2011;48: 243–250. doi:10.1603/ME10017

128. Olejnícek J, Gelbic I. Differences in response to temperature and density between two strains of the mosquito, *Culex pipiens molestus* forskal. J Vector Ecol. 2000;25: 136–145.

129. Parker BM. Temperature and Salinity as Factors Influencing the Size and Reproductive Potentials of *Aedes dorsalis* (Diptera: Culicidae). Annals of the Entomological Society of America. 1982;75: 99–102. doi:10.1093/aesa/75.1.99

130. Centers for Disease Control and Prevention. West Nile Virus: Final Cumulative Maps & Data for 1999-2017 [Internet]. 2018 Dec. Available: https://www.cdc.gov/westnile/statsmaps/cumMapsData.html

131. Bivand R, Rundel C. rgeos: Interface to Geometry Engine - Open Source (GEOS) R Package version 0.4-1.

132. Harris I, Jones PD, Osborn TJ, Lister DH. Updated high-resolution grids of monthly climatic observations - the CRU TS3.10 Dataset: UPDATED HIGH-RESOLUTION GRIDS OF MONTHLY CLIMATIC OBSERVATIONS. International Journal of Climatology. 2014;34: 623–642. doi:10.1002/joc.3711

133. Hijmans RJ. raster: Geographic data analysis and modeling, R package version 2.2.31.

134. Curren EJ, Lindsey NP, Fischer M, Hills SL. St. Louis Encephalitis Virus Disease in the United States, 2003–2017. The American Journal of Tropical Medicine and Hygiene. 2018;99: 1074–1079. doi:10.4269/ajtmh.18-0420

135. Lindsey NP, Staples JE, Fischer M. Eastern Equine Encephalitis Virus in the United States, 2003–2016. The American Journal of Tropical Medicine and Hygiene. 2018;98: 1472–1477. doi:10.4269/ajtmh.17-0927

136. Petersen LR, Brault AC, Nasci RS. West Nile Virus: Review of the Literature. JAMA. 2013;310: 308. doi:10.1001/jama.2013.8042

137. Ronca SE, Murray KO, Nolan MS. Cumulative Incidence of West Nile Virus Infection, Continental United States, 1999–2016. Emerging Infectious Diseases. 2019;25: 325–327. doi:10.3201/eid2502.180765

138. Government of Canada. Surveillance of West Nile virus [Internet]. Government of Canada; 2018 Dec. Available: https://www.canada.ca/en/public-health/services/diseases/west-nile-virus/surveillance-west-nile-virus.html

139. European Centre for Disease Prevention and Control. Surveillance and disease data for West Nile fever [Internet]. European Centre for Disease Prevention and Control; 2018 Dec. Available: https://ecdc.europa.eu/en/west-nile-fever/surveillance-and-disease-data

140. World Health Organization. Rift Valley Fever Fact Sheet [Internet]. World Health Organization; 2018 Feb. Available: https://www.who.int/en/news-room/fact-sheets/detail/rift-valley-fever

Table 1: Properties of six viruses transmitted by an overlapping network of mosquito vectors. Sources: WNV [22,23,130,136–139]; SLEV [23,26]; EEEV [23,27]; WEEV [23]; SINV [24]; RVFV [25,29,71,140].

Virus (*genus*)	Primary vector spp.	Geographic range	Presentation & mortality	Epidemiology & Ecology
West Nile virus (WNV, *Flavivirus*)	*Cx. pipiens*, *Cx. quinquefasciatus*, *Cx. tarsalis*	Globally distributed	Febrile illness and encephalitis. 10% mortality in neuro-invasive cases. Long-term physical & cognitive disabilities.	The most common mosquito-borne disease in North America. Since invading in 1999, 7 million estimated infections, 22,999 neuro-invasive cases, and 2,163 deaths in US; 5,614 reported cases in Canada. Typically 100-300 cases annually in Europe, but over 1500 in 2018. Poor surveillance in Africa, but seroprevalence ~80% in some areas. Birds are main reservoir/amplification hosts.
St. Louis Encephalitis virus (SLEV, *Flavivirus*)	*Cx. quinquefasciatus*, *Cx. tarsalis*	North America, primarily western, midwestern, & southern US	Encephalitis. 5-15% mortality in diagnosed cases.	97 cases and 5 deaths recorded in US from 2008-2017. Birds are main reservoir/amplification hosts.
Eastern Equine Encephalitis virus (EEEV, *Alphavirus*)	*Ae. triseriatus*, *Cs. melanura*	North America, primarily in eastern & midwestern US	Febrile illness and encephalitis. 33% mortality in diagnosed cases. Long-term cognitive disabilities.	71 cases and 30 deaths recorded in US from 2008-2017. Birds are main reservoir/amplification hosts.
Western Equine Encephalitis virus (WEEV, *Alphavirus*)	*Cx. tarsalis*	North America, primarily in western & midwestern US	Febrile illness and encephalitis. Low mortality, except in infants.	The CDC does not report WEEV infection. Birds are main reservoir/amplification hosts. WEEV is derived from a recombinant event between the ancestors of EEEV and SINV.
Sindbis virus (SINV, *Alphavirus*), also called Pogosta, Ockelbo, & Karelian Fever	*Cx. torrentium*, *Cx. pipiens, Cx. univittatus*	Old world & Australia, primarily northern Europe & southern Africa	Febrile illness, rash, and joint pain. No mortality, but long-term disability.	Poor surveillance except in Finland, where annual incidence is 2–26 per 100,000 people and seroprevalence can reach ~40%. Birds are main reservoir/amplification hosts. Long-distance migratory birds may spread the virus between temperate zones in Northern and Southern hemispheres.
Rift Valley Fever virus (RVFV, *Phlebovirus*)	*Ae. mcintoshi, Ae. ochraceus, Ae. vexans, Cx. pipiens, Cx. poicilipes, Cx. theileri* and many more	Africa & the Middle East	Febrile illness and encephalitis. <1% mortality in total cases. 50% mortality in hemorrhagic cases, permanent blindness in 50% of ocular cases (<2% of cases).	Livestock are main reservoir/amplification hosts, and suffer mortality and abortion after being infected by mosquitoes. Most transmission to humans occurs via direct contact with infected livestock. Vertical transmission in vectors (via dormant eggs) can initiate epidemics. In eastern and southern Africa, there are large epidemics every 5-15 years driven by rainfall and blooms of *Ae. spp*. from low-lying flooded areas known as *dambos*.

Table 2: Thermal optima and limits for transmission of mosquito-borne pathogens. Median temperature of the lower thermal limit (T_{min}), optimum, and upper thermal limit (T_{max}), with 95% credible intervals in parentheses.

NOTE: For publication, this should be one table with 5 columns (no repeated R_0 model column).

R_0 Model	T_{min} (ºC)	Optimum (ºC)	T_{max} (ºC)
From this study:			
EEEV in *Ae. triseriatus*	11.7 (8.8 – 16.3)	22.7 (22.0 – 23.6)	31.9 (31.1 – 33.0)
WEEV in *Cx. tarsalis*	8.6 (6.3 – 13.0)	23.0 (22.0 – 24.7)	31.9 (30.3 – 35.2)
SINV in *Cx. pipiens*	9.4 (6.9 – 13.3)	23.2 (21.7 – 24.6)	33.8 (28.2 – 37.0)
WNV in *Cx. univittatus*	11.0 (8.0 – 15.3)	23.8 (22.7 – 25.0)	33.6 (31.2 – 36.9)
WNV in *Cx. tarsalis*	12.1 (9.6 – 15.2)	23.9 (22.9 – 25.9)	32.0 (30.6 – 38.6)
SLEV in *Cx. tarsalis*	12.9 (11.0 – 14.8)	24.1 (23.1 – 26.0)	32.0 (30.6 – 38.5)
WNV in *Cx. pipiens*	16.8 (14.9 – 17.8)	24.5 (23.6 – 25.5)	34.9 (32.9 – 37.6)
WNV in *Cx. quinquefasciatus*	19.0 (14.1 – 20.9)	25.2 (23.9 – 27.1)	31.8 (31.1 – 32.2)
RVFV in *Ae. taeniorhynchus*	10.6 (8.6 – 14.4)	25.9 (23.8 – 27.1)	37.8 (34.4 – 39.1)
SINV in *Ae. taeniorhynchus*	9.7 (8.3 – 13.6)	26.0 (23.9 – 27.3)	37.8 (34.4 – 39.2)
From previous studies:			
Falciparum malaria [3]	19.1 (16.0 – 23.2)	25.4 (23.9 – 27.0)	32.6 (29.4 – 34.3)
DENV in *Ae. albopictus* [4]	16.2 (13.0 – 19.8)	26.4 (25.4 – 27.6)	31.4 (29.5 – 34.0)
Ross River virus [6]	17.0 (15.8 – 18.0)	26.4 (26.0 – 26.6)	31.4 (30.4 – 33.0)
ZIKV in *Ae. aegypti* [7]	22.8 (20.5 – 23.8)	28.9 (28.2 – 29.6)	34.5 (34.1 – 36.2)
DENV in *Ae. aegypti* [4]	17.8 (14.6 – 21.2)	29.1 (28.4 – 29.8)	34.5 (34.1 – 35.8)

R_0 Model	Thermal breadth (ºC)
From this study:	
EEEV in *Ae. triseriatus*	20.0 (15.4 – 23.0)
WEEV in *Cx. tarsalis*	23.3 (18.2 – 27.0)
SINV in *Cx. pipiens*	23.8 (17.3 – 28.6)
WNV in *Cx. univittatus*	22.5 (18.2 – 26.3)
WNV in *Cx. tarsalis*	20.1 (16.3 – 26.7)
SLEV in *Cx. tarsalis*	19.2 (16.5 – 25.6)
WNV in *Cx. pipiens*	18.2 (15.8 – 21.2)
WNV in *Cx. quinquefasciatus*	12.7 (10.6 – 17.6)
RVFV in *Ae. taeniorhynchus*	27.0 (21.8 – 29.7)
SINV in *Ae. taeniorhynchus*	27.7 (22.6 – 30.0)
From previous studies:	
Falciparum malaria [3]	13.2 (8.3 – 17.1)
DENV in *Ae. albopictus* [4]	15.2 (11.2 – 19.3)
Ross River virus [6]	14.2 (12.8 – 16.2)
ZIKV in *Ae. aegypti* [7]	11.7 (10.4 – 14.5)
DENV in *Ae. aegypti* [4]	16.7 (13.2 – 20.2)

Table 3: Predicted optima for transmission of West Nile virus. Predicted optima for transmission from this study and previous models.

R_0 Model	Optimum (ºC)
From this study:	
WNV in *Cx. pipiens*	24.5
WNV in *Cx. quinquefasciatus*	25.2
WNV in *Cx. tarsalis*	23.9
WNV in *Cx. univittatus*	23.8
From previous studies:	
WNV in *Cx. pipiens* [5]	24.9
WNV in *Cx. quinquefasciatus* [5]	24.3
WNV in *Cx. tarsalis* [5]	24.9
WNV in *Cx. pipiens* [68]	28
WNV in *Cx. pipiens molestus* [68]	28
WNV in *Cx.* and *Ae. spp.* [69]	35

Figure 1: Viruses transmitted by a community of vectors. The six viruses in this study (WNV = West Nile virus, SLEV = St. Louis Encephalitis virus, EEEV = Eastern Equine Encephalitis virus, WEEV = Western Equine Encephalitis virus, SINV = Sindbis virus, RVFV = Rift Valley Fever virus) and the *Culex* (*Cx.*), *Aedes* (*Ae.*), *Coquillettidia* (*Cq.*), and *Culiseta* (*Cs.*) vectors that are important for sustaining transmission to humans. Grey shading indicates an important vector-virus pair; hatching indicates available temperature-dependent data for infection traits (parasite development rate [*PDR*] and vector competence [*bc* or *b* and *c*]). The importance of each vector for transmission may vary over the geographic range of the virus. Infection data were available for SINV and RVFV in *Ae. taeniorhynchus*, although this North American mosquito does not occur in the endemic range of these pathogens. Data sources: [23–25,29,71].

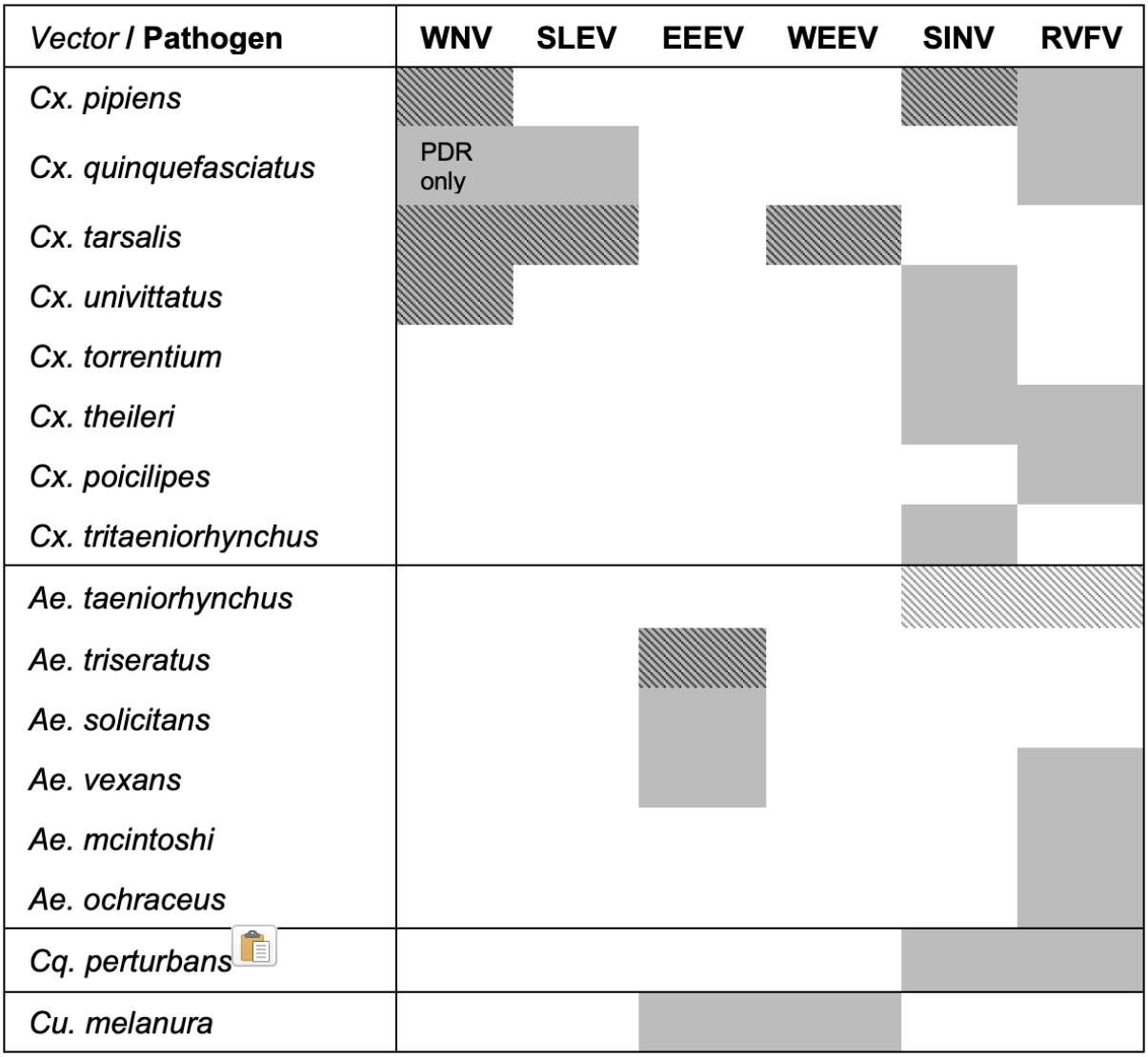

Figure 2: *Culex* spp. vectors of West Nile and other viruses have distinct but overlapping geographic distributions. The geographic distribution of the primary vectors of West Nile virus: (A) *Culex pipiens* (dark grey) and *Cx. quinquefasciatus* (red), adapted from [32,74]; (B) *Cx. tarsalis* (blue), northern boundary from [75], southern boundary based on data from the Global Biodiversity Information Facility.

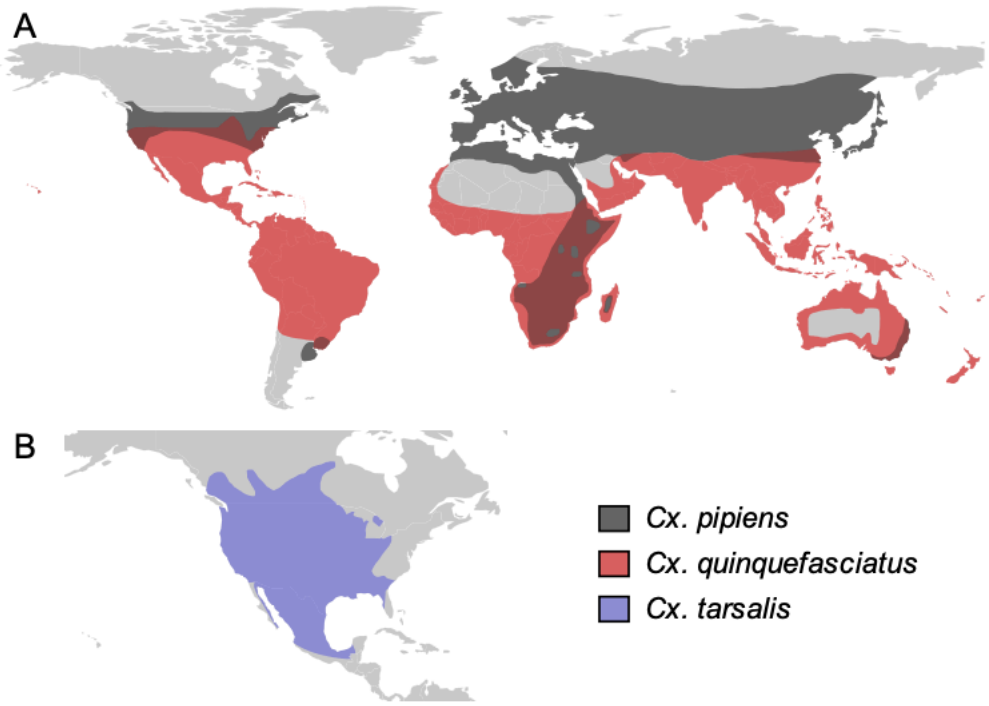

Figure 3: *Culex* spp. mosquito traits respond strongly and consistently to temperature. The thermal responses of mosquito traits for the North American vectors of West Nile virus: *Culex pipiens* (dark grey), *Cx. quinquefasciatus* (red), and *Cx. tarsalis* (blue). (A) Mosquito development rate (*MDR*), (B) larval-to-adult survival (*pLA*), (C) biting rate (*a*), and (D) adult lifespan (*lf*). Points without error bars are reported means from single studies; points with error bars are averages of means from multiple studies (+/- standard error, for visual clarity only; thermal responses were fit to reported means, see Figs S2–5). Solid lines are posterior means; shaded areas are 95% credible intervals. See Fig S1 for thermal responses for *Aedes taeniorhynchus*, *Aedes triseriatus*, *Ae. vexans*, *Culiseta melanura*.

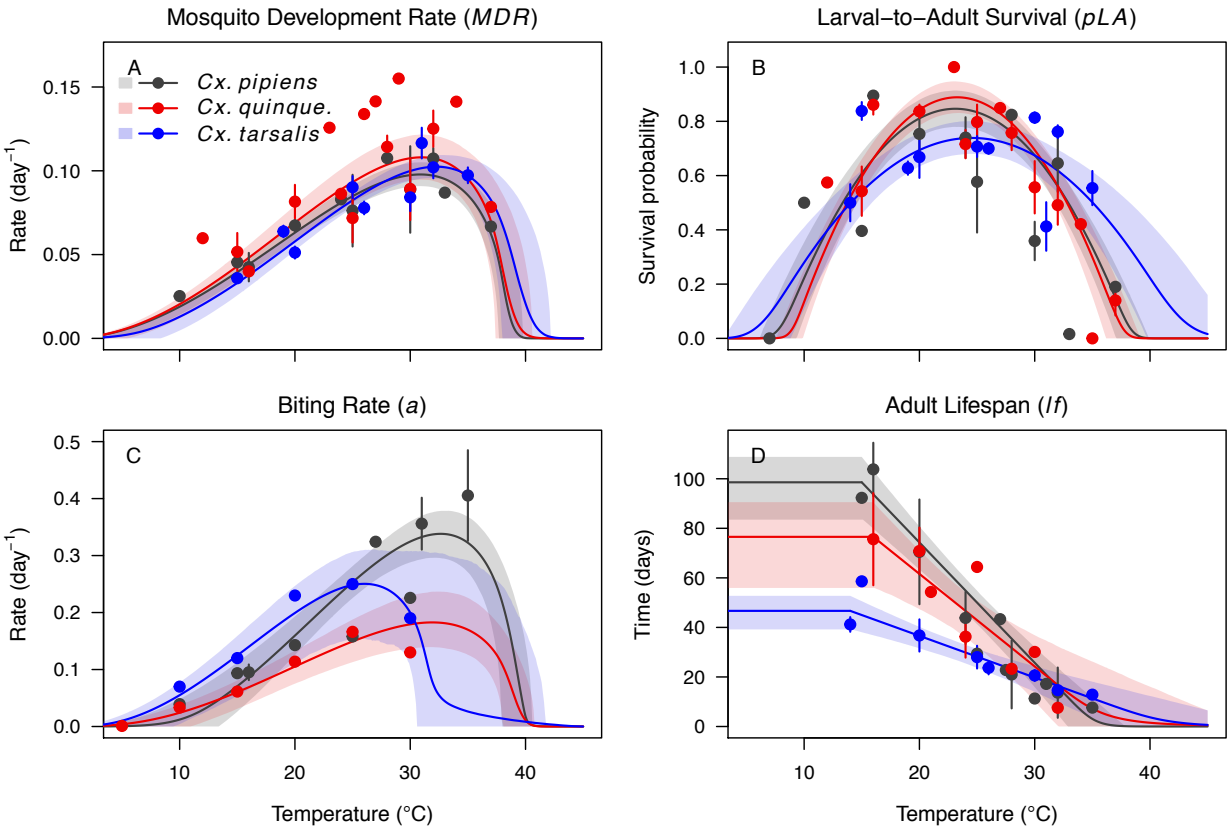

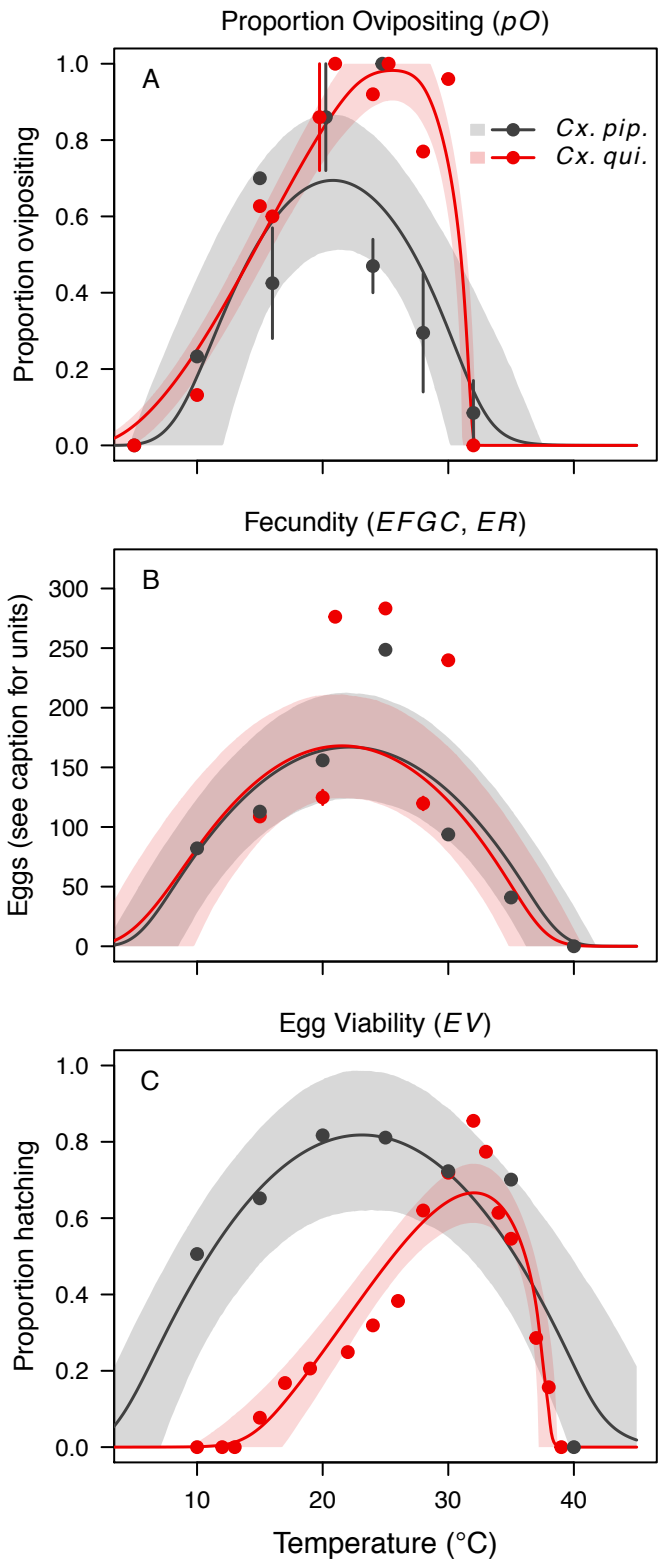

Figure 4: *Culex pipiens* and *Cx. quinquefasciatus* fecundity traits respond strongly to temperature but with different functional forms. The thermal responses of mosquito traits for the primary vectors of West Nile virus: *Culex pipiens* (dark grey) and *Cx. quinquefasciatus* (red). (A) Proportion ovipositing (*pO*), (B) fecundity (eggs per female per gonotrophic cycle, *EFGC,* or eggs per raft, *ER*), and (C) egg viability (*EV*). Points without error bars are reported means from single studies; points with error bars are averages of means from multiple studies (+/- standard error, for visual clarity only; thermal responses were fit to reported means, see Fig S6). Solid lines are posterior distribution means; shaded areas are 95% credible intervals. See Fig S1 for thermal responses for *Ae. vexans*, *Cx. theileri*, and *Culiseta melanura*.

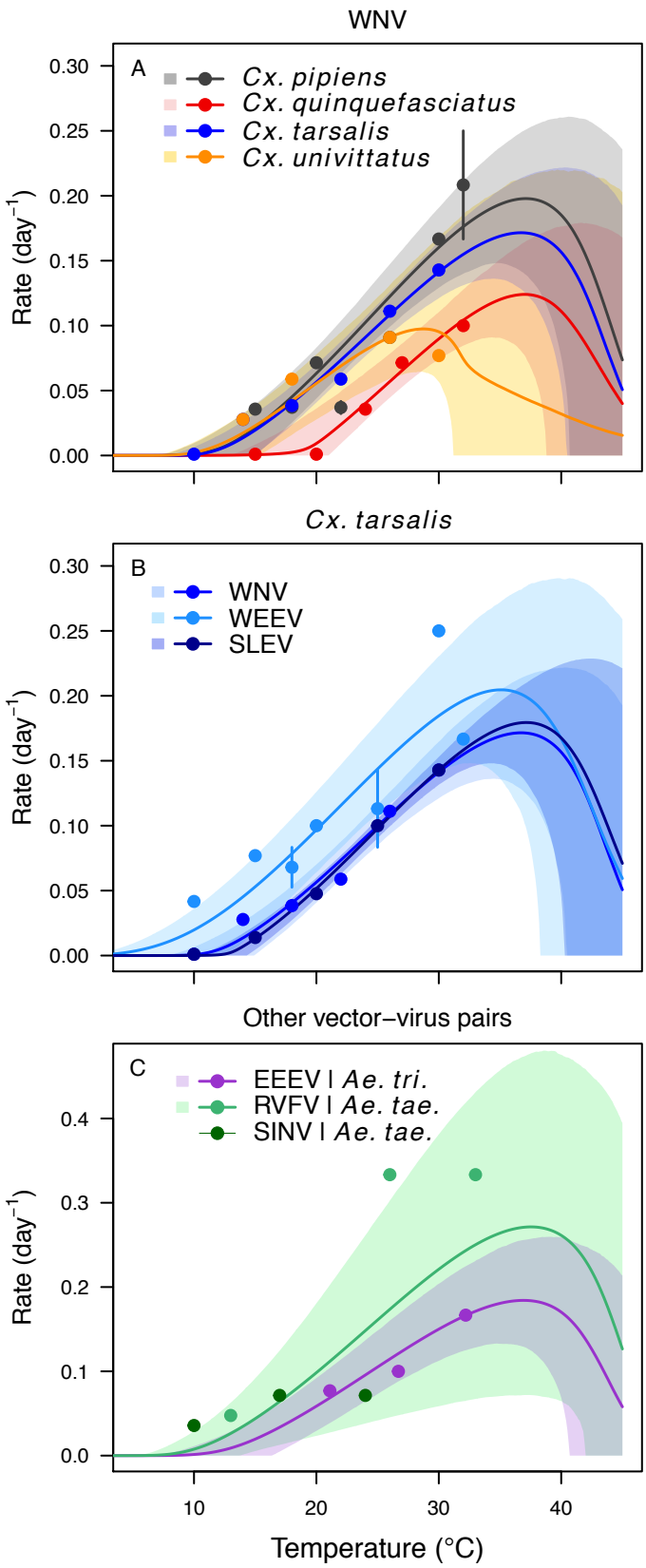

Figure 5: Pathogen development rates have high thermal optima. Thermal responses of pathogen development rate (*PDR*). (A) West Nile virus in *Culex pipiens* (dark grey), *Cx. quinquefasciatus* (red), *Cx. tarsalis* (blue), and *Cx. univitattus* (orange). (B) Three viruses in *Cx. tarsalis*: West Nile virus (same as in A, blue), Western Equine Encephalitis virus (light blue), and St. Louis Encephalitis virus (dark blue). (C) Eastern Equine Encephalitis virus in *Aedes triseriatus* (violet), Rift Valley Fever virus in *Ae. taeniorhynchus* (light green), Sindbis virus in *Ae. taeniorhynchus* (dark green). We did not fit a thermal response for Sindbis virus in *Ae. taeniorhynchus* because the limited data responded weakly to temperature and did not match our priors. We used informative priors based on thermal biology theory and data from other systems to fit the decrease at high temperatures (see *Model Overview*); other traits determined the upper limits of the R_0 models. Points without error bars are reported means from single studies; points with error bars are averages of means from multiple studies (+/- standard error, for visual clarity only; thermal responses were fit to reported means, see Fig S7). Solid lines are posterior distribution means; shaded areas are 95% credible intervals.

Figure 6: Vector competence responds strongly to temperature and varies across vector and virus species. Thermal responses of infection efficiency (*c*, # infected / # exposed; first column), transmission efficiency (*b*, # transmitting / # infected; second column) or vector competence (*bc*, # infected / # exposed; third column) for vector–virus pairs. First row (A,B,C): West Nile virus in *Culex pipiens* (dark grey), *Cx. tarsalis* (blue), and *Cx. univitattus* (yellow/orange). Second row: (D,E,F) Western Equine Encephalitis virus in *Cx. tarsalis* (light blue). Third row (G,H,I): Sindbis virus in *Aedes taeniorhynchus* (dark green), Sindbis virus in *Cx. pipiens* (light gray), St. Louis Encephalitis virus in *Cx. tarsalis* (dark blue), Eastern Equine Encephalitis virus in *Ae. triseriatus* (violet), and Rift Valley Fever virus in *Ae. taeniorhynchus* (light green). Points are means of replicates from single or multiple studies (+/- standard error, for visual clarity only; thermal responses were fit to replicate-level data, see Fig S8, Fig S9). Solid lines are posterior distribution means; shaded areas are 95% credible intervals.

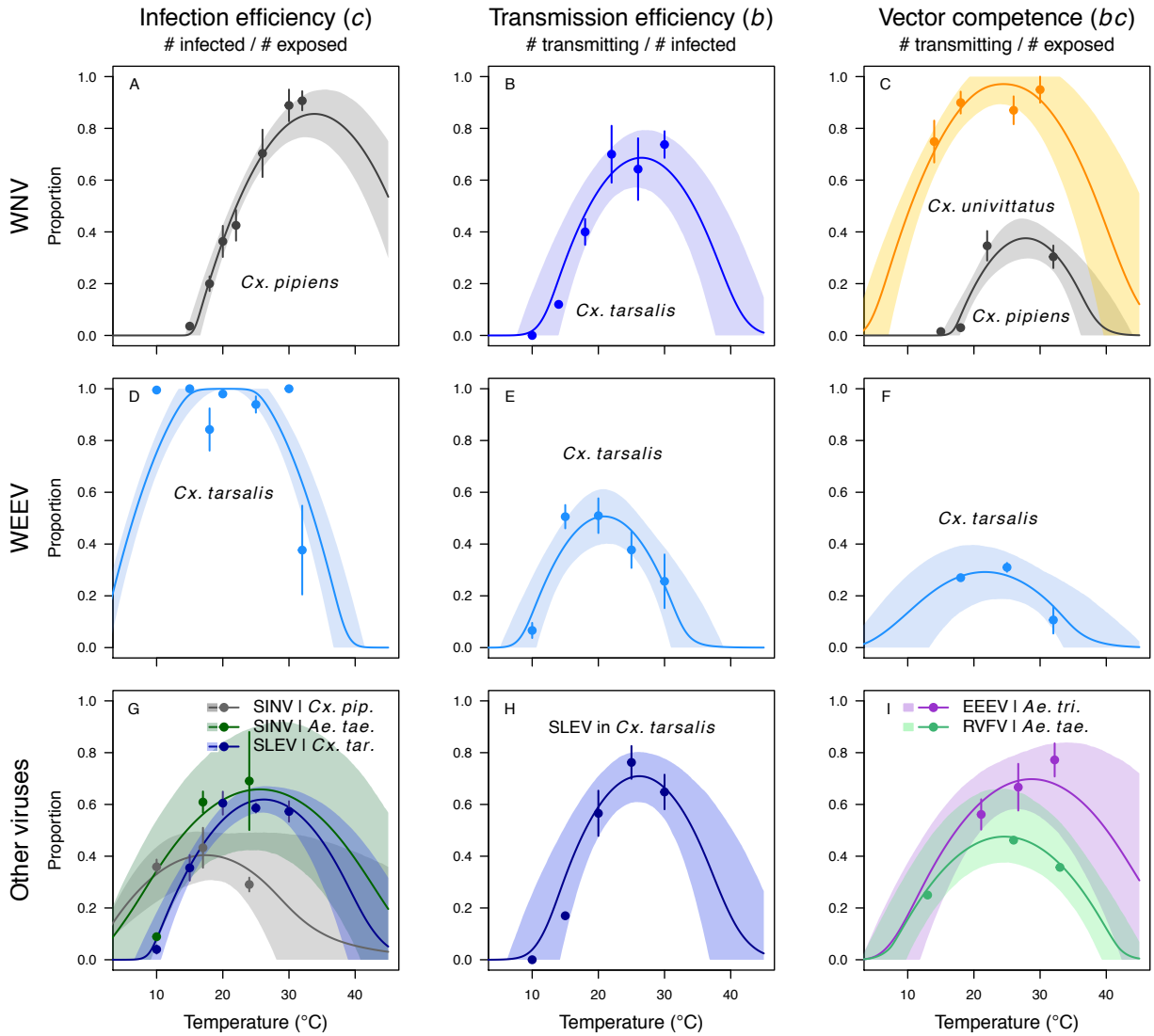

Figure 7: Unimodal thermal responses of transmission (relative R_0) for ten vector-virus pairs. Posterior mean relative R_0 for (A) West Nile virus (WNV) in *Culex pipiens* (dark grey), *Cx. tarsalis* (blue), *Cx. quinquefasciatus* (red), and *Cx. univitattus* (orange); (B) three viruses in *Cx. tarsalis*: WNV (same as in A, blue), Western Equine Encephalitis virus (WEEV, light blue), and St. Louis Encephalitis virus (SLEV, dark blue); (C) Sindbis virus (SINV) in *Aedes taeniorhynchus* (dark green) and *Cx. pipiens* (light grey), Rift Valley Fever virus (RVFV) in *Ae. taeniorhynchus* (light green), and Eastern Equine Encephalitis virus (EEEV) in *Ae. triseriatus* (violet). (D) Posterior median and uncertainty estimates for the lower thermal limit, optimum, and upper thermal limit. Points show medians, thick lines show middle 50% density, thin lines show 95% credible intervals.

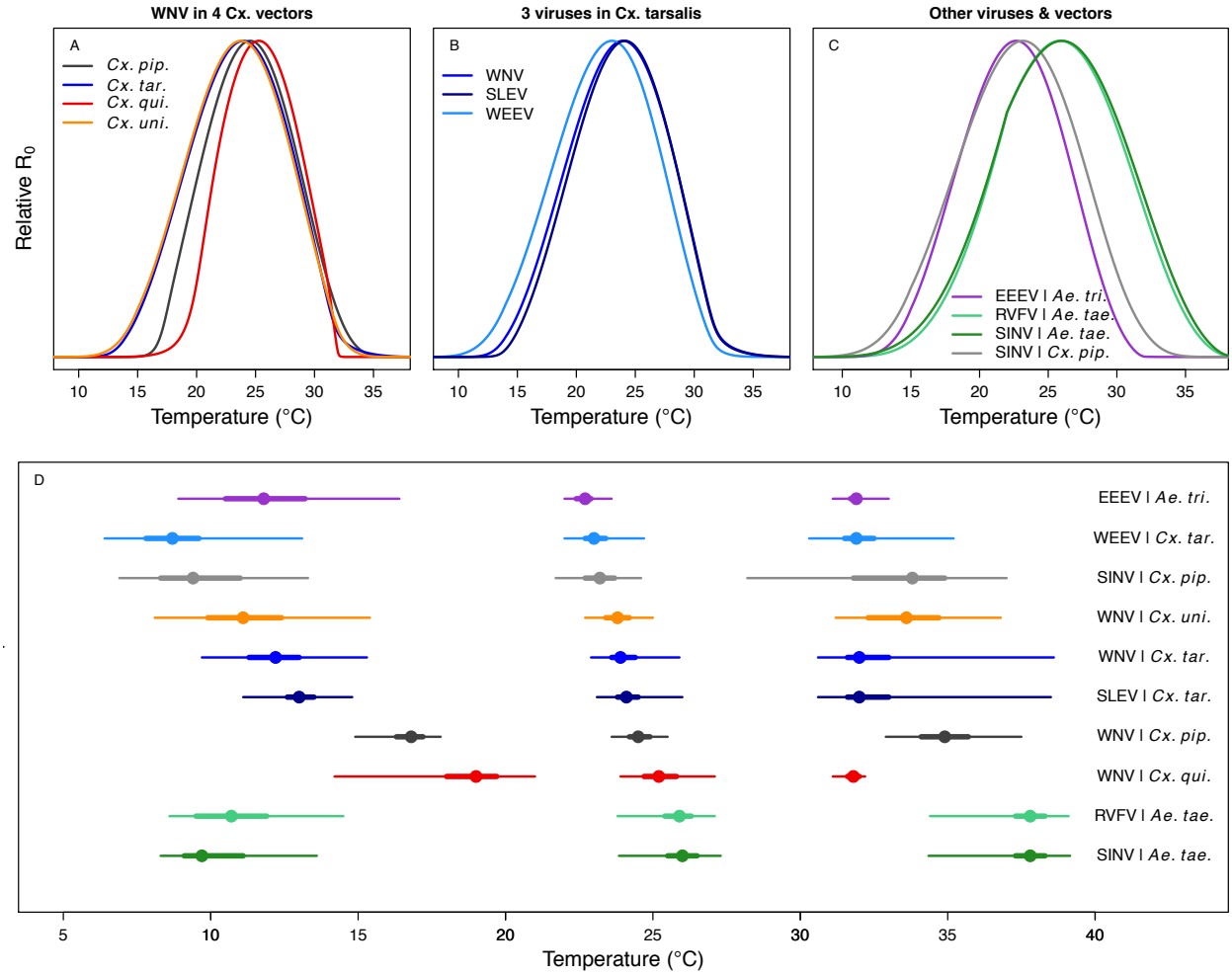

Figure 8: Incidence of human neuro-invasive West Nile disease across US counties responds unimodally to temperature, peaking at 23.9°C. Points are mean incidence (+/- SE) and mean temperature from May-September averaged from 2001-2016 for bins of 42 counties. Red contour is a locally estimated scatterplot smoothing (LOESS) regression (span = 0.6) fit to the raw county-level data (n = 3,109, binned for visual clarity). See Fig S23 for fits across a range of smoothing parameters.

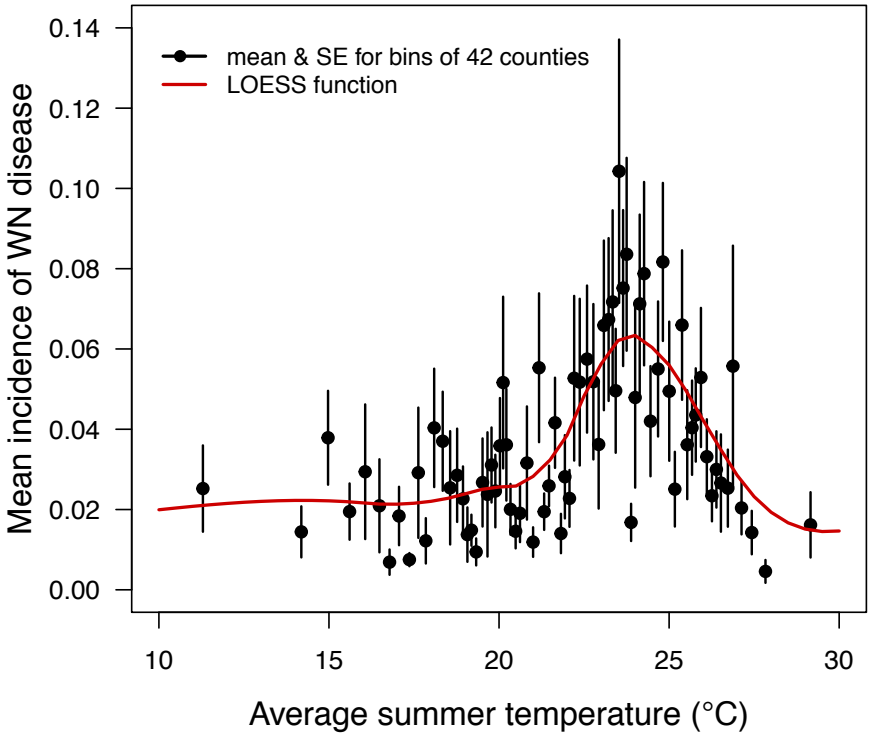

Figure 9: Temperature shapes the seasonal pattern of human cases of mosquito-borne viral diseases. Incidence (solid lines) lags behind predicted temperature-dependent R_0 (dashed lines) for human cases of neuro-invasive disease caused by West Nile virus (WNV, black), St. Louis encephalitis virus (SLEV, dark gray), and Eastern Equine Encephalitis virus (EEEV, light gray) by 2 months. This lag matches patterns in other mosquito-borne diseases, and is caused by the time required for mosquito populations to increase, become infectious, and bite humans, and for humans to present symptoms and seek medical care.

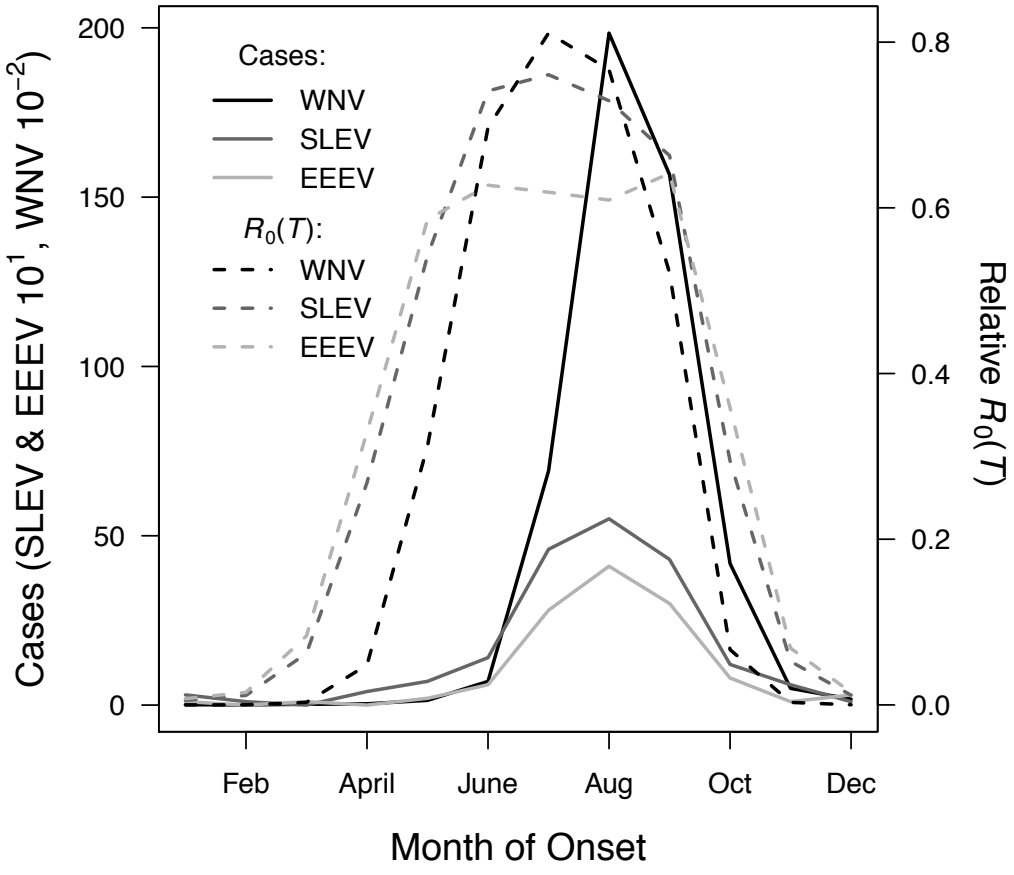

SUPPLEMENTAL MATERIAL for

Shocket et al. 'Transmission of West Nile virus and other temperate mosquito-borne viruses occurs at lower environmental temperatures than tropical mosquito-borne diseases'

List of Contents

1. Model, thermal response, and trait data information:
    a. R_0 model specifications 2
    b. Table S1: Trait thermal responses used in transmission (R_0) models 4
    c. Table S2-S6: Trait thermal response functions and data sources 5
    d. Table S7-S9: Priors for trait thermal response functions 9
2. Supplemental methods:
    a. Priors for trait thermal responses 12
    b. Sensitivity and uncertainty analyses 13
3. Supplemental figures:
    a. Fig S1: Mosquito trait thermal responses for additional vector species: *Aedes taeniorhynchus*, *Ae. triseriatus*, *Aedes vexans*, *Culex theileri* and *Culiseta melanura* 14
    b. Fig S2-9: Thermal responses for traits with individual data points 15
    c. Fig S10-19: Sensitivity and uncertainty analyses for R_0 models 23
    d. Fig S20: Histograms of T_{min}, optimum, and T_{max} for R_0 models 33
    e. Fig S21: Comparisons of alternative model parameterizations 34
    f. Fig S22: Comparison with previous transmission models for WNV 35
    g. Fig S23: LOESS models across varying span parameters 36
4. References 37

R_0 Model Specifications

The equation for R_0 (eq. 2 in main text) as a function of temperature (T) that was used in previous analyses [1–6] has fecundity measured as eggs per female per day (EFD):

$$\text{Full } R_0\text{: } R_0(T) = \left(\frac{a(T)^2 bc(T) e^{-\frac{\mu(T)}{PDR(T)}} EFD(T) EV(T) pLA(T) MDR(T)}{N\, r\, \mu(T)^3}\right)^{1/2} \qquad \text{eq. 2}$$

Fecundity data were not available directly as eggs per female per day, so we had to transform the available data to obtain the quantities needed for these models. The data for *Cx. pipiens* were reported as eggs per female per gonotrophic cycle ($EFGC$). To obtain EFD, we needed to divide $EFGC$ by the length of the gonotrophic cycle. In general, the gonotrophic cycle is assumed to be approximately the inverse of the biting rate. In fact, our 'biting rate' (a) data were observations of gonotrophic cycle duration. Accordingly, $EFD = EFGC * a$, resulting in the following equation for R_0:

$$R_0(T) = \left(\frac{a(T)^3 bc(T) e^{-\frac{\mu(T)}{PDR(T)}} EFGC(T) EV(T) pLA(T) MDR(T)}{N\, r\, \mu(T)^3}\right)^{1/2} \qquad \text{eq. S1}$$

Similarly, the fecundity data for *Cx. quinquefasciatus* were reported as eggs per raft (ER). Females lay rafts once per gonotrophic cycle. Thus, in order to obtain an approximation to EFD (eggs per female per day), we again divide by the number of days per gonotrophic cycle and, further, we multiply by the proportion of females ovipositing (pO), since not every female lays an egg raft. These changes result in the following equation for R_0:

$$R_0(T) = \left(\frac{a(T)^3 bc(T) e^{-\frac{\mu(T)}{PDR(T)}} ER(T) pO(T) EV(T) pLA(T) MDR(T)}{N\, r\, \mu(T)^3}\right)^{1/2} \qquad \text{eq. S2}$$

The remaining parameters that depend on temperature (T) are: adult mosquito mortality (μ, the inverse of lifespan [lf]), pathogen development rate (PDR, the inverse of the extrinsic incubation

period: the time required for exposed mosquitoes to become infectious), egg viability (proportion of eggs hatching into larvae, *EV*), proportion of larvae surviving to adulthood (*pLA*), and mosquito development rate (*MDR*, the inverse of the development period), and vector competence (*bc*, the proportion of exposed mosquitoes that become infectious). Vector competence is the product of infection efficiency (*c*, the proportion of exposed mosquitoes that develop a disseminated infection) and transmission efficiency (*b,* the proportion of infected mosquitoes that become infectious, with virus present in saliva). The form of vector competence varied between models based on the availability of data: $bc(T)$ [reported a single parameter], $c(T)*b(T)$ [both parameters reported separately], $c(T)$ only, or $b(T)$ only (see Table S1). The two remaining parameters do not depend on temperature: human density (N) and the rate at which infected hosts recover and become immune (r).

Table S1: Trait thermal responses used in transmission (R_0) models. Viruses: West Nile (WNV), Eastern and Western Equine Encephalitis (EEEV and WEEV), St. Louis Encephalitis (SLEV), Sindbis (SINV), and Rift Valley Fever (RVFV). *Ae. vex.* = *Ae. vexans, Cs. mel.* = *Culiseta melanura*; all other vectors (*Cx.* = *Culex*) listed under model names. Traits are: fecundity (as eggs/female/gonotrophic cycle [*EFGC*] or eggs per raft*proportion ovipositing [*ER*pO*]), egg viability (*EV*), larval-to-adult survival (*pLA*), mosquito development rate (*MDR*), lifespan (*lf*), biting rate (*a*), vector competence (*bc*, *b*c*, *b*, or *c*, as available), and parasite development rate (*PDR*). The WNV–*Cx. quinquefasciatus* model uses eq. S2 (*ER*pO*); the EEEV–*Ae. triseriatus* model uses *EFGC* from *Cx. pipiens* and *pO* from *Cs. melanura*; all other models use eq. S1 (*EFGC*). When data were missing for a vector–virus pair, we substituted the most conservative (i.e., least restrictive of transmission) trait thermal response from a vector that occurs within the geographic range of disease transmission. Several models had multiple potentially valid choices for traits; we explain and show compare these alternative models with the main text versions in Fig S21. Checkmarks indicate a thermal response from the vector in the model name. The parasite development rate data for SINV was insensitive to temperature (Fig 4), so the trait thermal response was omitted from the SINV models ('NA').

Model: virus–vector	***EFGC* or *ER*pO***	***EV***	***pLA***	***MDR***	***lf***	***a***	***bc, c*b c, or b***	***PDR***
WNV–*Cx. pipiens*	✓	✓	✓	✓	✓	✓	✓ (bc)	✓
WNV–*Cx. quinquefasciatus*	✓	✓	✓	✓	✓	✓	*Cx. uni.* (c*b)	✓
WNV–*Cx. tarsalis*	*Cx. pip.*	*Cx. pip*	✓	✓	✓	✓	✓ (b)	✓
WNV–*Cx. univittatus*	*Cx. pip.*	*Cx. pip.*	*Cx. pip.*	*Cx. pip.*	*Cx. pip.*	*Cx. pip.*	✓ (bc)	✓
WEEV–*Cx. tarsalis*	*Cx. pip.*	*Cx. pip.*	✓	✓	✓	✓	✓ (c*b)	✓
SLEV–*Cx. tarsalis*	*Cx. pip.*	*Cx. pip.*	✓	✓	✓	✓	✓ (c*b)	✓
EEEV–*Ae. triseriatus*	*Cx. pip.*, *Cs. mel.*	*Cx. pip.*	✓	✓	*Cx. pip.*	*Cs. mel.*	✓ (bc)	✓
SINV–*Cx. pipiens*	✓	✓	✓	✓	✓	✓	✓ (c)	NA
SINV–*Ae. taeniorhynchus*	*Cx. pip.*	*Ae. vex.*	*Ae. vex.*	*Ae. vex.*	✓	*Cx. pip.*	✓ (c)	NA
RVFV–*Ae. taeniorhynchus*	*Cx. pip.*	*Cx. the.*	*Ae. vex.*	*Ae. vex.*	✓	*Cx. pip.*	✓ (bc)	✓

Table S2: Trait thermal response functions and data sources: biting rate and fecundity traits. Asymmetrical responses fit with Brière function (**B**): $B(T) = qT(T - T_{min})(T_{max} - T)^{1/2}$; symmetrical responses fit with quadratic function (**Q**): $Q(T) = -q(T - T_{min})(T - T_{max})$. Median function coefficients and optima (with 95% credible intervals).

Trait / System	***F(x)***	***q* (CIs)**	***T_{min}* (CIs)**	***T_{max}* (CIs)**	***T_{opt}* (CIs)**
Biting rate (*a*)					
Cx. pipiens	B	$1.70 \cdot 10^{-4}$	9.4	39.6	32.7
[7–10]		($1.18–2.29 \cdot 10^{-4}$)	(2.8–13.4)	(37.9–40.6)	(31.3–33.6)
Cx. quinquefasciatus	B	$7.28 \cdot 10^{-5}$	3.1	39.3	31.9
[7,11]		($5.31–11.8 \cdot 10^{-5}$)	(0.1–10.9)	(38.0–40.8)	(30.6–33.3)
Cx. tarsalis	B	$1.67 \cdot 10^{-4}$	2.3	32.0	25.9
[11]		($0.87–2.56 \cdot 10^{-4}$)	(0.1–9.4)	(30.6–41.7)	(24.8–33.9)
Cs. melanura	B	$1.87 \cdot 10^{-4}$	7.8	31.8	26.4
[12]		($1.49–2.31 \cdot 10^{-4}$)	(5.5–11.4)	(31.0–33.4)	(25.7–27.9)
Fecundity					
Cx. pipiens (*EFGC*)	Q	$5.98 \cdot 10^{-1}$	5.3	38.9	22.1
[10]		($4.31–7.91 \cdot 10^{-1}$)	(2.6–8.5)	(36.2–41.8)	(20.1–24.4)
Cx. quinquefasciatus (*ER*)	Q	$6.36 \cdot 10^{-1}$	5.0	37.7	21.4
[13,14]		($4.50–9.05 \cdot 10^{-1}$)	(1.3–9.8)	(34.8–40.7)	(18.9–24.4)
Proportion ovipositing (*pO*)					
Cx. pipiens	Q	$4.45 \cdot 10^{-3}$	8.2	33.2	20.8
[7,15]		($2.54–7.77 \cdot 10^{-3}$)	(4.6–12.1)	(30.1–37.5)	(18.6–23.4)
Cx. quinquefasciatus	B	$6.67 \cdot 10^{-4}$	1.7	31.8	24.9
[7,13,15]		($5.80–7.91 \cdot 10^{-4}$)	(0.2–4.8)	(31.1–32.2)	(21.8–26.0)
Cs. melanura	Q	$6.31 \cdot 10^{-3}$	8.7	33.6	20.7
[12]		($4.52–7.89 \cdot 10^{-3}$)	(6.9–10.4)	(32.5–35.4)	(16.9–22.3)
Egg viability (*EV*)					
Ae. vexans		$1.24 \cdot 10^{-3}$	0	55.5	27.6
[16]		($0.73–1.95 \cdot 10^{-3}$)	(0–1.6)	(45.9–74.1)	(20.4–34.0)
Cx. pipiens	Q	$2.11 \cdot 10^{-3}$	3.2	42.6	23.0
[10]		($1.36–3.05 \cdot 10^{-3}$)	(0.5–7.1)	(39.7–48.3)	(20.7–26.3)
Cx. quinquefasciatus	B	$0.47 \cdot 10^{-3}$	13.6	38.0	32.1
[13,17]		($0.34–0.62 \cdot 10^{-3}$)	(9.3–16.8)	(37.2–38.7)	(31.3–32.7)
Cx. theileri	Q	$2.54 \cdot 10^{-3}$	5.5	45.4	23.6
[18]		($1.86–3.41 \cdot 10^{-3}$)	(2.6–8)	(42.4–49.0)	(18.2–27.0)

Data from additional species used for fitting priors only. Fecundity (*ER*): *Cx. pipiens molestus* [13], *Cx. pipiens pallens* [14], and *Ae. dorsalis* [19]. Proportion ovipositing (*pO*): *Cx. pipiens molestus* [13] and *Ae. dorsalis* [19]. Egg viability (*EV*): *Cx. pipiens molestus* [13], *Aedes dorsalis* [20], and *Ae. nigromaculis* [21].

Table S3: Trait thermal response functions and data sources: larval traits. Asymmetrical responses fit with Brière function (**B**): $B(T) = qT(T - T_{min})(T_{max} - T)^{1/2}$; symmetrical responses fit with quadratic function (**Q**): $Q(T) = -q(T - T_{min})(T - T_{max})$. Median function coefficients and optima (with 95% credible intervals).

Trait / System	***F(x)***	***q* (CIs)**	***T_{min}* (CIs)**	***T_{max}* (CIs)**	***T_{opt}* (CIs)**
Mosquito Dev. Rate (*MDR*)					
Ae. triseriatus	B	$4.30 \cdot 10^{-5}$	0.8	36.5	29.3
[22]		($3.01–5.83 \cdot 10^{-5}$)	(0–7.5)	(34.6–39.5)	(27.8–31.9)
Ae. vexans	B	$4.33 \cdot 10^{-5}$	1.9	38.2	30.9
[23,24]		($3.34–5.50 \cdot 10^{-5}$)	(0.1–10.5)	(37.0–39.5)	(29.8–32.2)
Cx. pipiens	B	$3.76 \cdot 10^{-5}$	0.1	38.5	30.9
[7–9,15,25–27]		($3.36–4.47 \cdot 10^{-5}$)	(0–4.0)	(37.6–39.8)	(30.2–31.9)
Cx. quinquefasciatus	B	$4.14 \cdot 10^{-5}$	0.1	38.6	31.0
[7,15,22,28,29]		($3.46–5.26 \cdot 10^{-5}$)	(0–5.5)	(37.4–40.6)	(30.0–32.6)
Cx. tarsalis	B	$4.12 \cdot 10^{-5}$	4.3	39.9	32.3
[30–32]		($3.15–5.47 \cdot 10^{-5}$)	(0–8.4)	(37.9–42.2)	(31.0–34.0)
Cs. melanura	B	$2.74 \cdot 10^{-5}$	8.6	37.6	31.1
[33]		($1.64–4.72 \cdot 10^{-5}$)	(0–16.8)	(35.1–40.4)	(28.7–33.7)
Larval survival (p_{LA})					
Ae. triseriatus	Q	$3.26 \cdot 10^{-3}$	8.3	35.7	22.0
[22,34]		($1.95–5.18 \cdot 10^{-3}$)	(4.9–11.4)	(32.9–39.7)	(19.9–24.6)
Ae. vexans	Q	$3.29 \cdot 10^{-3}$	9.1	40.8	25.0
[23,24]		($2.65–4.24 \cdot 10^{-3}$)	(8.1–10.6)	(38.4–43.6)	(23.9–26.2)
Cx. pipiens	Q	$3.60 \cdot 10^{-3}$	7.8	38.4	23.1
[7–9,15,25–27]		($2.96–4.42 \cdot 10^{-3}$)	(6.1–9.3)	(37.1–39.9)	(22.2–24.0)
Cx. quinquefasciatus	Q	$4.26 \cdot 10^{-3}$	8.9	37.7	23.3
[7,14,15,22,28,29,35]		($3.51–5.17 \cdot 10^{-3}$)	(7.6–9.9)	(36.2–39.2)	(22.5–24.0)
Cx. tarsalis	Q	$2.12 \cdot 10^{-3}$	5.9	43.1	24.6
[30–32]		($1.52–3.08 \cdot 10^{-3}$)	(3.0–8.8)	(39.8–47.5)	(22.9–26.4)
Cs. melanura	Q	$3.03 \cdot 10^{-3}$	10.1	36.2	23.2
[33]		($1.55–5.68 \cdot 10^{-3}$)	(5.7–15.1)	(32.8–40.7)	(20.4–26.5)

Data from additional species used for fitting priors only. Mosquito Development Rate (*MDR*): *Cx. pipiens molestus* [36,37], *Cx. pipiens pallens* [36], *Cx. restuans* [8,22,31,38], *Cx. salinarius* [22], *Ae. solicitans* [22], and *Ae. nigromaculis* [23]. Larval survival (p_{LA}): *Cx. pipiens molestus* [35,37], *Cx. pipiens pallens* [14], *Cx. restuans* [8,15,22,31,38], *Cx. salinarius* [22], *Ae. sollicitans* [22], *Ae. nigromaculis* [23].

Table S4: Trait thermal response functions and data sources: vector competence traits. Asymmetrical responses fit with Brière function (**B**): $B(T) = qT(T - T_{min})(T_{max} - T)^{1/2}$; symmetrical responses fit with quadratic function (**Q**): $Q(T) = -q(T - T_{min})(T - T_{max})$. Median function coefficients and optima (with 95% credible intervals).

Trait / System	***F(x)***	***q* (CIs)**	***T_{min}* (CIs)**	***T_{max}* (CIs)**	***T_{opt}* (CIs)**
Transmission efficiency (*b*)					
SLEV | *Cx. tarsalis* [39]	Q	$2.98 \cdot 10^{-3}$ ($1.63–5.31 \cdot 10^{-3}$)	10.8 (6.2–14.2)	41.6 (36.8–49.1)	26.2 (23.5–29.7)
WEEV | *Cx. tarsalis* [39]	Q	$3.17 \cdot 10^{-3}$ ($1.65–5.06 \cdot 10^{-3}$)	8.2 (5.1–10.7)	33.5 (31.0–38.9)	20.9 (19.2–23.2)
WNV | *Cx. tarsalis* [40]	Q	$2.94 \cdot 10^{-3}$ ($1.91–4.48 \cdot 10^{-3}$)	11.3 (7.6–14.0)	41.9 (37.7–47.0)	26.6 (23.9–29.3)
Infection efficiency (*c*)					
SINV | *Ae. taeniorhynchus* [41]	Q	$1.24 \cdot 10^{-3}$ ($0.75–2.17 \cdot 10^{-3}$)	1.4 (0–9.1)	48.4 (40.8–57.1)	25.4 (21.0–31.1)
SINV | *Cx. pipiens* [42]	Q	$1.33 \cdot 10^{-3}$ ($0.47–2.30 \cdot 10^{-3}$)	0 (0–0)	35.0 (28.1–61.1)	17.5 (14.1–30.5)
WNV | *Cx. pipiens* [43,44]	Q	$2.56 \cdot 10^{-3}$ ($2.05–3.19 \cdot 10^{-3}$)	15.6 (14.3–16.6)	52.2 (48.4–56.6)	33.9 (31.9–36.1)
SLEV | *Cx. tarsalis* [39]	Q	$2.03 \cdot 10^{-3}$ ($1.28–3.07 \cdot 10^{-3}$)	8.8 (6.6–10.6)	43.7 (38.9–51.4)	26.2 (24.2–29.7)
WEEV | *Cx. tarsalis* [39,45]	Q	$3.04 \cdot 10^{-3}$ ($2.52–3.68 \cdot 10^{-3}$)	1.3 (0.4–2.9)	38.8 (36.7–41.5)	15.5 (13.4–19.7)
Vector competence (*bc*)					
RVFV | *Ae. taeniorhynchus* [46]	Q	$1.51 \cdot 10^{-3}$ ($1.03–2.05 \cdot 10^{-3}$)	7.1 (2.8–9.8)	42.3 (39.3–46.5)	24.7 (22.0–27.0)
EEEV | *Ae. triseriatus* [47]	Q	$1.51 \cdot 10^{-3}$ ($0.96–2.24 \cdot 10^{-3}$)	7.0 (2.9–11.9)	50.3 (42.3–63.1)	28.8 (23.6–35.8)
WNV | *Cx. pipiens* [43]	Q	$3.05 \cdot 10^{-3}$ ($1.68–4.87 \cdot 10^{-3}$)	16.8 (15–17.9)	38.9 (36.1–44.1)	27.8 (26.6–30.1)
WEEV | *Cx. tarsalis* [45]	Q	$1.17 \cdot 10^{-3}$ ($0.55–2.36 \cdot 10^{-3}$)	5.1 (0.6–13.3)	37.0 (33.5–46.0)	21.4 (18.1–27.3)
WNV | *Cx. univittatus* [48]	Q	$2.32 \cdot 10^{-3}$ ($1.58–3.68 \cdot 10^{-3}$)	4.2 (1.5–7.1)	45.2 (39.6–53.0)	23.7 (19.4–27.3)

Table S5: Trait thermal response functions and data sources: parasite development rate. Asymmetrical responses fit with Brière function (**B**): $B(T) = qT(T - T_{min})(T_{max} - T)^{1/2}$; symmetrical responses fit with quadratic function (**Q**): $Q(T) = -q(T - T_{min})(T - T_{max})$. Median function coefficients and optima (with 95% credible intervals).

Trait / System	***F(x)***	***q* (CIs)**	***T_{min}* (CIs)**	***T_{max}* (CIs)**	***T_{opt}* (CIs)**
Parasite Dev. Rate (*PDR*)					
RVFV | *Ae. taeniorhynchus* [46]	B	$8.84 \cdot 10^{-5}$ ($2.51–15.5 \cdot 10^{-5}$)	9.0 (5.4–13.8)	45.9 (41.9–50.3)	37.8 (34.5–41.3)
EEEV | *Ae. triseriatus* [47]	B	$7.05 \cdot 10^{-5}$ ($5.21–9.68 \cdot 10^{-5}$)	11.6 (7.0–16.4)	44.8 (40.6–49.4)	37.2 (33.8–41.1)
WNV | *Cx. pipiens* [43,44]	B	$7.38 \cdot 10^{-5}$ ($5.38–9.94 \cdot 10^{-5}$)	11.4 (7.3–15.0)	45.2 (40.7–50.3)	37.5 (33.8–41.6)
WNV | *Cx. quinquefasciatus* [49]	B	$7.12 \cdot 10^{-5}$ ($4.58–10.2 \cdot 10^{-5}$)	19.0 (12.9–21.0)	44.1 (38.8–50.4)	37.7 (33.6–42.7)
SLEV | *Cx. tarsalis* [39]	B	$7.11 \cdot 10^{-5}$ ($5.60–8.95 \cdot 10^{-5}$)	12.8 (10.3–14.3)	45.2 (40.2–51.5)	37.7 (33.8–42.6)
WEEV | *Cx. tarsalis* [39,45]	B	$6.43 \cdot 10^{-5}$ ($4.44–10.4 \cdot 10^{-5}$)	4.0 (0–12.6)	44 .0 (38.3–50.9)	35.7 (31.0–41.4)
WNV | *Cx. tarsalis* [40]	B	$6.57 \cdot 10^{-5}$ ($5.11–8.85 \cdot 10^{-5}$)	11.2 (7.9–14.9)	44.7 (40.4–49.4)	37.0 (33.6–40.9)
WNV | *Cx. univittatus* [48]	B	$7.54 \cdot 10^{-5}$ ($4.13–11.1 \cdot 10^{-5}$)	10.2 (7.1–15.3)	34.4 (31.2–51.1)	28.8 (26.1–42.5)
SINV | *Ae. taeniorhynchus* [41]	NA	Not fitted because lack of temperature sensitivity			

Table S6: Trait thermal response functions and data sources: lifespan. Responses fit with a linear function (**L**): $L(T) = -mT + z$. Median function coefficients and T_{max} (with 95% credible intervals).

Trait / System	***F(x)***	***m***	***z***	***Tmax = z/m***
Lifespan (*lf*)				
Ae. taeniorhynchus [50]	L	2.02 (1.59–3.19)	85.9 (73.8–117.6)	42.7 (34.5–48.5)
Cx. pipiens [9,15,51]	L	4.86 (3.83–5.84)	169.8 (142.1–195.6)	34.9 (32.9–37.9)
Cx. quinquefasciatus [15,35]	L	3.80 (1.85–5.29)	136.3 (86.8–174.0)	35.9 (32.1–48.5)
Cx. tarsalis [30]	L	1.69 (1.12–2.24)	69.6 (55.8–83.5)	41.3 (36.6–50.8)

Data from additional species used for fitting priors only. Lifespan (*lf*): *Cx. pipiens molestus* [35,36], *Cx. pipiens pallens* [36], and *Cx. restuans* [15].

Table S7: Priors for trait thermal response functions: mosquito traits with unimodal responses. Gamma distribution parameters (α [shape] and β [rate]) for priors for fitting thermal response parameters (T_{min}, T_{max}, and q). Scaled variances are noted in parentheses, either by the system name (applied to priors all parameters) or by individual parameters. See *Supplemental Methods: Priors for trait thermal responses*.

Trait / System	***q*: *α***	***q*: *β***	***T_{min}*: *α***	***T_{min}*: *β***	***T_{max}*: *α***	***T_{max}*: *β***
Biting rate (*a*)						
Cx. pipiens (0.5)	8.84	64200	1.91	0.367	103	3.00
Cx. quinquefasciatus	39.1 (0.1)	234133 (0.1)	8.82 (0.1)	0.997 (0.1)	2992	75.8
Cx. tarsalis	40.1 (0.05)	227752 (0.05)	18.7 (0.05)	1.745 (0.05)	2891	73.1
Cs. melanura	35.4 (0.75)	229694 (0.75)	7.77 (0.75)	0.895 (0.75)	2714 (0.1)	68.5 (0.1)
Fecundity						
Cx. pipiens (*EFGC*) (3)	9.23	15.6	2.38	0.419	139	3.52
Cx. quinquefasciatus (*ER*)	19.1	30.44	2.87	0.600	486	13.2
Prop. ovipositing (*pO*)						
Cx. pipiens (0.5)	9.50	1823	14.8	1.495	263	7.14
Cx. quinquefasciatus	32.9	55242	1.41	0.397	3346	106
Cs. melanura	14.4	2635	22.0	2.254	588	16.8
Egg viability (*EV*)						
Ae. vexans (0.01)	26.6	12259	11.6	1.916	486	10.8
Cx. pipiens (0.2)	29.4	14525	8.83	1.579	514	11.1
Cx. quinquefasciatus (0.1)	101	262268	1.08	1.032	1361	34.9
Cx. theileri	5.86	2266	4.46	0.591	266	6.06
Mos. dev. rate (*MDR*)						
Ae. triseriatus (0.2)	118	2697528	1.93	0.703	5542	145
Ae. vexans (0.5)	119	2739401	1.89	0.689	6661	174
Cx. pipiens (0.1)	71.9	1545915	2.03	0.596	2912	76.5
Cx. quinquefasciatus (0.1)	113	2569782	1.81	0.651	5900	155
Cx. tarsalis (0.1)	129	2940582	1.49	0.660	6431	169
Cs. melanura (0.1)	129	2941063	1.78	0.685	6915	181
Larval survival (p_{LA})						
Ae. triseriatus (0.05)	163	46723	231	27.3	4667	122
Ae. vexans (0.05)	135	37701	210	24.6	4040	107
Cx. pipiens (0.1)	102	27382	217	24.2	2872	76.7
Cx. quinquefasciatus (0.1)	88.8	26461	123	14.8	2608	68.4
Cx. tarsalis (0.025)	94.6	23240	237	26.2	2564	69.5
Cs. melanura (0.05)	148.9	41533	239	27.8	4391	116

Table S8: Priors for trait thermal response functions: infection traits. Gamma distribution parameters (α [shape] and β [rate]) for priors for fitting thermal response parameters (T_{min}, T_{max}, and q). Scaled variances are noted in parentheses, either by the system name (applied to priors all parameters) or by individual parameters. See *Supplemental Methods: Priors for trait thermal responses*.

Trait / System	***q*: *α***	***q*: *β***	***T_{min}*: *α***	***T_{min}*: *β***	***T_{max}*: *α***	***T_{max}*: *β***
Transmission efficiency (*b*)	7.72	3202	9.97	1.268	114	2.9
SLEV | *Cx. tarsalis* (0.5)	9.49	2373	79.6	6.181	153	3.74
WEEV | *Cx. tarsalis* (0.1)	8.46	3056	12.1	1.455	134	3.5
WNV | *Cx. tarsalis*	7.72	3202	9.97	1.268	114	2.9
Infection efficiency (*c*)						
SINV | *Ae. taeniorhynchus* (0.1)	61.7	45102	2.49	0.815	1214	25.1
SINV | *Cx. pipiens* (0.01)	57.3	40236	2.64	0.799	1124	23.28
WNV | *Cx. pipiens*	28.5	15944	1.44	0.852	237	5.393
SLEV | *Cx. tarsalis*	65.2 (0.01)	46656 (0.01)	1.67 (0.01)	0.692 (0.01)	1071 (0.1)	22.2 (0.1)
WEEV | *Cx. tarsalis* (0.01)	82.2	35791	392	30.502	1264	26.1
Vector competence (*bc*)						
RVFV | *Ae. taeniorhynchus* (2)	8.4	4775	2.316	0.421	147	3.39
EEEV | *Ae. triseriatus*	6.68 (3)	3612 (3)	2.027 (3)	0.383 (3)	119 (0.01)	2.86 (0.01)
WNV | *Cx. pipiens* (0.5)	17.6	7857	1.403	0.534	219	5.42
WEEV | *Cx. tarsalis* (0.5)	9.56	5344	3.021	0.498	180	4.05
WNV | *Cx. univittatus*	13.7 (0.01)	2327 (0.01)	380 (0.01)	22.434 (0.01)	527 (0.1)	14.4 (0.1)
Parasite dev. rate (*PDR*)						
RVFV | *Ae. taeniorhynchus*	20.2 (0.2)	331065 (0.2)	8.69 (2)	0.893 (2)	227 (2)	4.96 (2)
EEEV | *Ae. triseriatus* (2)	13.2	167635	6.76	0.609	183	4.05
WNV | *Cx. pipiens*	8.71 (2)	113904 (2)	3.51 (5)	0.356 (5)	140 (2)	3.17 (2)
WNV | *Cx. quinquefasciatus*	15.8	201154	8.09	0.772	202	4.44
SLEV | *Cx. tarsalis*	11.8	151149	6.31	0.584	179	3.97
WEEV | *Cx. tarsalis*	10.3	117795	9.97 (0.05)	0.768 (0.05)	162	3.62
WNV | *Cx. tarsalis* (2)	11.7	148079	5.92	0.541	169	3.77
WNV | *Cx. univittatus*	12.3	146439	9.02 (3)	0.773 (3)	174 (0.2)	3.87 (0.2)

Table S9: Priors for trait thermal response functions: lifespan. Gamma distribution parameters (α [shape] and β [rate]) for priors for fitting thermal response parameters (*m* and *z*). Scaled variances are noted in parentheses, either by the system name (applied to priors all parameters) or by individual parameters. See *Supplemental Methods: Priors for trait thermal responses*.

Trait / System **(var.)**	***m*: *α***	***m*: *β***	**z: *α***	**z: *β***
Lifespan (*lf*)				
Ae. taeniorhynchus (0.01)	119	52.9	268	3.19
Cx. pipiens (0.01)	117	42.4	238	2.39
Cx. quinquefasciatus (0.01)	110	32.9	207	1.78
Cx. tarsalis (0.1)	124	43.0	249	2.42

Supplemental Methods: Priors for trait thermal responses

We used gamma distribution parameters (α [shape] and β [rate]) for informative priors for each thermal response parameter (Brière and quadratic functions: T_{min}, T_{max}, and q); linear functions: m and z). First, we fit a thermal response function (with uniform priors) to all the *Aedes* and *Culex* data for a given trait except that of the focal vector species or vector–virus pair (i.e., the parameters for the priors for a for *Culex pipiens* were fit to the a data for all species except *Cx. pipiens*). Then we used the 'MASS' package in R to fit a gamma distribution hyperparameters to the distribution from each thermal response parameters.

The mean of the gamma distribution is equal to α/β, while the variance is determined by the magnitude of the parameters (smaller values = higher variance). When fitting thermal responses, the appropriate strength for the priors depends on the amount of data used to fit the priors and the amount of the data for the focal trait. Prior strengths can be modified by scaling the variance (i.e., multiplying the gamma parameters by <1 to increase the variance or >1 to decrease the variance) without impacting the mean. In many cases we had to increase the variance because of the large number of data points used to fit priors. In a few cases, we had to decrease the variation (e.g., to constrain T_{max} for Briere functions for *PDR* where we had no observations at high temperatures, in order to make it so *PDR* would not constrain R_0 where there was no data).

Supplemental Methods: Sensitivity and uncertainty analyses

We performed two sensitivity analyses and one uncertainty analysis to understand what traits were most important for determining and contributing to uncertainty in the thermal limits and optima. For the first sensitivity analysis, we calculated the partial derivatives of R_0 with respect to each trait across temperature (T) and multiplied it by the derivative of the trait with temperature (i.e., the slope of the thermal response). Equations S3-S6 (below) apply to both versions of the R_0 model (eqs. S1 and S2). Equation S3 is for to all traits (x) that appear once in the numerator. Equation S4, for biting rate (a), differs from previous analyses [2–6] because biting rate was cubed to account for fecundity measured per gonotrophic cycle rather than per day. Equation S5 is for parasite development rate (PDR), and equation S6 is for lifespan (lf).

$$\frac{\partial R_0}{\partial x} \cdot \frac{\partial x}{\partial T} = \frac{R_0}{2x} \cdot \frac{\partial x}{\partial T} \qquad \text{eq. S3}$$

$$\frac{\partial R_0}{\partial a} \cdot \frac{\partial a}{\partial T} = \frac{3R_0}{2a} \cdot \frac{\partial a}{\partial T} \qquad \text{eq. S4}$$

$$\frac{\partial R_0}{\partial PDR} \cdot \frac{\partial PDR}{\partial T} = \frac{R_0}{2\, lf\, PDR^2} \cdot \frac{\partial PDR}{\partial T} \qquad \text{eq. S5}$$

$$\frac{\partial R_0}{\partial lf} \cdot \frac{\partial lf}{\partial T} = \frac{R_0(1+3PDR)}{2\, PDR\, lf^2} \cdot \frac{\partial lf}{\partial T} \qquad \text{eq. S6}$$

For the second sensitivity analysis, we held single traits constant while allowing all other traits to vary with temperature. For the uncertainty analysis, we calculated the 'total uncertainty' across temperature as the width of the 95% highest posterior density (HPD) interval across temperature for the full model. Then, we calculated the HPD for 'uncertainty for each trait' by fixing all traits except the focal trait at their posterior median value across temperature, while keeping the full posterior sample of the focal trait. Then, we divided the uncertainty for each trait by the total uncertainty, calculated across temperature, to estimate the proportion of uncertainty in R_0 that was due to the uncertainty in the focal trait.

Figure S1: Thermal responses for mosquito traits in additional vector species: *Ae. taeniorhynchus* (green), *Ae. triseriatus* (violet), *Aedes vexans* (teal), *Cx. theileri* (pink), and *Culiseta melanura* (brown). (A) Mosquito development rate (*MDR*), (B) larval-to-adult survival (*pLA*), and (C) biting rate (*a*), (D) lifespan (*lf*), (E) proportion ovipositing (*pO*) and (F) egg viability (*EV*). Points without error bars are reported means from single studies; points with error bars are averages of means from multiple studies (+/- standard error, for visual clarity only; thermal responses were fit to reported means). Solid lines are posterior distribution means; shaded areas are 95% credible intervals.

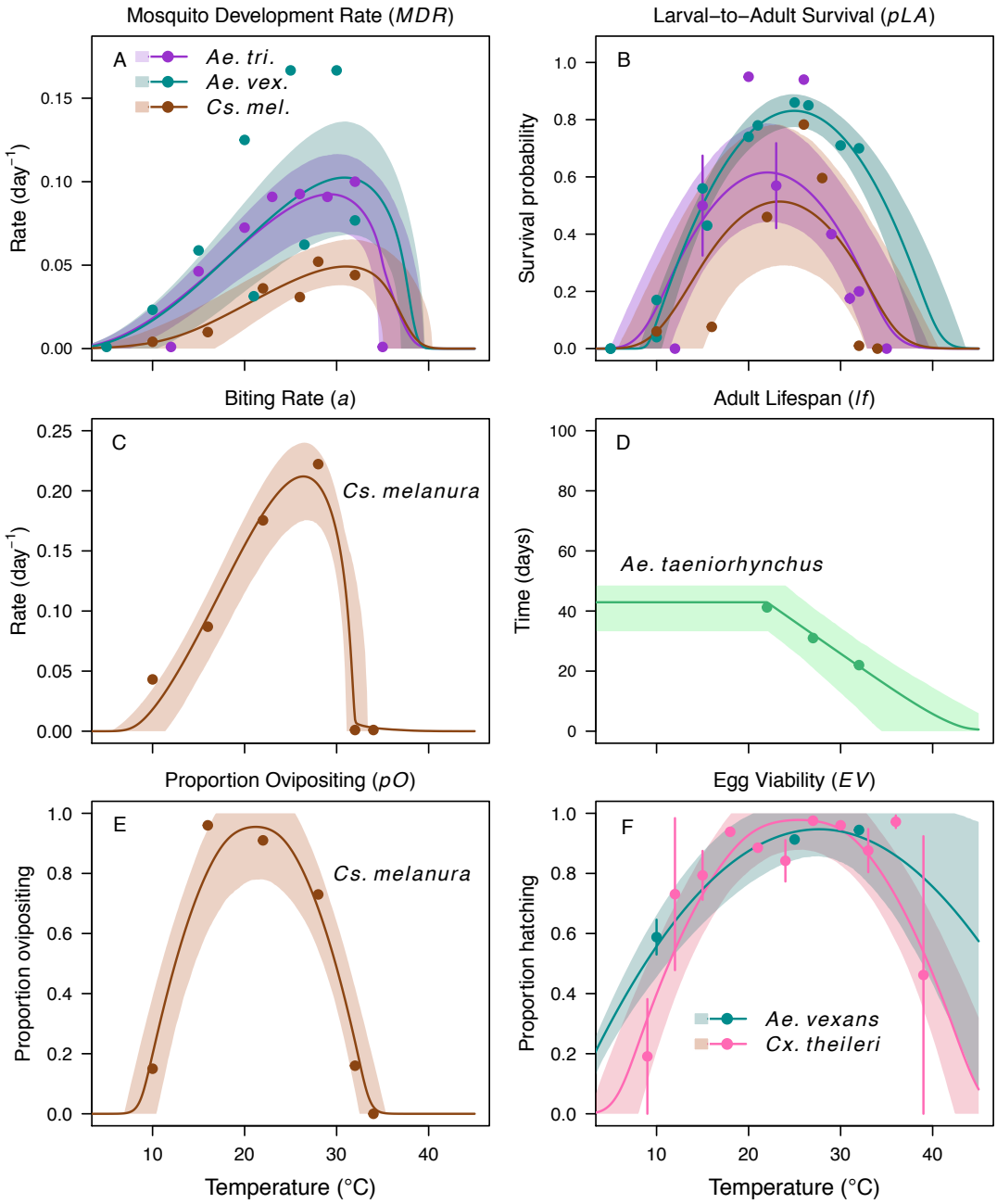

Figure S2: Thermal responses for biting rate (*a*) showing individual data points. (A) C*ulex pipiens*, (B), *Cx. quinquefasciatus*, (C) *Cx. tarsalis*, and (D) *Culiseta melanura*.

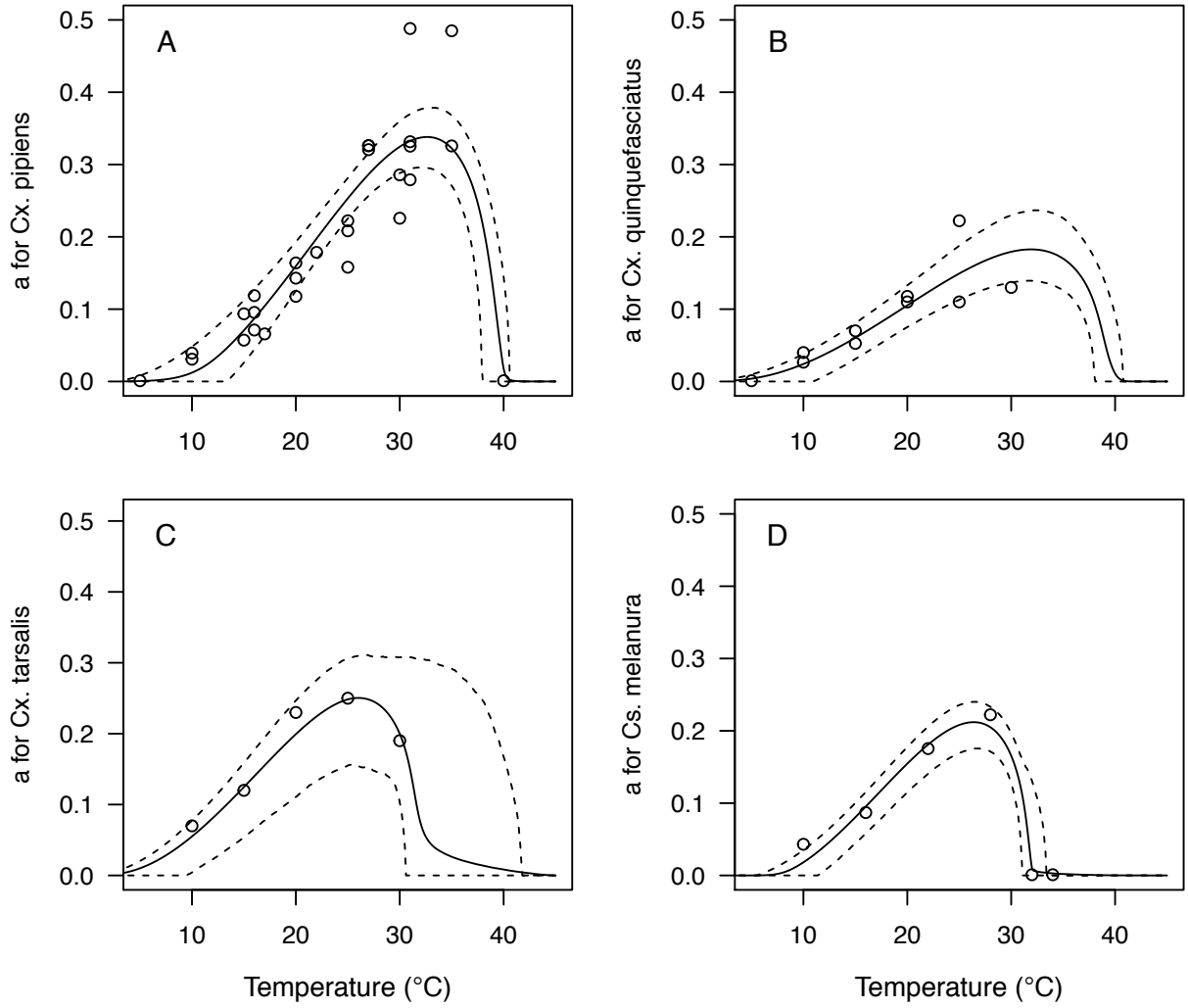

Figure S3: Thermal responses for larval-to-adult survival (*pLA*) showing individual data points. (A) *Culex pipiens*, (B), *Cx. quinquefasciatus*, (C) *Cx. tarsalis*, (D) *Aedes vexans*, (E) *Ae. triseriatus*, and (F) *Culiseta melanura*.

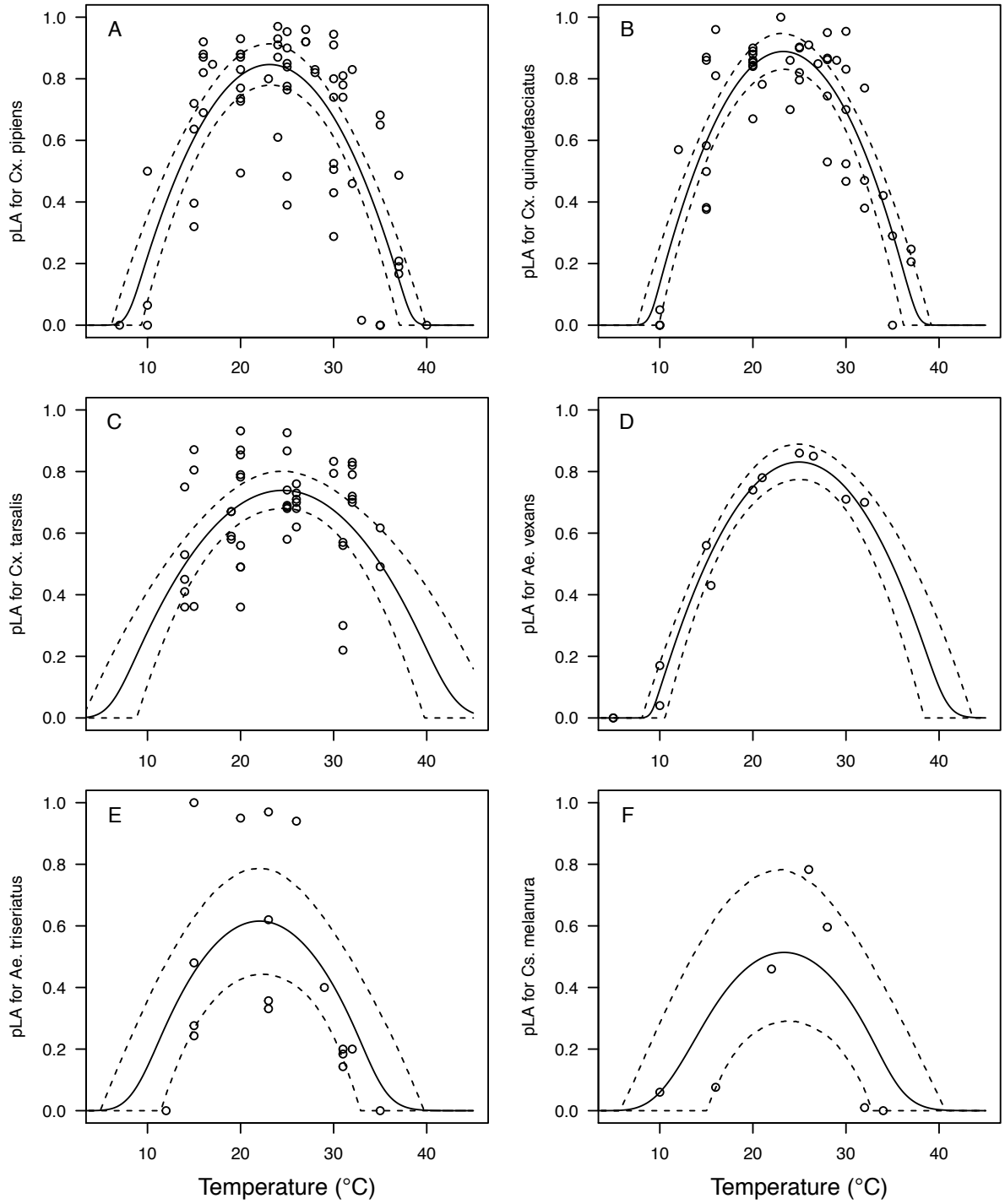

Figure S4: Thermal responses for mosquito development rate (*MDR*) showing individual data points. (A) *Culex pipiens*, (B), *Cx. quinquefasciatus*, (C) *Cx. tarsalis*, (D) *Aedes vexans*, (E) *Ae. triseriatus*, and (F) *Culiseta melanura*.

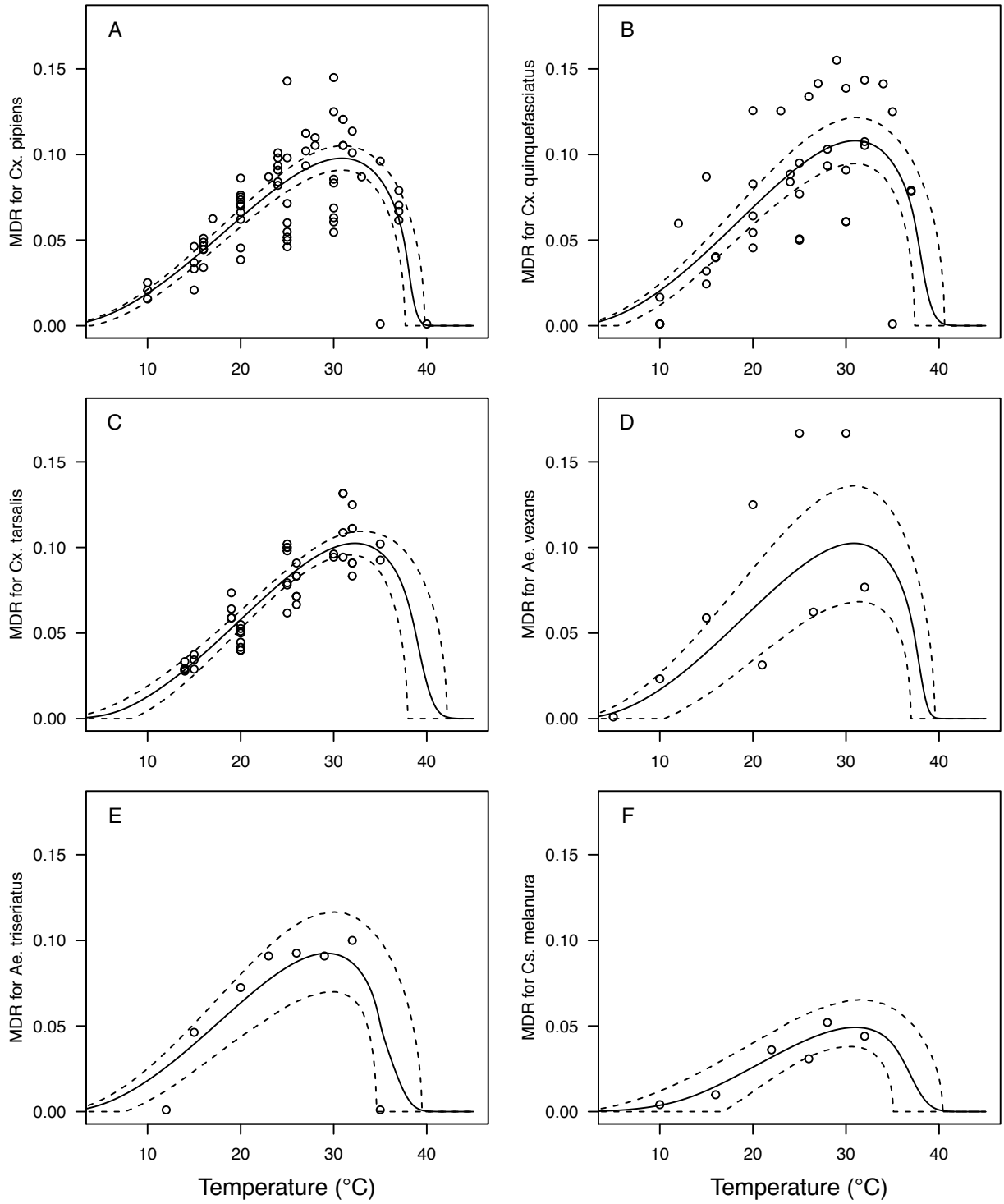

Figure S5: Thermal responses for adult mosquito lifespan (*lf*) showing individual data points. (A) *Culex pipiens*, (B), *Cx. quinquefasciatus*, (C) *Cx. tarsalis*, and (D) *Aedes taeniorhynchus*. When data were reported by sex, only female data were used.

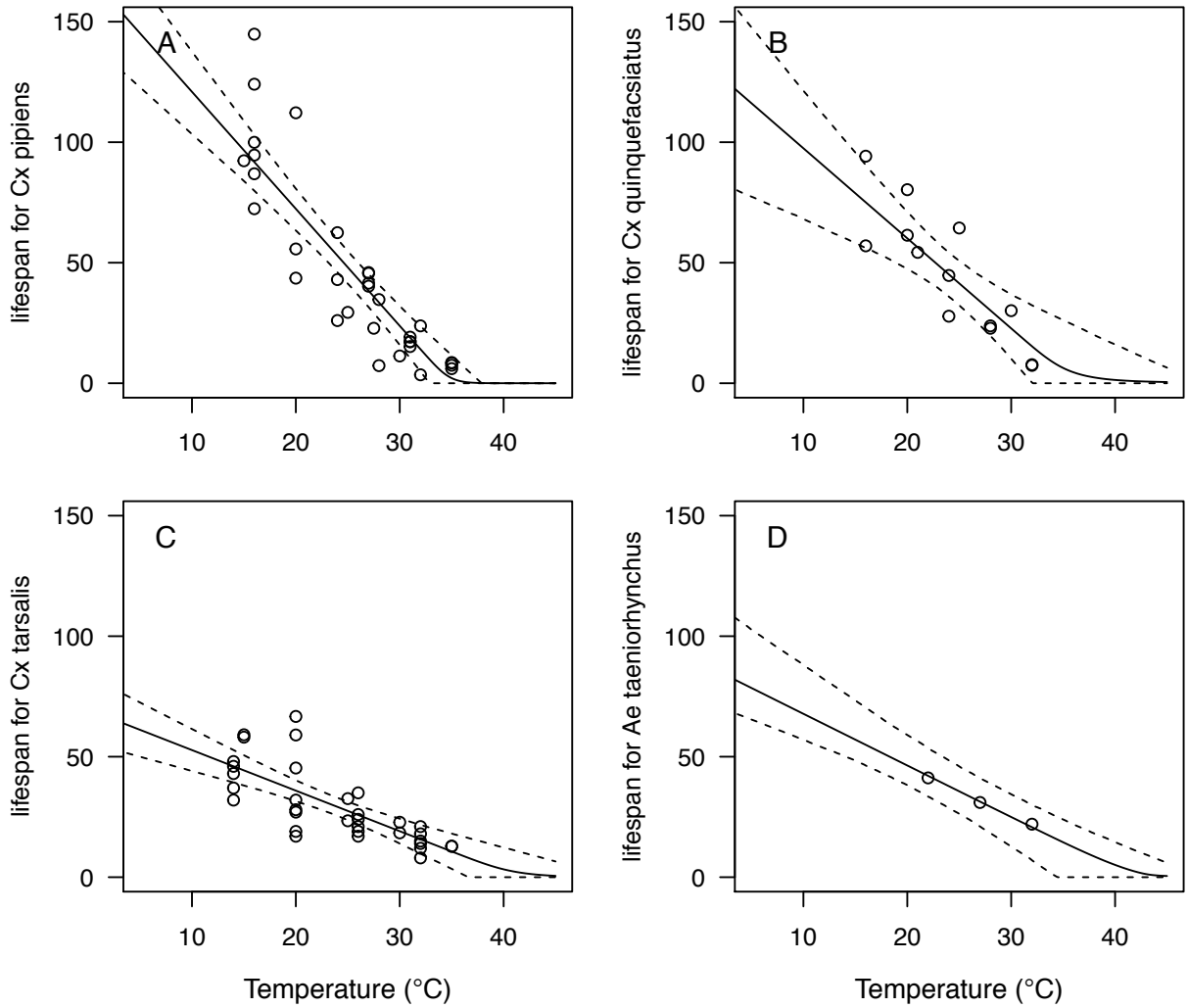

Figure S6: Thermal responses for fecundity traits showing individual data points. Traits: (A) Reproduction measured as eggs per female per gonotrophic cycle (*EFGC*), (B) reproduction measured as eggs per raft (*ER*) (C–E) proportion ovipositing (*pO*), and (F–I) egg viability (*EV*). Vector species: (A,C,F) *Culex pipiens*, (B,D,G), *Cx. quinquefasciatus*, (E) *Culiseta melanura*, (H) *Cx. theileri*, and (I) *Aedes vexans*.

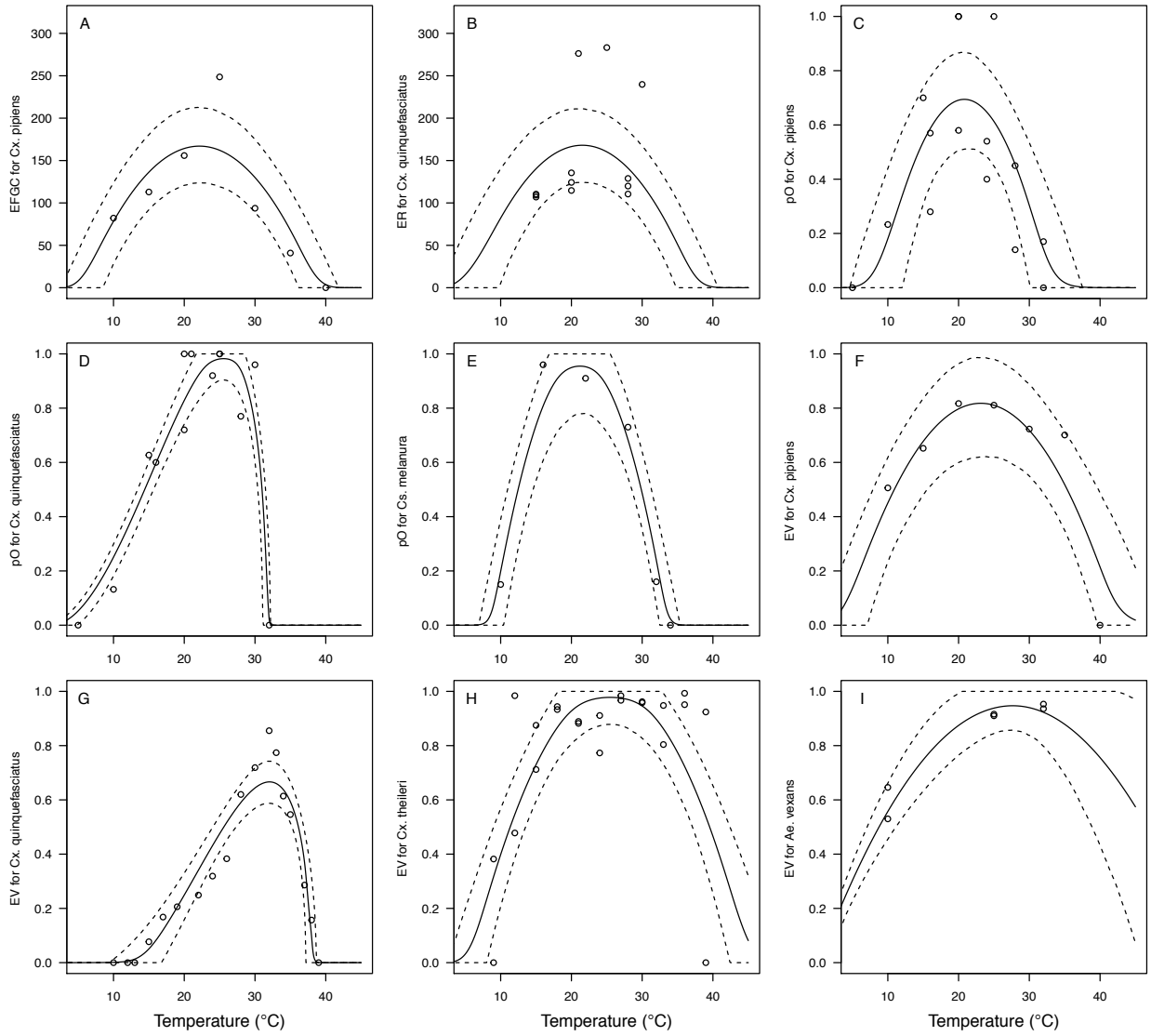

Figure S7: Thermal responses for pathogen development rate (*PDR*) showing individual data points. (A) West Nile virus (WNV) in *Culex pipiens*, (B), WNV in *Cx. quinquefasciatus*, (C) WNV in *Cx. tarsalis*, (D) WNV in *Cx. univittatus*, (E) St. Louis Encephalitis virus (SLEV) in *Cx. tarsalis*, (F) Western Equine Encephalitis virus (WEEV) in *Cx. tarsalis*, and (G) Eastern Equine Encephalitis virus (EEEV) in *Aedes triseriatus*.

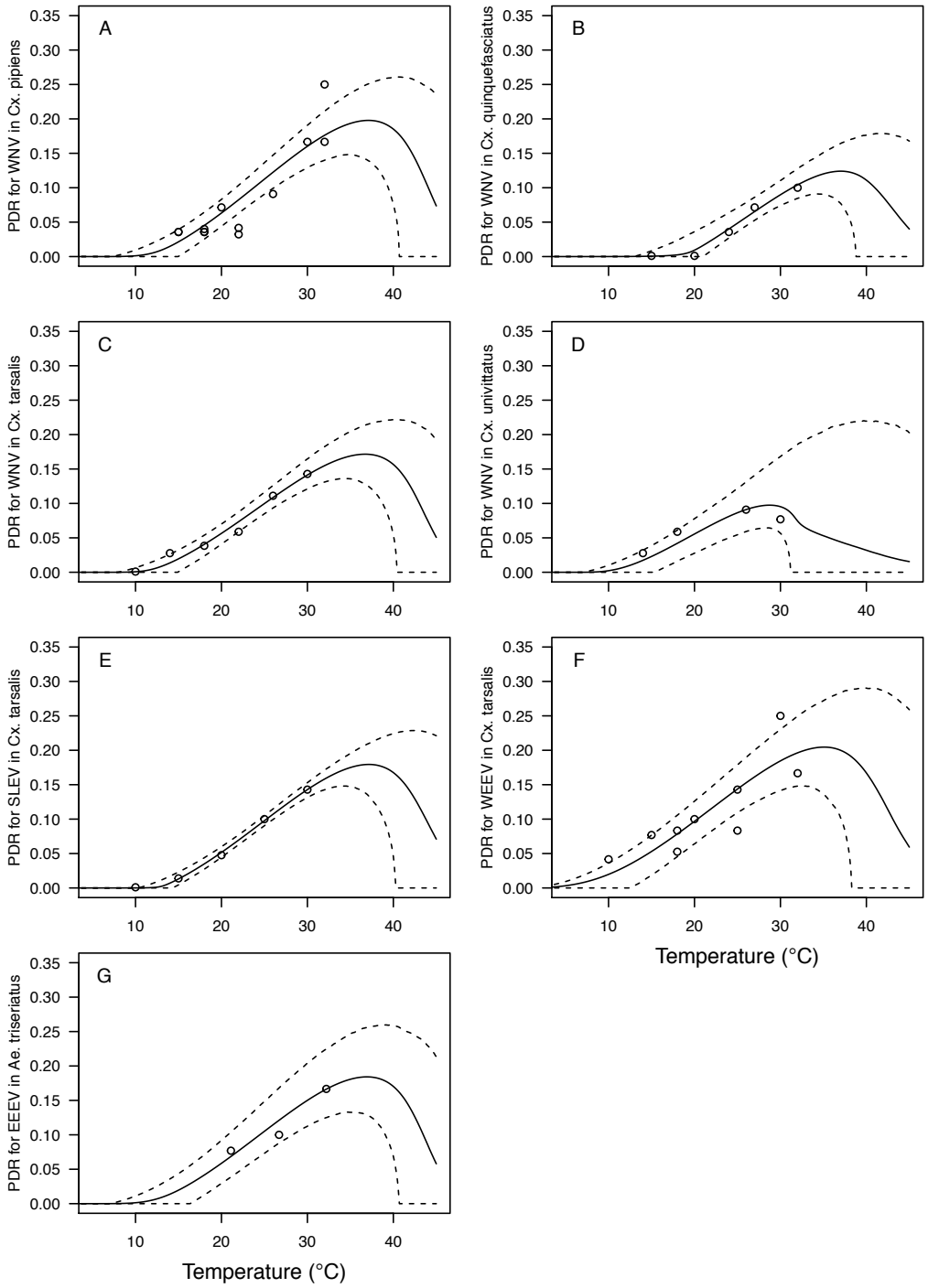

Figure S8: Thermal responses for vector competence traits in *Culex tarsalis*, showing individual data points. Traits: (A,B,F) transmission efficiency (*b*, # transmitting / # infected), (C,E) infection efficiency (*c*, # infected / # exposed), and (D) vector competence (*bc*, # infected / # exposed). Viruses: (A) West Nile virus (WNV), (B–D) Western Equine Encephalitis virus (WEEV), (E,F) St. Louis Encephalitis virus (SLEV).

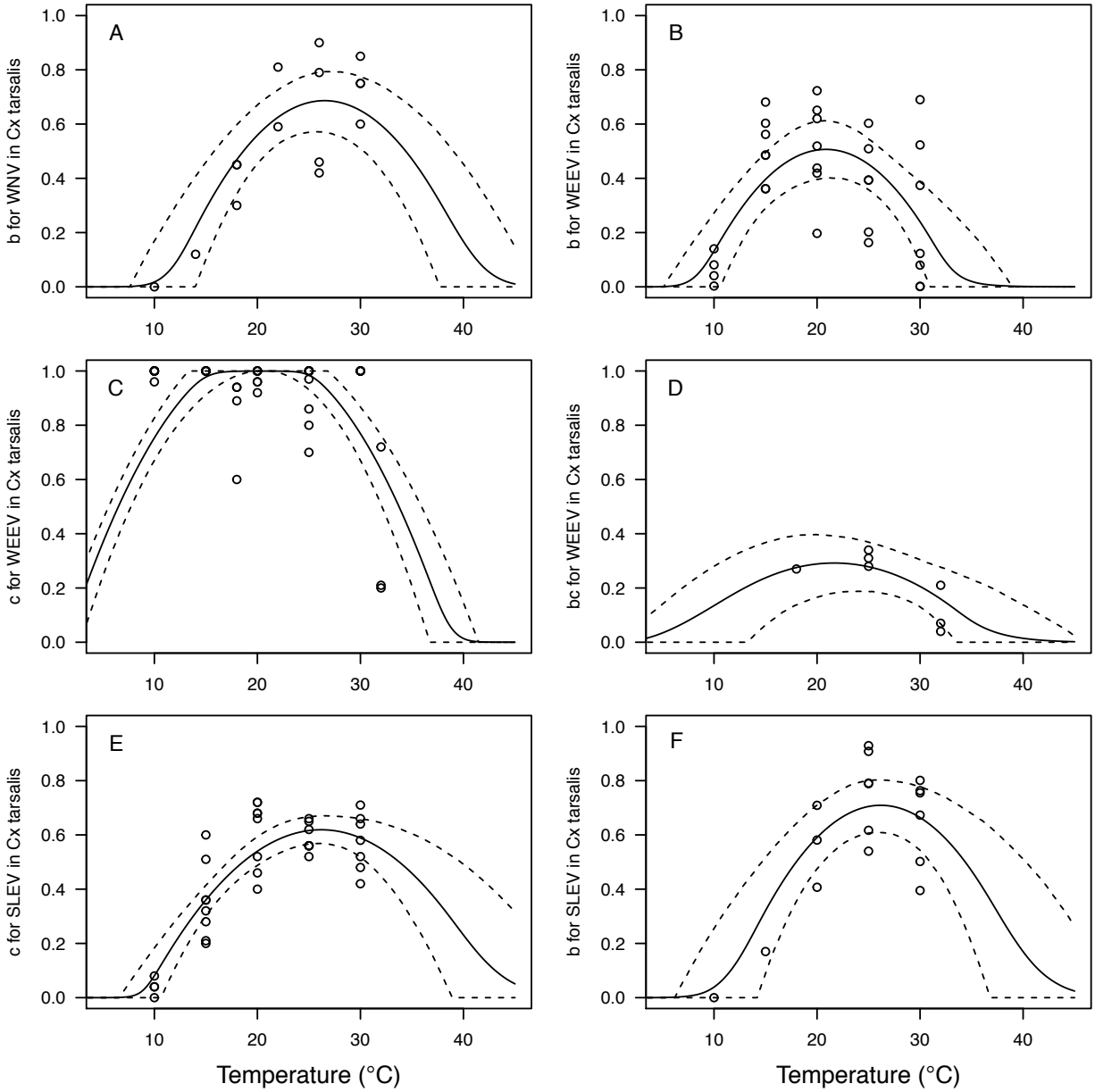

Figure S9: Thermal responses for vector competence traits showing individual data points. Traits: (A,E,F) infection efficiency (*c*, # infected / # exposed) and (B,C,D,G) vector competence (*bc*, # infected / # exposed). Viruses and vectors: (A,B) West Nile virus (WNV) in *Culex pipiens*, (C) WNV in *Cx. univittatus*, (D) Eastern Equine Encephalitis virus (EEEV) in *Ae. triseriatus*, (E) Sindbis virus (SINV) in *Culex pipiens*, (F) SINV in *Aedes taeniorhynchus*, and (G) RVFV in *Ae. taeniorhynchus*

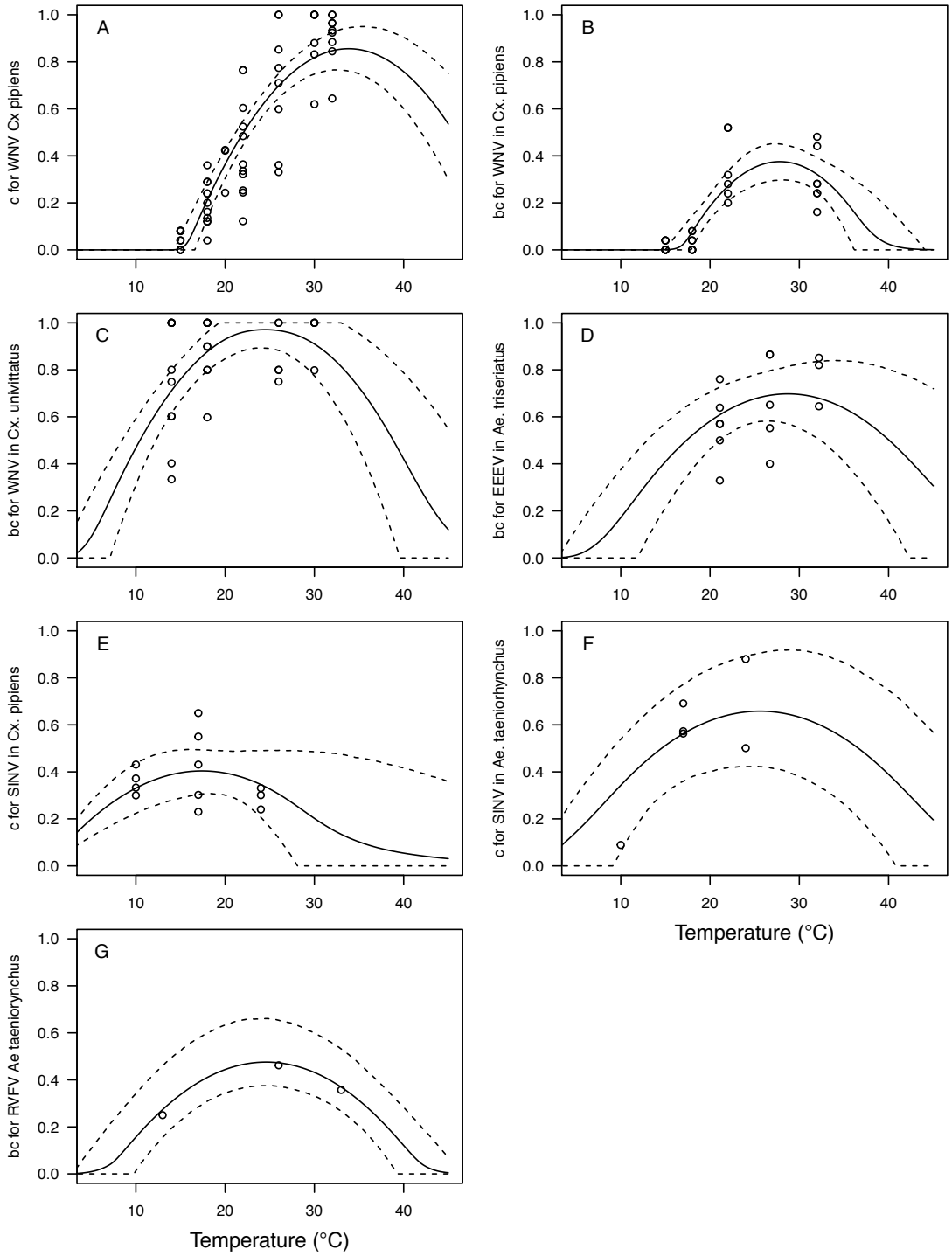

Figure S10: Temperature-dependent R_0, sensitivity analyses, and uncertainty analysis for model of West Nile Virus (WNV) in *Culex pipiens*. (A) Median temperature-dependent R_0 (black line) with 95% credible intervals (dashed red lines). (B) Sensitivity analysis #1: derivative with respect to temperature for R_0 (black) and partial derivatives with respect to temperature for each trait. (C) Sensitivity analysis #2: relative R_0 calculated with single traits held constant. (D) Uncertainty analysis using highest posterior density (HPD) interval widths: the proportion of total uncertainty due to each trait. (B-D) Trait colors: biting rate (*a*, red), vector competence (*bc*, orange), adult lifespan (*lf*, green), parasite development rate (*PDR*, cyan), fecundity (*EFGC*, light blue), egg viability (*EV*, dark blue), larval survival (*pLA*, purple), and mosquito development rate (*MDR*, pink). All traits from *Cx. pipiens*.

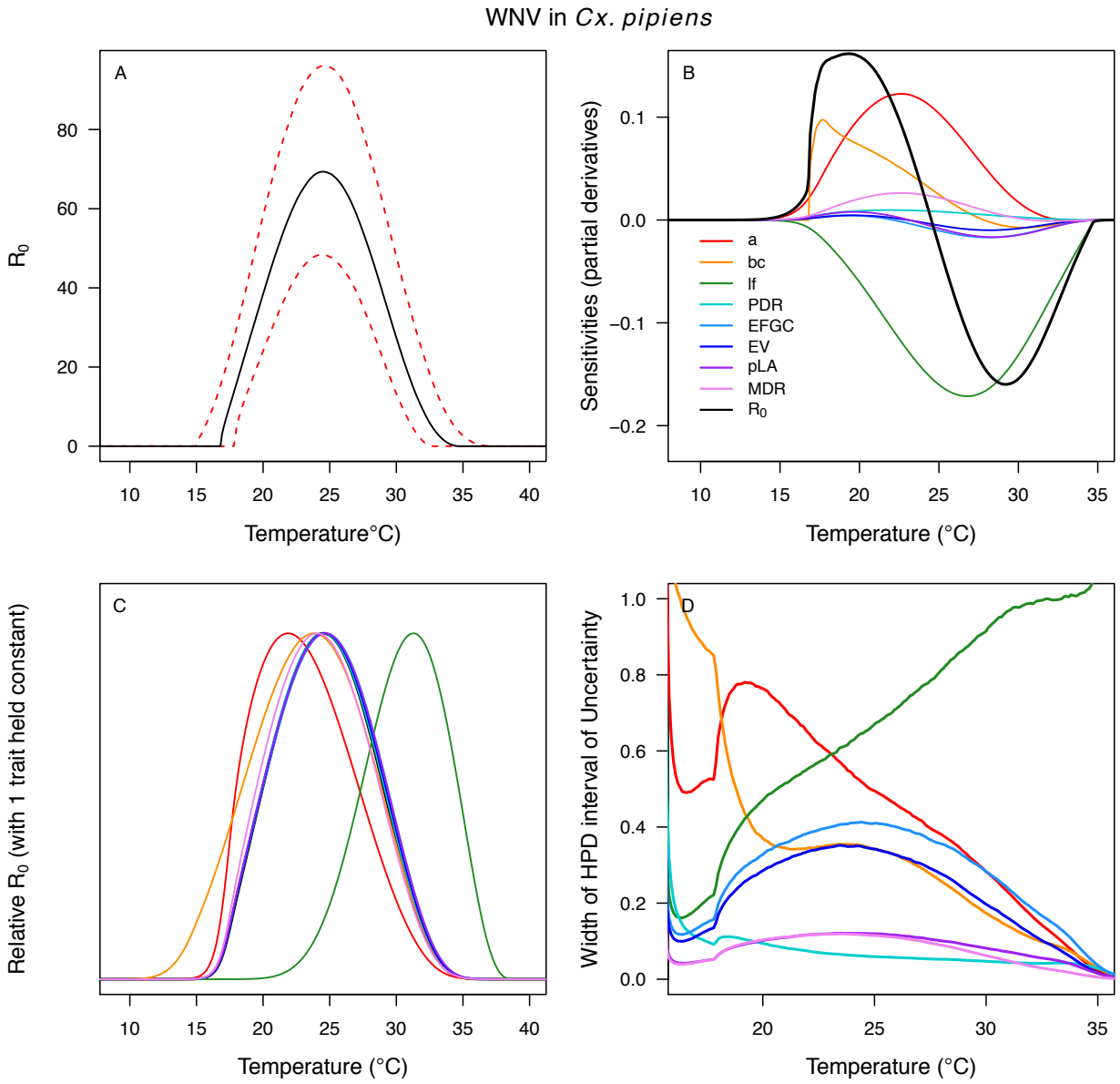

Figure S11: Temperature-dependent R_0, sensitivity analyses, and uncertainty analysis for model of West Nile Virus (WNV) in *Culex quinquefasciatus*. (A) Median temperature-dependent R_0 (black line) with 95% credible intervals (dashed red lines). (B) Sensitivity analysis #1: derivative with respect to temperature for R_0 (black) and partial derivatives with respect to temperature for each trait. (C) Sensitivity analysis #2: relative R_0 calculated with single traits held constant. (D) Uncertainty analysis using highest posterior density (HPD) interval widths: the proportion of total uncertainty due to each trait. (B-D) Trait colors: biting rate (*a*, red), vector competence (*bc*, orange), adult lifespan (*lf*, green), parasite development rate (*PDR*, cyan), fecundity (*EFGC*, light blue), egg viability (*EV*, dark blue), larval survival (*pLA*, purple), mosquito development rate (*MDR*, pink), and proportion ovipositing (*pO*, grey). Vector competence (*bc*) from *Cx. univitattus*; all other traits from *Cx. quinquefasciatus*.

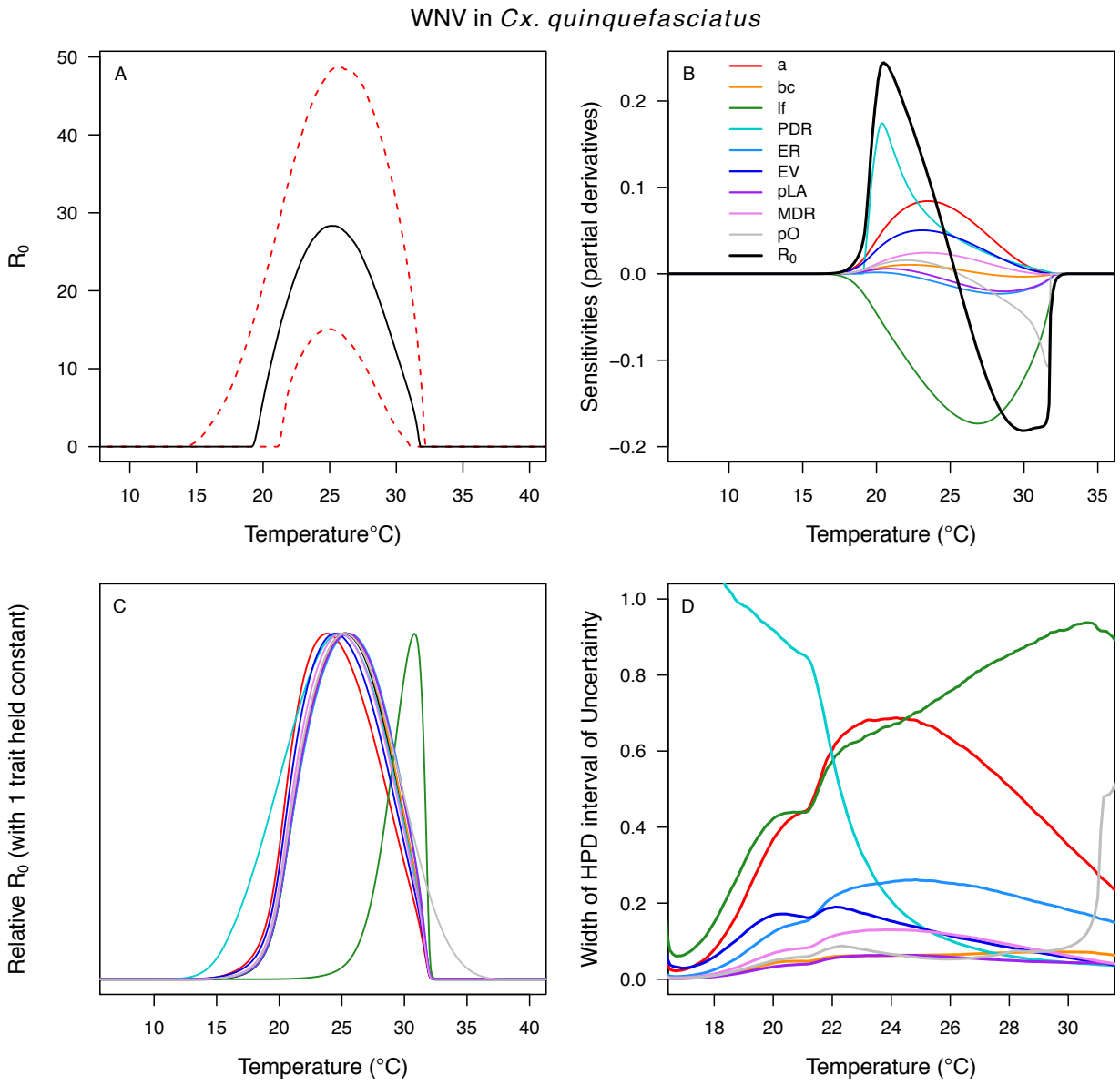

Figure S12: Temperature-dependent R_0, sensitivity analyses, and uncertainty analysis for model of West Nile Virus (WNV) in *Culex tarsalis*. (A) Median temperature-dependent R_0 (black line) with 95% credible intervals (dashed red lines). (B) Sensitivity analysis #1: derivative with respect to temperature for R_0 (black) and partial derivatives with respect to temperature for each trait. (C) Sensitivity analysis #2: relative R_0 calculated with single traits held constant. (D) Uncertainty analysis using highest posterior density (HPD) interval widths: the proportion of total uncertainty due to each trait. (B-D) Trait colors: biting rate (*a*, red), transmission efficiency (*b*, orange), adult lifespan (*lf*, green), parasite development rate (*PDR*, cyan), fecundity (*EFGC*, light blue), egg viability (*EV*, dark blue), larval survival (*pLA*, purple), and mosquito development rate (*MDR*, pink). Fecundity (*EFGC*) and egg viability (*EV*) from *Cx. pipiens*; all other traits from *Cx. tarsalis*.

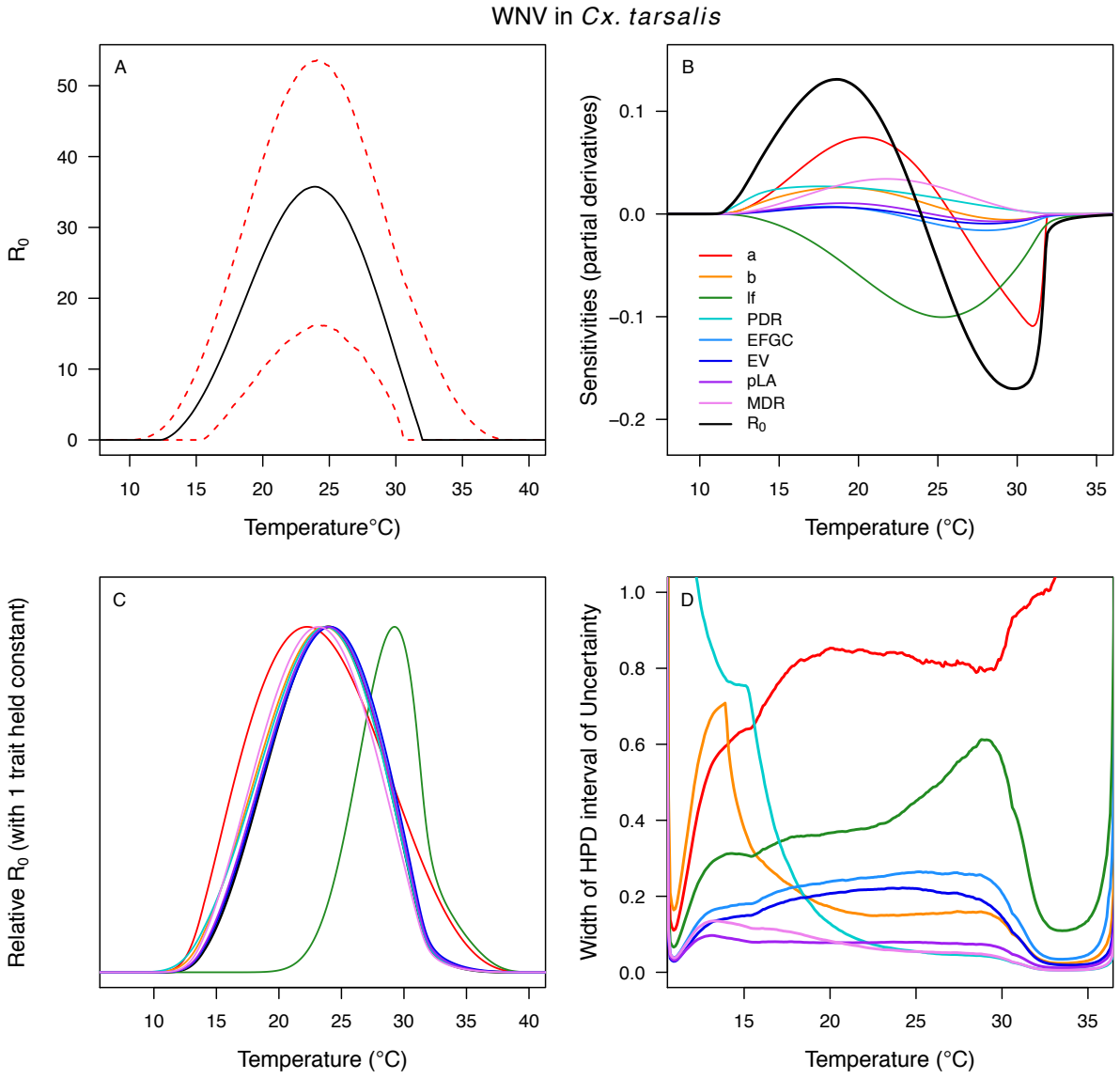

Figure S13: Temperature-dependent R_0, sensitivity analyses, and uncertainty analysis for model of West Nile Virus (WNV) in *Culex univittatus*. (A) Median temperature-dependent R_0 (black line) with 95% credible intervals (dashed red lines). (B) Sensitivity analysis #1: derivative with respect to temperature for R_0 (black) and partial derivatives with respect to temperature for each trait. (C) Sensitivity analysis #2: relative R_0 calculated with single traits held constant. (D) Uncertainty analysis using highest posterior density (HPD) interval widths: the proportion of total uncertainty due to each trait. (B-D) Trait colors: biting rate (*a*, red), vector competence (*bc*, orange), adult lifespan (*lf*, green), parasite development rate (*PDR*, cyan), fecundity (*EFGC*, light blue), egg viability (*EV*, dark blue), larval survival (*pLA*, purple), and mosquito development rate (*MDR*, pink). Infection traits (*bc* and *PDR*) from *Cx. univittatus*; all other traits from *Cx. pipiens*.

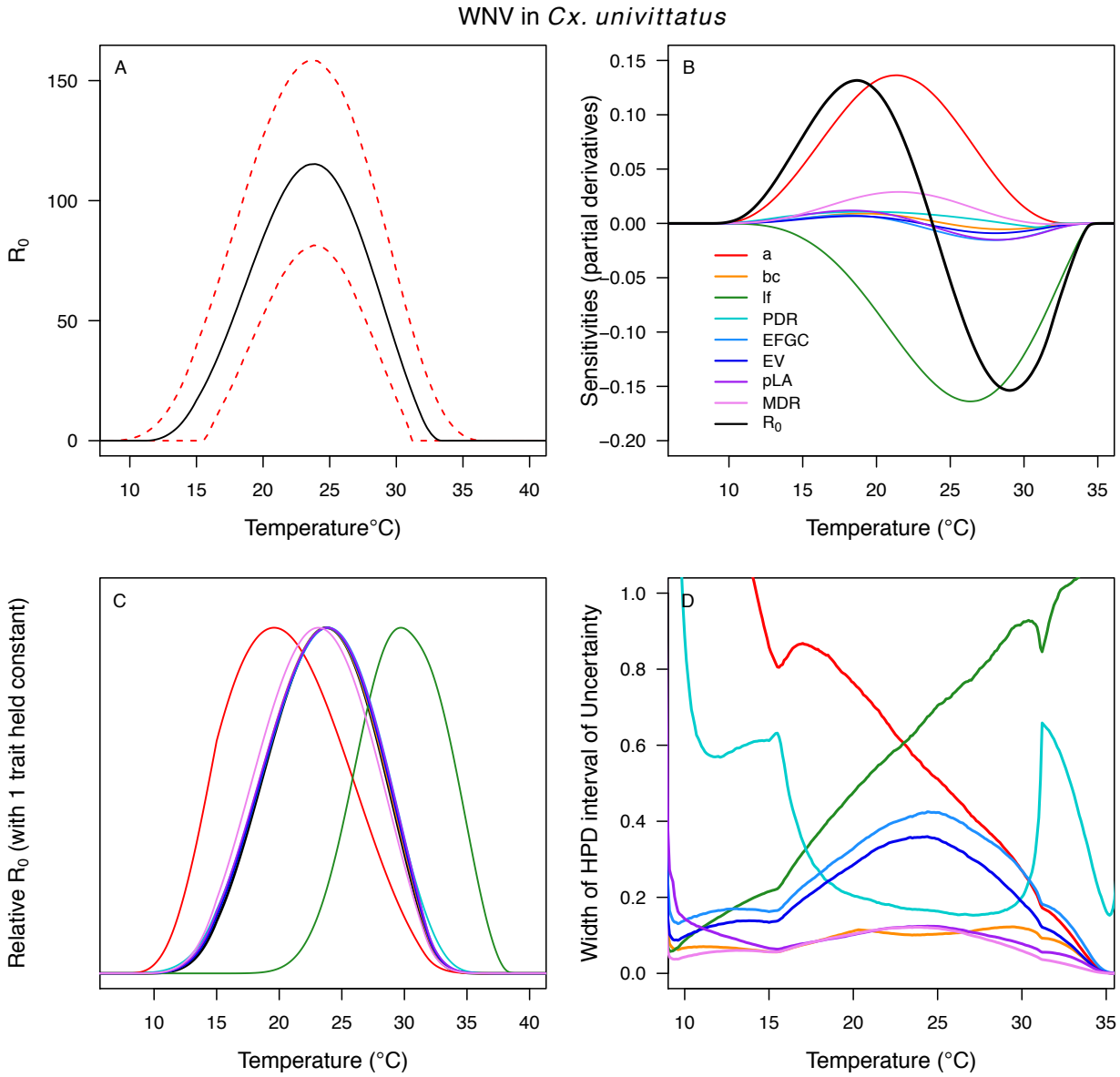

Figure S14: Temperature-dependent R_0, sensitivity analyses, and uncertainty analysis for St. model of St. Louis Encephalitis Virus (SLEV) in *Culex tarsalis*. (A) Median temperature-dependent R_0 (black line) with 95% credible intervals (dashed red lines). (B) Sensitivity analysis #1: derivative with respect to temperature for R_0 (black) and partial derivatives with respect to temperature for each trait. (C) Sensitivity analysis #2: relative R_0 calculated with single traits held constant. (D) Uncertainty analysis using highest posterior density (HPD) interval widths: the proportion of total uncertainty due to each trait. (B-D) Trait colors: biting rate (*a*, red), transmission efficiency (*b*, orange), infection efficiency (*c*, brown), adult lifespan (*lf*, green), parasite development rate (*PDR*, cyan), fecundity (*EFGC*, light blue), egg viability (*EV*, dark blue), larval survival (*pLA*, purple), and mosquito development rate (*MDR*, pink). Fecundity (*EFGC*) and egg viability (*EV*) from *Cx. pipiens*; all other traits from *Cx. tarsalis*.

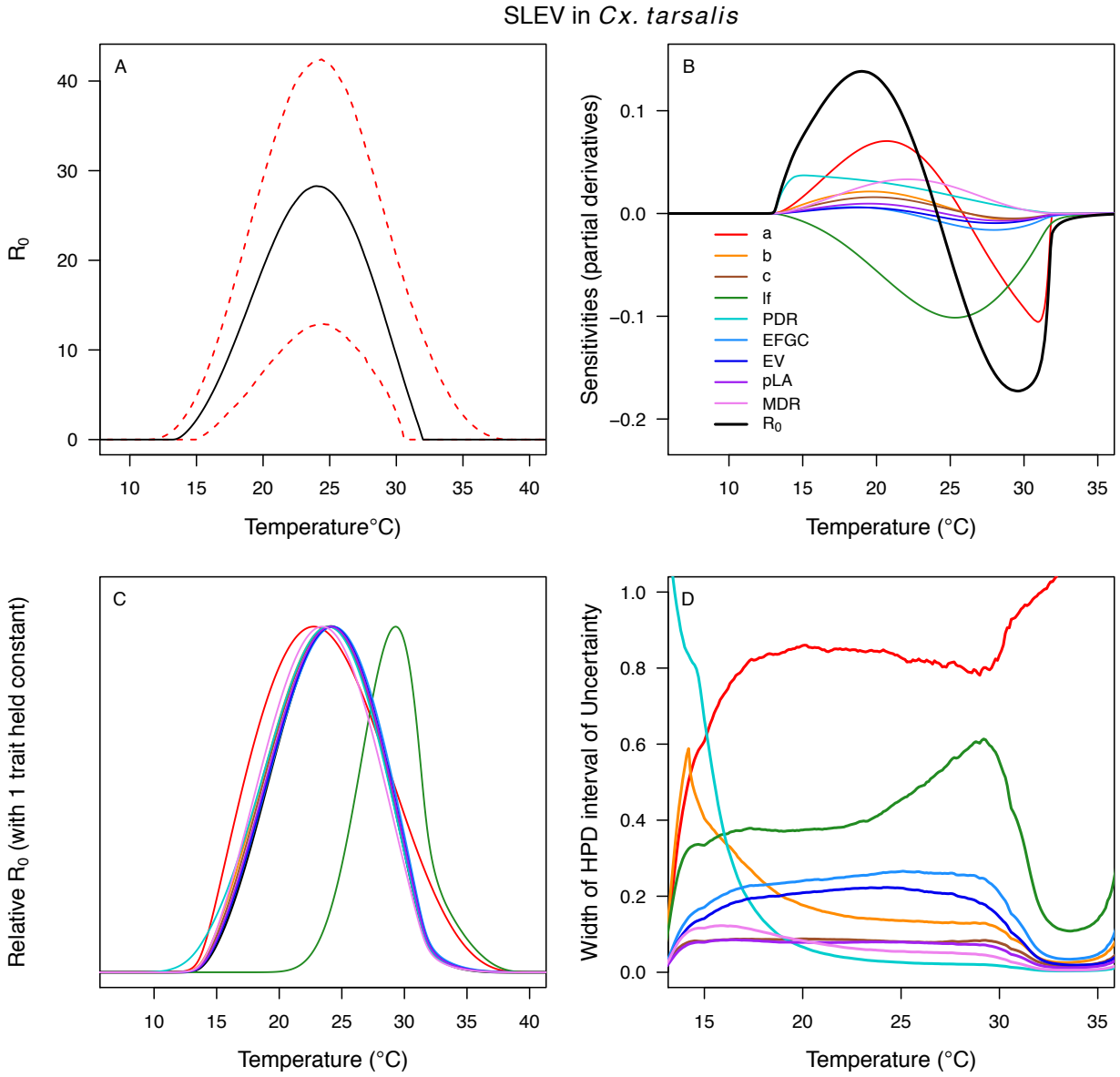

Figure S15: Temperature-dependent R_0, sensitivity analyses, and uncertainty analysis for model of Western Equine Encephalitis Virus (WEEV) in *Culex tarsalis*. (A) Median temperature-dependent R_0 (black line) with 95% credible intervals (dashed red lines). (B) Sensitivity analysis #1: derivative with respect to temperature for R_0 (black) and partial derivatives with respect to temperature for each trait. (C) Sensitivity analysis #2: relative R_0 calculated with single traits held constant. (D) Uncertainty analysis using highest posterior density (HPD) interval widths: the proportion of total uncertainty due to each trait. (B-D) Trait colors: biting rate (*a*, red), transmission efficiency (*b*, orange), infection efficiency (*c*, brown), adult lifespan (*lf*, green), parasite development rate (*PDR*, cyan), fecundity (*EFGC*, light blue), egg viability (*EV*, dark blue), larval survival (*pLA*, purple), and mosquito development rate (*MDR*, pink). Fecundity (*EFGC*) and egg viability (*EV*) from *Cx. pipiens*; all other traits from *Cx. tarsalis*.

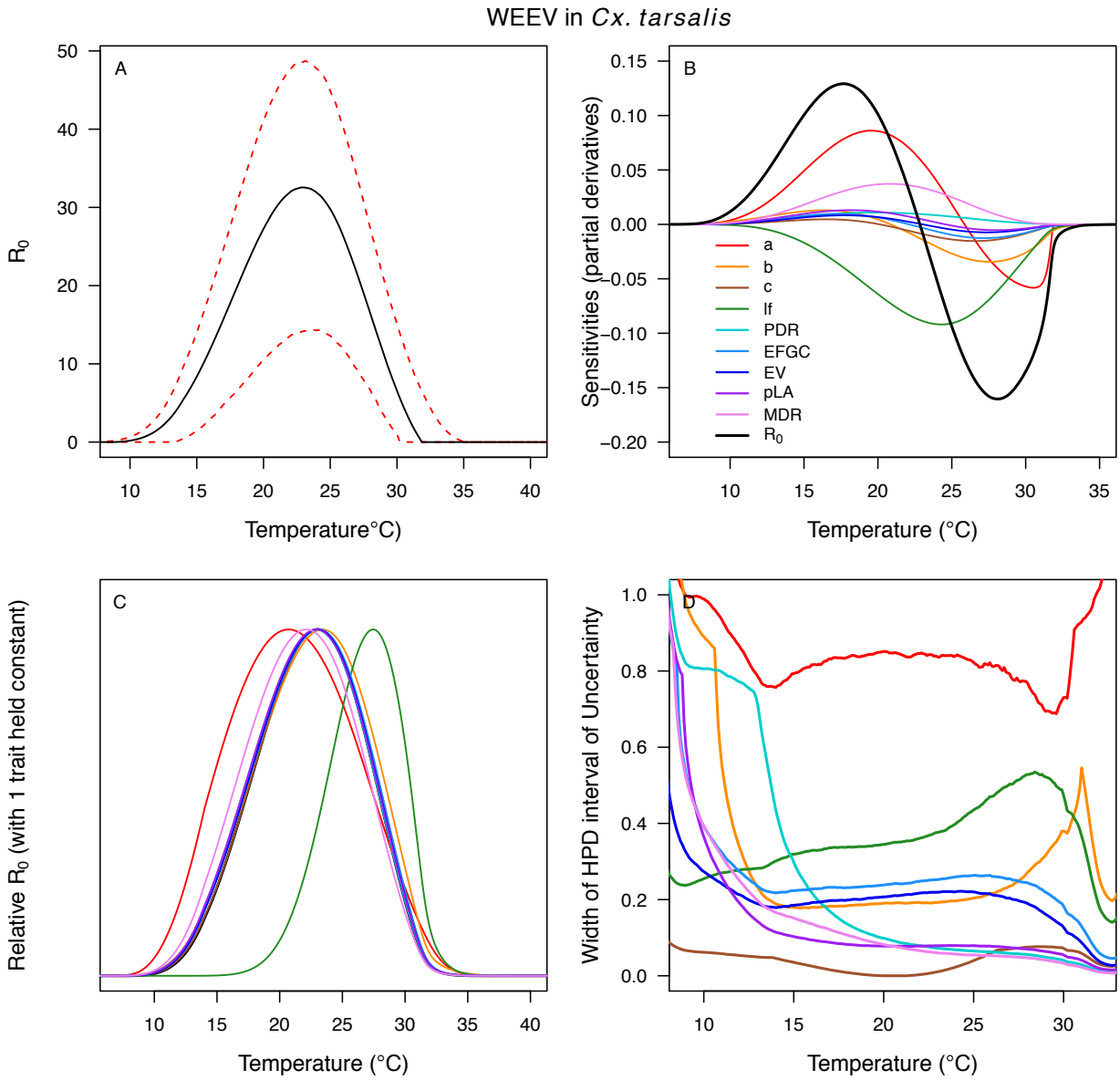

Figure S16: Temperature-dependent R_0, sensitivity analyses, and uncertainty analysis for model of Eastern Equine Encephalitis Virus in *Aedes triseriatus*. (A) Median temperature-dependent R_0 (black line) with 95% credible intervals (dashed red lines). (B) Sensitivity analysis #1: derivative with respect to temperature for R_0 (black) and partial derivatives with respect to temperature for each trait. (C) Sensitivity analysis #2: relative R_0 calculated with single traits held constant. (D) Uncertainty analysis using highest posterior density (HPD) interval widths: the proportion of total uncertainty due to each trait. (B-D) Trait colors: biting rate (*a*, red), vector competence (*bc*, orange), adult lifespan (*lf*, green), parasite development rate (*PDR*, cyan), fecundity (*EFGC*, light blue), egg viability (*EV*, dark blue), larval survival (*pLA*, purple), mosquito development rate (*MDR*, pink), and proportion ovipositing (*pO*, grey). Fecundity (*EFGC*), egg viability (*EV*), and lifespan (*lf*) from *Cx. pipiens*; biting rate (*a*) and proportion ovipositing (*pO*) from *Culiseta melanura*; all other traits from *Ae. triseriatus*. Note: technically fecundity as eggs per female per gonotrophic cycle (*EFGC*) has already accounted for the proportion ovipositing (*pO*). However, we selected this trait fit because it was very similar to the *ER* thermal response from *Cx. quinquefasciatus*, but slightly wider (more conservative).

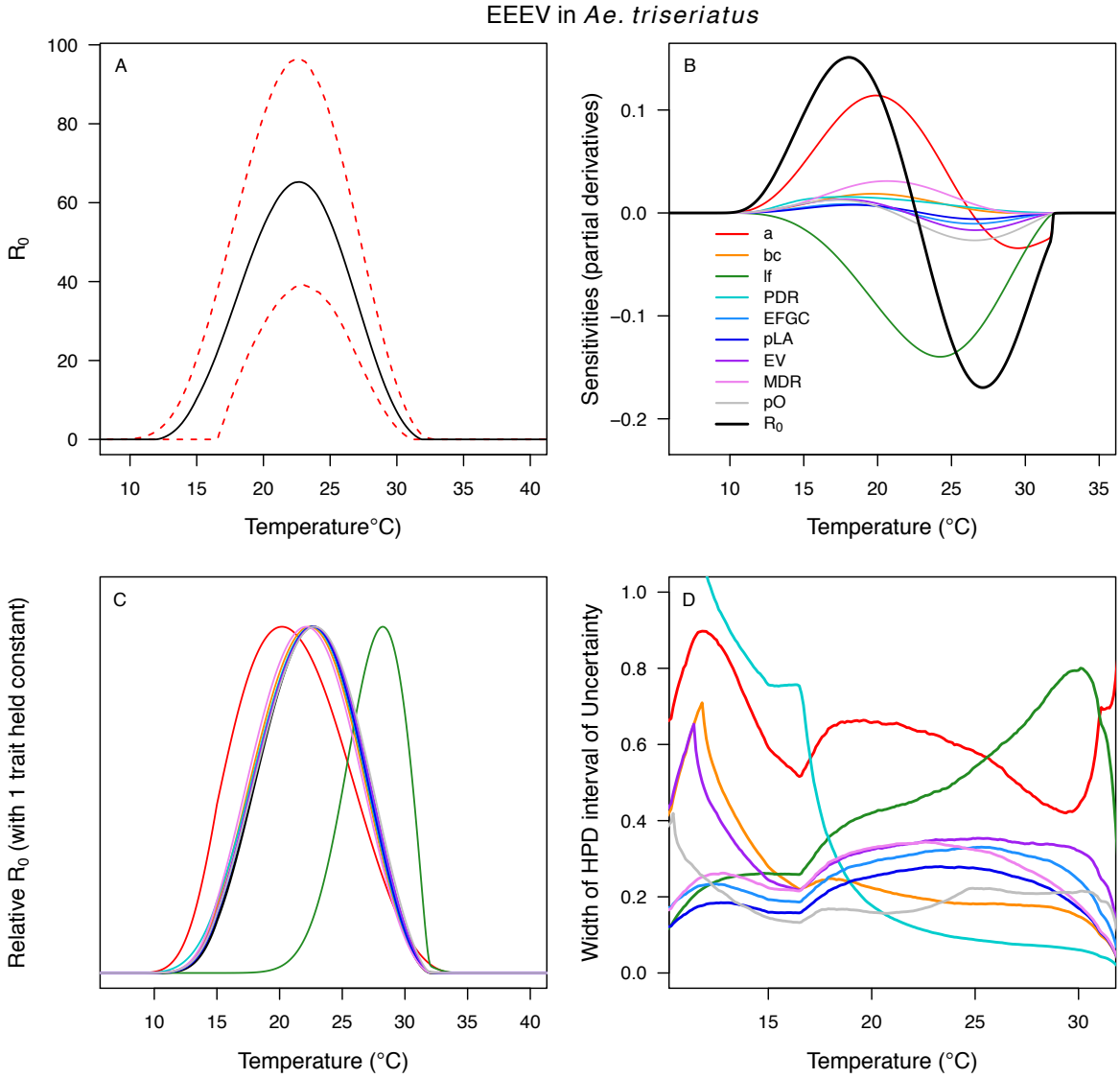

Figure S17: Temperature-dependent R_0, sensitivity analyses, and uncertainty analysis for model of Sindbis Virus in *Culex pipiens*. (A) Median temperature-dependent R_0 (black line) with 95% credible intervals (dashed red lines). (B) Sensitivity analysis #1: derivative with respect to temperature for R_0 (black) and partial derivatives with respect to temperature for each trait. (C) Sensitivity analysis #2: relative R_0 calculated with single traits held constant. (D) Uncertainty analysis using highest posterior density (HPD) interval widths: the proportion of total uncertainty due to each trait. (B-D) Trait colors: biting rate (*a*, red), infection efficiency (*c*, brown), adult lifespan (*lf*, green), fecundity (*EFGC*, light blue), egg viability (*EV*, dark blue), larval survival (*pLA*, purple), and mosquito development rate (*MDR*, pink). All traits from *Cx. pipiens*. NOTE: The raw R_0 calculation used $PDR = 1$, which is not biologically reasonable trait value.

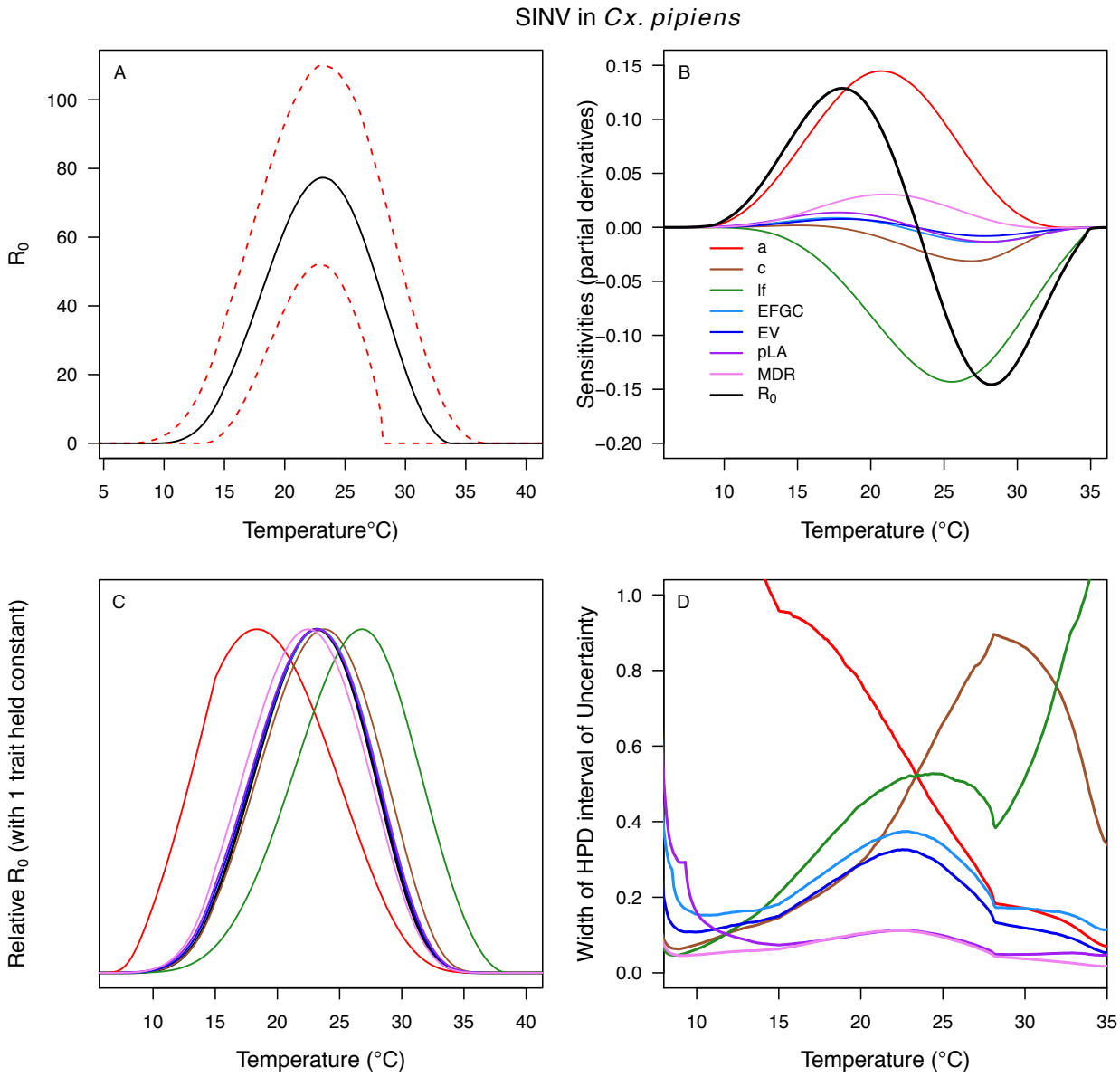

Figure S18: Temperature-dependent R_0, sensitivity analyses, and uncertainty analysis for model of Sindbis Virus in *Aedes taeniorhynchus*. (A) Median temperature-dependent R_0 (black line) with 95% credible intervals (dashed red lines). (B) Sensitivity analysis #1: derivative with respect to temperature for R_0 (black) and partial derivatives with respect to temperature for each trait. (C) Sensitivity analysis #2: relative R_0 calculated with single traits held constant. (D) Uncertainty analysis using highest posterior density (HPD) interval widths: the proportion of total uncertainty due to each trait. (B-D) Trait colors: biting rate (*a*, red), infection efficiency (*c*, brown), adult lifespan (*lf*, green), fecundity (*EFGC*, light blue), egg viability (*EV*, dark blue), larval survival (*pLA*, purple), and mosquito development rate (*MDR*, pink). Fecundity (*EFGC*) and biting rate (*a*) from *Culex pipiens*; egg viability (EV) and larval traits (*pLA* and *MDR*) from *Ae. vexans*; all other traits from *Ae. taeniorhynchus*. NOTE: The raw R_0 calculation used *PDR* = 1, which is not biologically reasonable trait value.

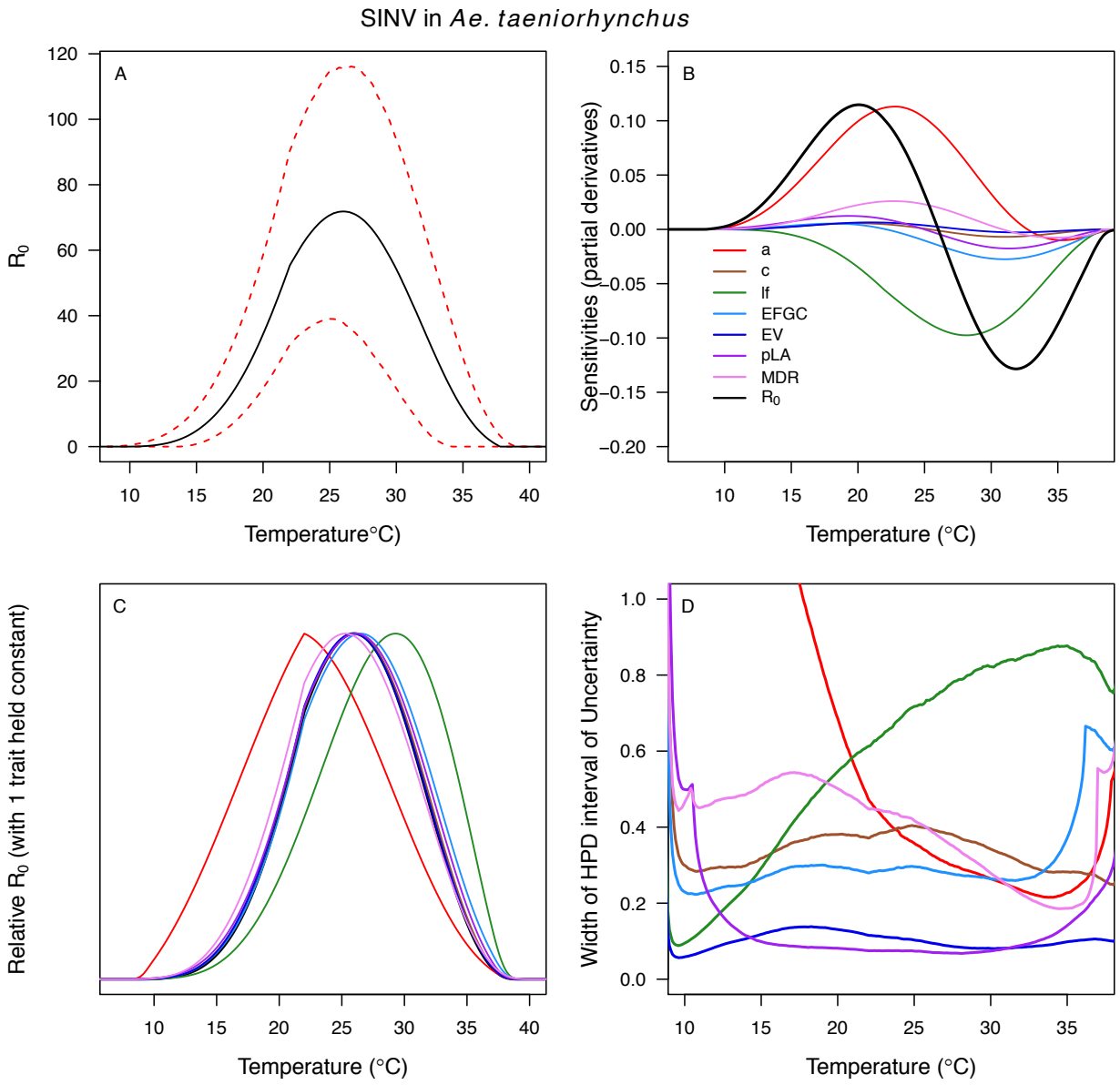

Figure S19: Temperature-dependent R_0, sensitivity analyses, and uncertainty analysis for model of Rift Valley Fever Virus in *Aedes taeniorhynchus*. (A) Median temperature-dependent R_0 (black line) with 95% credible intervals (dashed red lines). (B) Sensitivity analysis #1: derivative with respect to temperature for R_0 (black) and partial derivatives with respect to temperature for each trait. (C) Sensitivity analysis #2: relative R_0 calculated with single traits held constant. (D) Uncertainty analysis using highest posterior density (HPD) interval widths: the proportion of total uncertainty due to each trait. (B-D) Trait colors: biting rate (*a*, red), vector competence (*bc*, orange), adult lifespan (*lf*, green), parasite development rate (*PDR*, cyan), fecundity (*EFGC*, light blue), egg viability (*EV*, dark blue), larval survival (*pLA*, purple), and mosquito development rate (*MDR*, pink). Fecundity (*EFGC*) and biting rate (*a*) from *Culex pipiens*; egg viability (EV) from *Cx. theileri*; larval traits (*pLA* and *MDR*) from *Ae. vexans*; all other traits from *Ae. taeniorhynchus*.

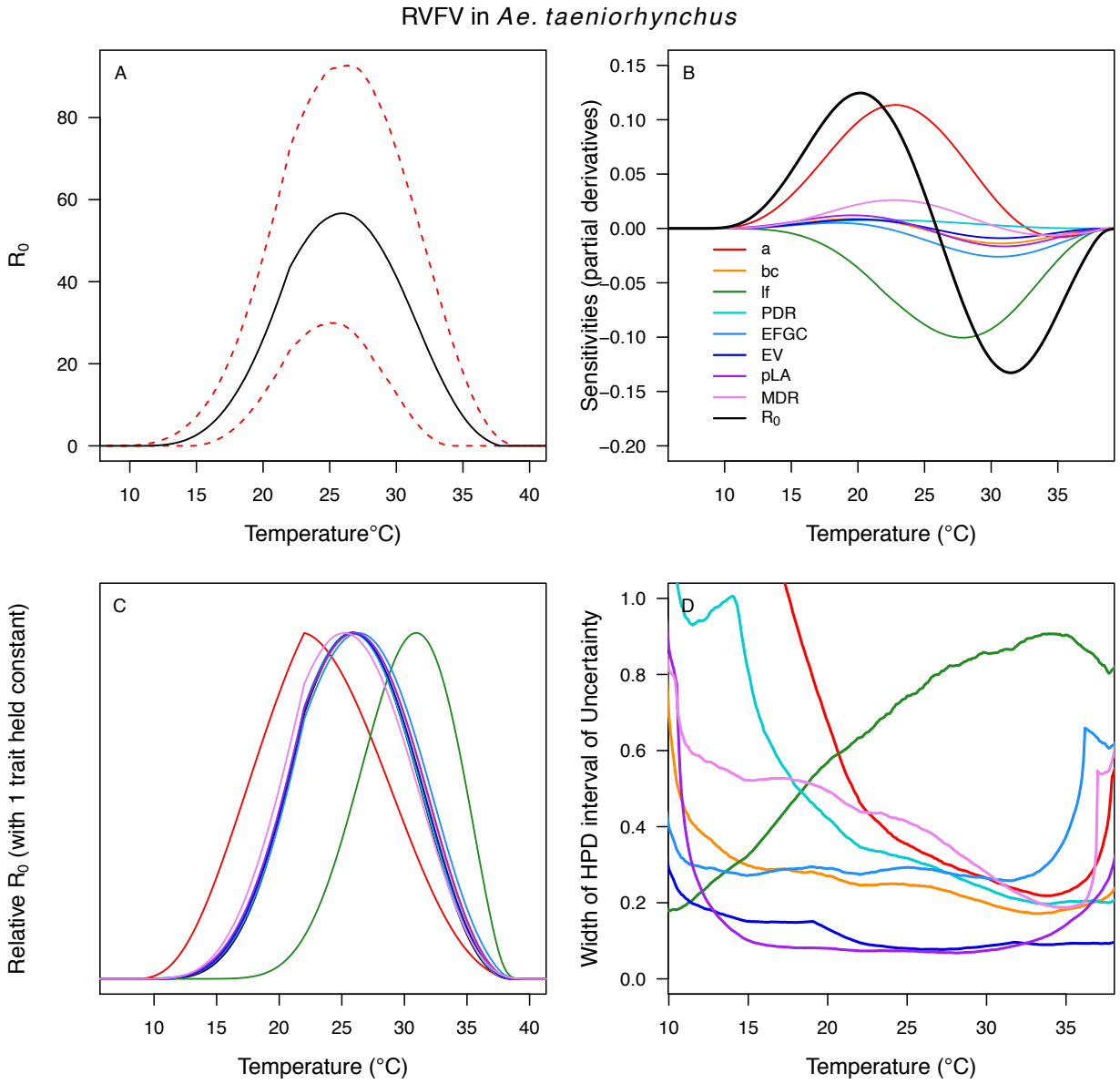

Figure S20: Histograms of T_{min}, optimum, and T_{max} for transmission (R_0) models. T_{min} (left column), optimum (center column), and T_{max} (right column). Top row (A-C): West Nile virus (WNV) in four vectors: *Culex pipiens* (grey), *Cx. quinquefasciatus* (red), *Cx. tarsalis* (blue), and *Cx. univitattus* (orange). Middle row (D-F): three viruses in *Cx. tarsalis*: WNV (same as in top row, bright blue), Western Equine Encephalitis virus (WEEV, light blue), and St. Louis Encephalitis virus (SLEV, dark blue). Bottom row (H-J): Sindbis virus (SINV) in *Aedes taeniorhynchus* (grey), SINV in *Cx. pipiens* (dark green), Rift Valley Fever virus (RVFV) in *Ae. taeniorhynchus* (light green), and Eastern Equine Encephalitis virus (EEEV) in *Ae. triseriatus* (purple).

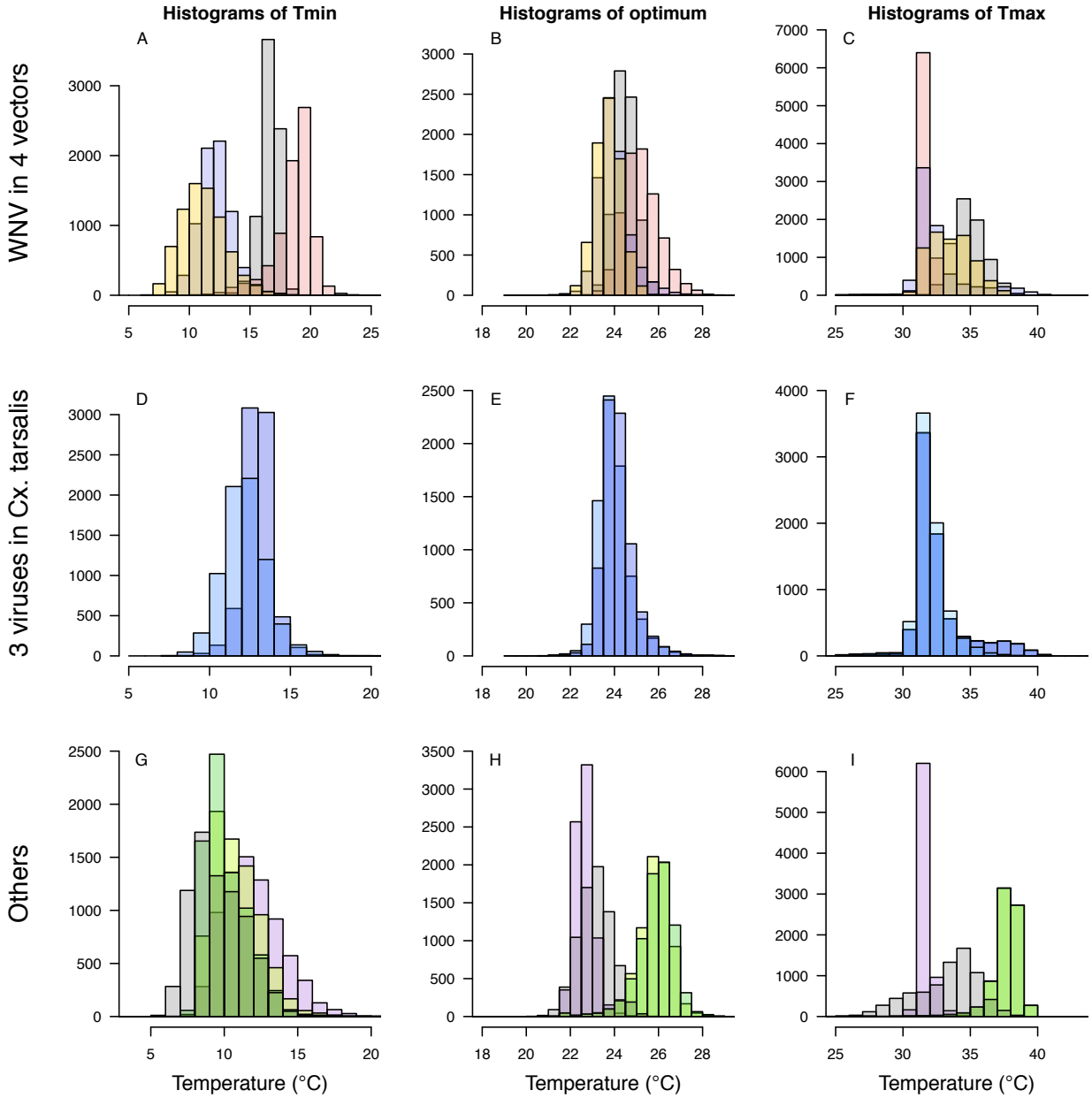

Figure S21: Comparing alternative model parameterizations. Several models had multiple potentially valid choices for traits; we show these alternative models here to show that they make very little difference, except in D. (A) Models for EEEV in *Ae. triseriatus* with larval traits (larval-to-adult survival [*pLA*] and mosquito development rate [*MDR*]) from *Ae. triseriatus* (violet, from the main text) and larval traits from *Cs. melanura* (black). We also show larval traits from *Cs. melanura* without proportion ovipositing (*pO*) in the model (grey), since the thermal responses for *EFCG* (eggs per female per gonotrophic cycle, in *Cx. pipiens*) and *ER* (eggs per raft, in *Cx. quinquefasciatus*) were nearly identical even though the units were different, probably because the ER data were not very informative and the priors strongly shaped the thermal response. (B) Models for WNV in *Cx. quinquefasciatus*, with (light red, from the main text) and without (dark red) the thermal response for fecundity (as eggs per raft, *ER*), for the same reason as in A. (C) Models for WEEV in *Cx. tarsalis* with vector competence estimated by infection efficiency (*c*, Fig 6D) and transmission efficiency (*b*, Fig 6E) measured separately (blue, from the main text) or by vector competence measured as a single trait (*bc*, Fig 6F; light blue). (D) Models for RVFV in *Ae. taeniorhynchus* with lifespan from *Ae. taeniorhynchus* (light green, from the main text) or from *Cx. pipiens* (dark green). We chose the *Ae. taeniorhynchus* version for the main text because it is the same species the infection traits (*PDR*, *bc*) were measured in, and that choice strongly impacted the results.

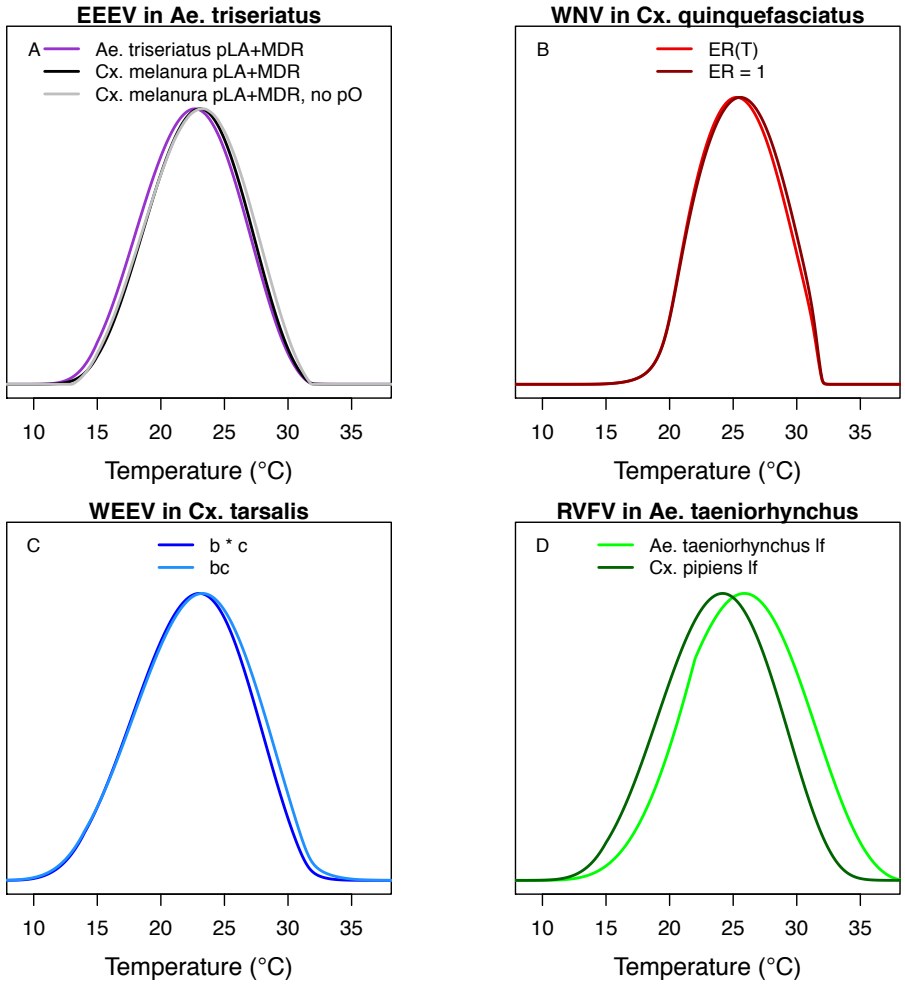

Figure S22: Comparison with previous R_0 models for transmission of West Nile virus. Models taken from this paper (solid lines: *Cx. pipiens* [grey], *Cx. quinquefasciatus* [red], *Cx. tarsalis* [blue], and *Cx. univittatus* [orange]), from Paull et al. 2017 [49] (dashed lines: *Cx. pipiens* [grey], *Cx. quinquefasciatus* [red], and *Cx. tarsalis* [blue]), from Vogels et al. 2017 [52] (*Cx. pipiens* [grey] and *Cx. pipiens molestus* [black]), and from Kushmaro et al. 2015 [53] (not species specific, dot-dashed line [brown]).

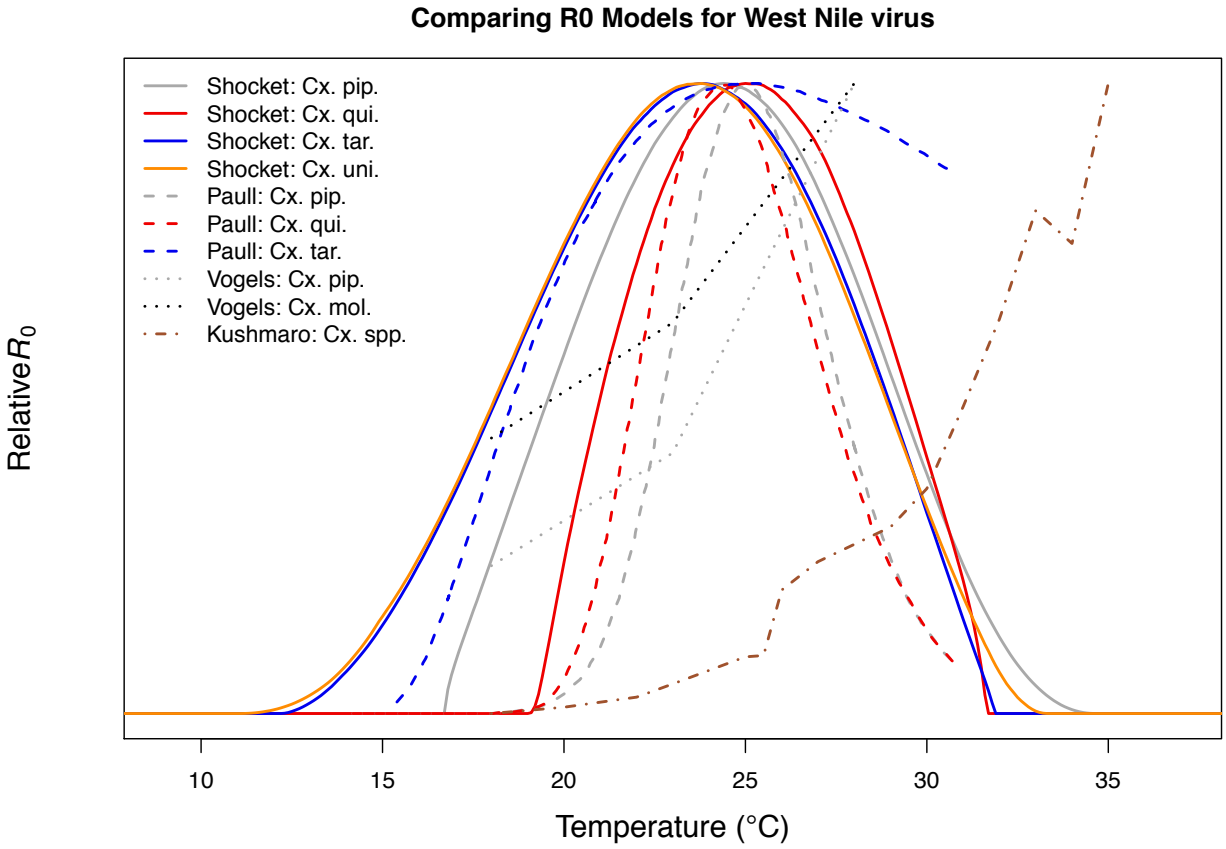

Figure S23: LOESS models of WNV incidence across varying smoothing parameters. Points are means for bins of 42 counties (+/- SE). Lines are locally estimated scatterplot smoothing (LOESS) regression models with different smoothing (span) parameters: 0.1 (red), 0.25 (orange), 0.5 (green), 0.6 (cyan), 0.75 (light blue), 1 (dark blue), and 2 (violet). Models were fit to raw county-level data (n = 3,109, binned for visual clarity). We chose the model presented in the main text (span = 0.6) because it appropriately balances overfitting and underfitting the data.

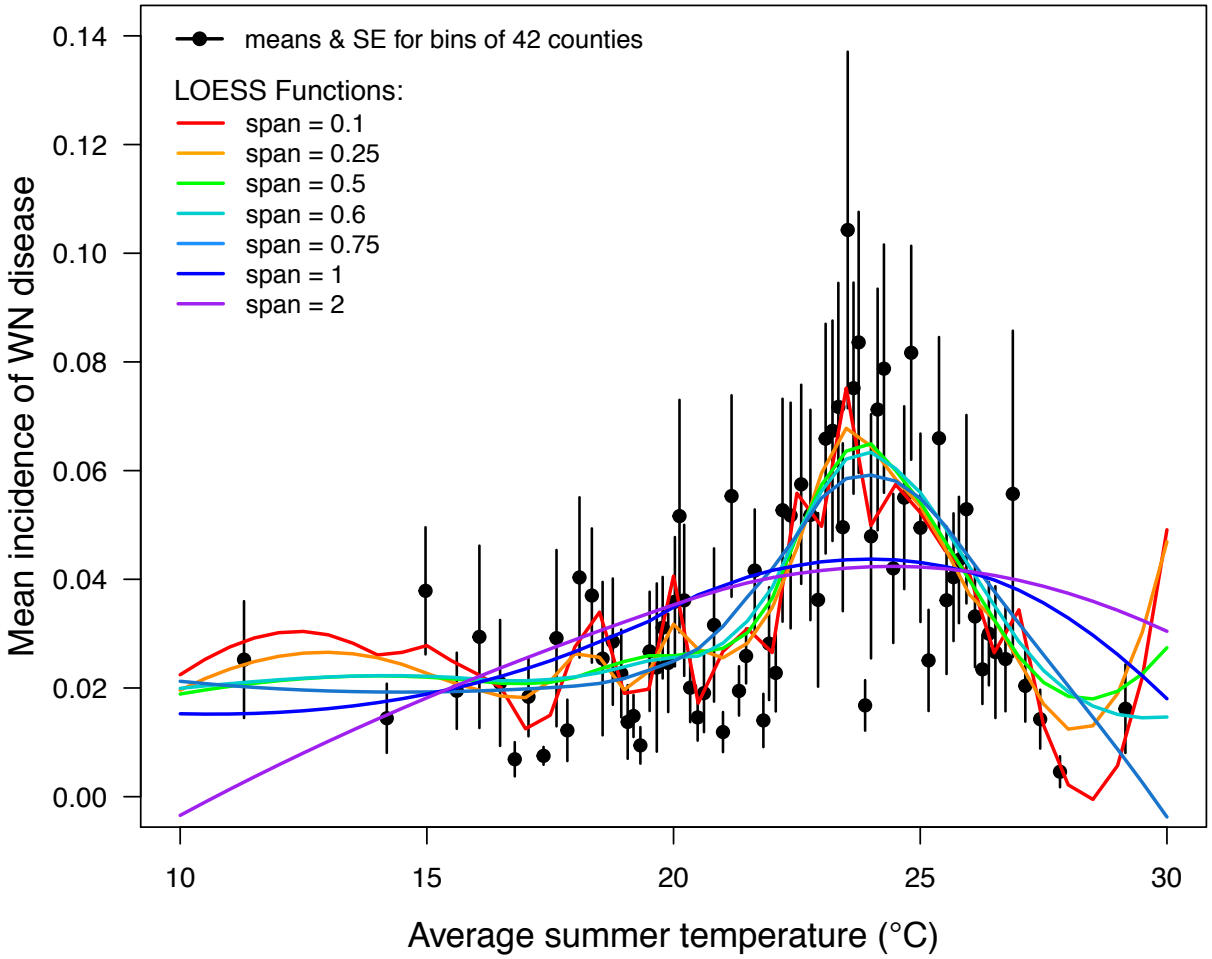

References

1. Parham PE, Michael E. Modeling the effects of weather and climate change on malaria transmission. Environmental Health Perspectives. 2010;118: 620–626. doi:10.1289/ehp.0901256

2. Mordecai EA, Paaijmans KP, Johnson LR, Balzer C, Ben-Horin T, de Moor E, et al. Optimal temperature for malaria transmission is dramatically lower than previously predicted. Ecology letters. 2013;16: 22–30. doi:10.1111/ele.12015

3. Johnson LR, Ben-Horin T, Lafferty KD, McNally A, Mordecai E, Paaijmans KP, et al. Understanding uncertainty in temperature effects on vector-borne disease: A Bayesian approach. Ecology. 2015;96: 203–213. doi:10.1890/13-1964.1

4. Mordecai EA, Cohen JM, Evans MV, Gudapati P, Johnson LR, Lippi CA, et al. Detecting the impact of temperature on transmission of Zika, dengue, and chikungunya using mechanistic models. PLOS Neglected Tropical Diseases. 2017;11: e0005568. doi:10.1371/journal.pntd.0005568

5. Shocket MS, Ryan SJ, Mordecai EA. Temperature explains broad patterns of Ross River virus transmission. eLife. 2018;7. doi:10.7554/eLife.37762

6. Tesla B, Demakovsky LR, Mordecai EA, Ryan SJ, Bonds MH, Ngonghala CN, et al. Temperature drives Zika virus transmission: evidence from empirical and mathematical models. Proceedings of the Royal Society B: Biological Sciences. 2018;285: 20180795. doi:10.1098/rspb.2018.0795

7. Tekle A. The Physiology of Hibernation and Its Role in the Geographical Distribution of Populations of the *Culex Pipiens* Complex. The American Journal of Tropical Medicine and Hygiene. 1960;9: 321–330. doi:10.4269/ajtmh.1960.9.321

8. Madder DJ, Surgeoner GA, Helson BV. Number of generations, egg production, and developmental time of Culex pipiens and Culex restauns (Diptera: Culicidae) in southern Ontario. J Med Entomol. 1983;20: 275–287.

9. Ruybal JE, Kramer LD, Kilpatrick AM. Geographic variation in the response of *Culex pipiens* life history traits to temperature. Parasites & Vectors. Parasites & Vectors; 2016;9. doi:10.1186/s13071-016-1402-z

10. Li J, Zhu G, Zhou H, Tang J, Cao J. Effect of temperature on the development of *Culex pipiens pallens*. Chin J Vector Biol & Control. 2017;28: 35–37.

11. Reisen WK, Milby MM, Presser SB, Hardy JL. Ecology of Mosquitoes and St. Louis Encephalitis Virus in the Los Angeles Basin of California, 1987–1990. Journal of Medical Entomology. 1992;29: 582–598. doi:10.1093/jmedent/29.4.582

12. Mahmood F, Crans WJ. A thermal heat summation model to predict the duration of the gonotrophic cycle of Culiseta melanura in nature. J Am Mosq Control Assoc. 1997;13: 92–94.

13. Oda T, Mori A, Ueda M, Kurokawa K, others. Effects of temperatures on the oviposition and hatching of eggs in *Culex pipiens molestus* and *Culex pipiens quinquefasciatus*. Tropical Medicine. 1980;22: 167–180.

14. Mogi M. Temperature and Photoperiod Effects on Larval and Ovarian Development of New Zealand Strains of *Culex quinquefasciatus* (Diptera: Culicidae). Annals of the Entomological Society of America. 1992;85: 58–66. doi:10.1093/aesa/85.1.58

15. Ciota AT, Matacchiero AC, Kilpatrick AM, Kramer LD. The Effect of Temperature on Life History Traits of *Culex* Mosquitoes. Journal of Medical Entomology. 2014;51: 55–62. doi:10.1603/ME13003

16. McHaffey DG. Photoperiod and temperature influences on diapause in eggs of the floodwater mosquito *Aedes vexans* (Meigen) (Diptera: Culicidae). J Med Entomol. 1972;9: 564–571.

17. Rayah EAE, Groun NAA. Effect of temperature on hatching eggs and embryonic survival in the mosquito Culex quinquefasciatus. Entomologia Experimentalis et Applicata. 1983;33: 349–351. doi:10.1111/j.1570-7458.1983.tb03281.x

18. Van der Linde TCD. Development rates and percentage hatching of Culex (Culex) theileri; Theobald (Diptera: Culicidae) eggs at various constant temperatures. Journal of the Entomological Society of Southern Africa,. 1990;53: 17–26.

19. Parker BM. Temperature and Salinity as Factors Influencing the Size and Reproductive Potentials of *Aedes dorsalis* (Diptera: Culicidae). Annals of the Entomological Society of America. 1982;75: 99–102. doi:10.1093/aesa/75.1.99

20. McHaffey DG, Harwood RF. Photoperiod and Temperature Influences on Diapause in Eggs of the Floodwater Mosquito, *Aedes Dorsalis* (Meigen) (Diptera: Culicidae)1. Journal of Medical Entomology. 1970;7: 631–644. doi:10.1093/jmedent/7.6.631

21. McHaffey DG. Photoperiod and temperature influences on diapause in eggs of the floodwater mosquito *Aedes nigromaculis* (Ludlow) (Diptera : Culicidae). Mosquito News. 1972;32: 51–61.

22. Shelton RM. The effect of temperatures on development of eight mosquito species. Mosquito News. 1973;33: 1–12.

23. Brust RA. WEIGHT AND DEVELOPMENT TIME OF DIFFERENT STADIA OF MOSQUITOES REARED AT VARIOUS CONSTANT TEMPERATURES. The Canadian Entomologist. 1967;99: 986–993. doi:10.4039/Ent99986-9

24. Trpiš M, Shemanchuk JA. EFFECT OF CONSTANT TEMPERATURE ON THE LARVAL DEVELOPMENT OF *AEDES VEXANS* (DIPTERA: CULICIDAE). The Canadian Entomologist. 1970;102: 1048–1051. doi:10.4039/Ent1021048-8

25. Mpho M, Callaghan A, Holloway GJ. Temperature and genotypic effects on life history and fluctuating asymmetry in a field strain of *Culex pipiens*. Heredity. 2002;88: 307–312. doi:10.1038/sj.hdy.6800045

26. Mpho M, Callaghan A, Holloway GJ. Effects of temperature and genetic stress on life history and fluctuating wing asymmetry in *Culex pipiens* mosquitoes. European Journal of Entomology. 2002;99: 405–412. doi:10.14411/eje.2002.050

27. Loetti V, Schweigmann N, Burroni N. Development rates, larval survivorship and wing length of *Culex pipiens* (Diptera: Culicidae) at constant temperatures. Journal of Natural History. 2011;45: 2203–2213. doi:10.1080/00222933.2011.590946

28. Rueda LM, Patel KJ, Axtell RC, Stinner RE. Temperature-dependent development and survival rates of *Culex quinquefasciatus* and *Aedes aegypti* (Diptera: Culicidae). J Med Entomol. 1990;27: 892–898.

29. Mpho M, Holloway GJ, Callaghan A. A comparison of the effects of organophosphate insecticide exposure and temperature stress on fluctuating asymmetry and life history traits in *Culex quinquefasciatus*. Chemosphere. 2001;45: 713–720.

30. Reisen WK. Effect of temperature on *Culex tarsalis* (Diptera: Culicidae) from the Coachella and San Joaquin Valleys of California. J Med Entomol. 1995;32: 636–645.

31. Buth JL, Brust RA, Ellis RA. Development time, oviposition activity and onset of diapause in *Culex tarsalis*, *Culex restuans* and *Culiseta inornata* in southern Manitoba. J Am Mosq Control Assoc. 1990;6: 55–63.

32. Dodson BL, Kramer LD, Rasgon JL. Effects of larval rearing temperature on immature development and West Nile virus vector competence of *Culex tarsalis*. Parasites & Vectors. 2012;5: 199. doi:10.1186/1756-3305-5-199

33. Mahmood F, Crans WJ. Effect of temperature on the development of Culiseta melanura (Diptera: Culicidae) and its impact on the amplification of eastern equine encephalomyelitis virus in birds. J Med Entomol. 1998;35: 1007–1012.

34. Teng H-J, Apperson CS. Development and Survival of Immature *Aedes albopictus* and *Aedes triseriatus* (Diptera: Culicidae) in the Laboratory: Effects of Density, Food, and Competition on Response to Temperature. Journal of Medical Entomology. 2000;37: 40–52. doi:10.1603/0022-2585-37.1.40

35. Oda T, Uchida K, Mori A, Mine M, Eshita Y, Kurokawa K, et al. Effects of high temperature on the emergence and survival of adult *Culex pipiens molestus* and *Culex quinquefasciatus* in Japan. J Am Mosq Control Assoc. 1999;15: 153–156.

36. Kiarie-Makara MW, Ngumbi PM, Lee D-K. Effects of Temperature on the Growth and Development of *Culex pipiens* Complex Mosquitoes (Diptera: Culicidae). Journal of Pharmacy and Biological Sciences. 2015;10: 1–10.

37. Olejnícek J, Gelbic I. Differences in response to temperature and density between two strains of the mosquito, *Culex pipiens molestus* forskal. J Vector Ecol. 2000;25: 136–145.

38. Muturi EJ, Lampman R, Costanzo K, Alto BW. Effect of Temperature and Insecticide Stress on Life-History Traits of Culex restuans and Aedes albopictus (Diptera: Culicidae). Journal of Medical Entomology. 2011;48: 243–250. doi:10.1603/ME10017

39. Reisen WK, Meyer RP, Presser SB, Hardy JL. Effect of temperature on the transmission of western equine encephalomyelitis and St. Louis encephalitis viruses by *Culex tarsalis* (Diptera: Culicidae). J Med Entomol. 1993;30: 151–160.

40. Reisen WK, Fang Y, Martinez VM. Effects of Temperature on the Transmission of West Nile Virus by *Culex tarsalis* (Diptera: Culicidae). Journal of Medical Entomology. 2006;43: 309–317. doi:10.1603/0022-2585(2006)043[0309:EOTOTT]2.0.CO;2

41. Turell MJ, Lundström JO. Effect of environmental temperature on the vector competence of *Aedes aegypti* and *Ae. taeniorhynchus* for Ockelbo virus. Am J Trop Med Hyg. 1990;43: 543–550.

42. Lundström JO, Turell MJ, Niklasson B. Effect of environmental temperature on the vector competence of *Culex pipiens and Cx. torrentium* for Ockelbo virus. Am J Trop Med Hyg. 1990;43: 534–542.

43. Kilpatrick AM, Meola MA, Moudy RM, Kramer LD. Temperature, viral genetics, and the transmission of West Nile virus by *Culex pipiens* mosquitoes. PLoS Pathogens. 2008;4. doi:10.1371/journal.ppat.1000092

44. Dohm DJ, O'Guinn ML, Turell MJ. Effect of environmental temperature on the ability of *Culex pipiens* (Diptera: Culicidae) to transmit West Nile virus. Journal of Medical Entomology. 2002;39: 221–225. doi:10.1603/0022-2585-39.1.221

45. Kramer LD, Hardy JL, Presser SB. Effect of temperature of extrinsic incubation on the vector competence of *Culex tarsalis* for western equine encephalomyelitis virus. Am J Trop Med Hyg. 1983;32: 1130–1139.

46. Turell MJ, Rossi CA, Bailey CL. Effect of Extrinsic Incubation Temperature on the Ability of *Aedes Taeniorhynchus* and *Culex Pipiens* to Transmit Rift Valley Fever Virus. The American Journal of Tropical Medicine and Hygiene. 1985;34: 1211–1218. doi:10.4269/ajtmh.1985.34.1211

47. Chamberlain RW, Sudia WD. The effects of temperature upon the extrinsic incubation of eastern equine encephalitis in mosquitoes. Am J Hyg. 1955;62: 295–305.

48. Cornel AJ, Jupp PG, Blackburn NK. Environmental Temperature on the Vector Competence of *Culex univittatus* (Diptera: Culicidae) for West Nile Virus. Journal of Medical Entomology. 1993;30: 449–456. doi:10.1093/jmedent/30.2.449

49. Paull SH, Horton DE, Ashfaq M, Rastogi D, Kramer LD, Diffenbaugh NS, et al. Drought and immunity determine the intensity of West Nile virus epidemics and climate change impacts. Proceedings of the Royal Society B: Biological Sciences. 2017;284: 20162078. doi:10.1098/rspb.2016.2078

50. Nayar JK. Effects of constant and fluctuating temperatures on life span of *Aedes taeniorhynchus* adults. Journal of Insect Physiology. 1972;18: 1303–1313. doi:10.1016/0022-1910(72)90259-4

51. Andreadis SS, Dimotsiou OC, Savopoulou-Soultani M. Variation in adult longevity of *Culex pipiens f. pipiens*, vector of the West Nile Virus. Parasitology Research. 2014;113: 4315–4319. doi:10.1007/s00436-014-4152-x

52. Vogels CBF, Hartemink N, Koenraadt CJM. Modelling West Nile virus transmission risk in Europe: effect of temperature and mosquito biotypes on the basic reproduction number. Scientific Reports. 2017;7. doi:10.1038/s41598-017-05185-4

53. Kushmaro A, Friedlander TA, Levins R. Temperature Effects on the Basic Reproductive Number (R0) Of West Nile Virus, Based On Ecological Parameters: Endemic Vs. New Emergence Regions. Journal of Tropical Diseases. 2015;s1. doi:10.4172/2329-891X.1000S1-001